Western Norway University of Applied Sciences

BACHELOR'S THESIS

Study of rechargeable iron-ion batteries fabrication using ionic liquid electrolyte

Carmen Bolufer Cruañes

Bachelor's in Chemical Engineering
Faculty of Engineering and Science/Department of Biomedical Laboratory Sciences and Chemical Engineering/Chemical Engineering/ Specialization Environmental Technology
Supervisor: Yansong Zhao

Submission Date: 29th May 2020

I confirm that the work is self-prepared and that references/source references to all sources used in the work are provided, cf. Regulation relating to academic studies and examinations at the Western Norway University of Applied Sciences (HVL), § 12-1.

Foreword

First of all, I would like to thank my supervisor Yansong Zhao for his supervision provided from the initial design and planning phases trough to the full implementation of the batteries. It has been an amazing opportunity to work on a real project of such importance at present as it is the study of iron-ion batteries. I also express special appreciation for all his help during the difficulties encountered when assembling the batteries.

Furthermore, I would like to thank Staff Engineer Hilde Kløften Duesund and Gerard Virgili Ayuso for practical guidance regarding instrumentation and general advice and support throughout the project.

Finally, a special thanks to Liyuan Li and Huishuang Zhao for the aid and broad knowledge provided in the study of iron-ion batteries and ionic liquids, respectively.

Bergen, 29th May 2020

Carmen Bolufer Cruañes

Abbreviations

Abbreviation	Definition
ILs	Ionic Liquids
LIBs	Lithium-ion Batteries
Li	Lithium
Na	Sodium
Mg	Magnesium
Fe	Iron
SEI	Solid Electrolyte Interphase
PILs	Polymer Ionic Liquids
Al	Aluminium
Bmim	1-Butyl-3-methylimidazolium
DMC	Dimethyl Carbonate
EC	Ethylene Carbonate
Li-S	Lithium-Sulphur
Li-O_2/air	Lithium-Oxygen/air
NIBs	Sodium-ion Batteries
EDLCs	Electric Double-Layer Capacitors
EVs	Electric Vehicles
AmimCl	1-Ally-3-methylimidazolium Chloride
DEC	Diethyl Carbonate
BF_4^-	Tetrafluoroborate
TFSI-	Bis(trifluoromethanesulfonyl)imide
FSI-	Bis(fluorosulfonyl)imide
SEI	Solid Electrolyte Interphase
PP13TFSI	N-methyl-N-propylpiperidinium bis(trifluoromethanesulfonyl)imide
TEMPOImIL	2,2,6,6-Tetramethyl-1-piperidinyloxy
RTILs	Room Temperature Ionic Liquids
TPGS-S	Surface Modified Sepiolite

LiTFSI	Lithium bis(trifluoromethanesulfonyl)imide
PYR14TFSI	1-Butyl-1-methylpyrrolidinium bis(trifluoromethanesulfonyl)imide
KSFA	Potassium bis(fluorosulfonyl)amide
PYR13FSA	1-Methyl-1-propylpyrrolidinium bis(trifluoromethanesulfonyl)amide
KTFSA	Potassium bis(trifluoromethanesulfonyl)amide
PYR14TFSA	1-Butyl-1-methylpyrrolidinium bis(trifluoromethanesulfonyl)amide
PYR13TFSA	1-Propyl-1-methylpyrrolidinium bis(trifluoromethanesulfonyl)amide
C_1C_2ImTFSI	1-Ethyl-2-methylimidazolium bis(trifluoromethanesulfonyl)imide
[PYR14]TfO	1-Butyl-1-methylpyrrolidinium trifluoromethylsulphonate
[EMIm]TfO	1-Ethyl-3-methylimidazolium trifluoromethylsulfonate
PYR13Cl	1-Methyl-1-propylpyrrolidinium chloride
EMIC-$AlCl_3$	1-Ethyl-3-methylimidazolium chloride
CV	Cyclic voltammetry
WE	Working Electrode
CE	Counter Electrode
RE	Reference Electrode
GHS	Globally Harmonized System for the Classification and Labelling of Chemicals
BmimCl	1-Butyl-3-methylimidazolium Chloride
$FeCl_3 \cdot 6\ H_2O$	Iron (III) chloride hexahydrate
$BmimFeCl_4$	1-Butyl-3-methylimidazolium tetrachloroferrate
$FePO_4$	Ferric phosphate
$Fe(CH_3COO)_3$	Iron (III) acetate
EC+DMC	Refers to the solution based on a ratio 1:1
Ni	Nickel
Cu	Copper

Abstract

Nowadays, rechargeable lithium-ion batteries are the energy storage devices most used. However, they have many disadvantages, including high cost, low security, and a shortage of lithium on earth in the near future. Consequently, an alternative option is needed. Iron-ion batteries are a new type of battery that have been recently introduced into the field of research and they seem to be a good option. Therefore, this thesis aims to improve the rechargeable iron-ion battery's properties in order to study its feasibility as a substitute for current batteries.

Using an ionic liquid electrolyte in the fabrication of iron-ion batteries is investigated. Ionic liquids are types of salts which are regarded as environmentally friendly solvents. In addition, ionic liquids have many advantages, including near zero vapor pressure, low flammability, and good ionic conductivity.

In this thesis, various electrolytes are prepared by mixing various concentration of ionic liquids in organic solvents. Physical properties, including density, viscosity and ionic conductivity are investigated and compared to obtain the optimal solution. Subsequently, these electrolytes are utilized to fabricate iron-ion battery. The performance of the batteries is investigated. Batteries are tested with various methods using Battery Testing System in order to obtain charge and discharge performance of batteries.

Keywords: Ionic liquids; electrolyte; iron-ion batteries; renewable energy; energy technology.

Sammendrag

I dag er oppladbare litium-ion-batterier de energilagringsenhetene som brukes mest. Litium-ion-batterier har flere ulemper som høye kostnader, lav sikkerhet og på lang sikt vil det bli mangel på litium. Det er dermed nødvendig med et alternativ som kan erstatte litium-ion-batteriene. Jern-ion-batterier er en ny type batteri som nylig har blitt introdusert i forskningsfeltet, og ser ut til å være et godt alternativ. Derfor har denne avhandlingen som mål å forbedre det oppladbare jern-ion-batteriets egenskaper for å studere muligheten til at det kan erstatte nåværende batterier.

Tilsetning av ioniske væsker i elektrolytten av jern-ion-batterier er foreslått. Ioniske væsker er typer salter som blir sett på som grønne løsningsmidler siden de ikke er skadelige for miljøet. Ioniske væsker har også flere fordeler, som lavt damptrykk, lav brennbarhet og god ionisk ledningsevne.

I denne avhandlingen blir forskjellige elektrolytter fremstilt ved å blande forskjellige mengder av ulike ioniske væsker og organiske løsningsmidler. De fysiske egenskapene som tetthet, viskositet og ionisk konduktivitet blir studert og sammenlignet for å finne den optimale løsningen. Deretter blir disse elektrolyttene introdusert hver og en i ett jern-ion-batteri for å se hvordan batteriet fungerer. Hvert batteri testes med forskjellige metoder i Landt Battery Testing System for å sammenligne hvordan parameterne endres når det gjelder elektrolytten som er tilsatt og metoden som brukes til å lade og utlade batteriet.

Nøkkelord: ioniske væsker; elektrolytt; jern-ion-batterier; fornybar energi; energiteknologi.

Contents

1. Introduction

1.1.Background

Due to the growing environmental pollution and shortage of fossil fuels, electrical energy storage devices such as batteries have attracted ever-increasing attention from all over the world. Lithium-ion batteries (LIBs) have improved significantly and dominated the mobile market over the last decade owing to their advantages in terms of high energy density and long cycle life. (1) However, lithium (Li) based batteries have many drawbacks such as low safety, high cost and a shortage of Li on the earth's crust in the near future. The latter is the main reason why many researchers have kept studying batteries in order to try to replace Li by another material with similar properties, for example, sodium (Na), magnesium (Mg) or iron (Fe). Amongst all of them, Fe is the cheapest one. Furthermore, Fe is the most abundant element in the universe and the second most abundant metal in the earth. Thus, there is a lot of Fe in the natural world which could be used for as long as ca. 1 million years for manufacturing Fe-ion batteries. (2)

Conventional batteries normally use a liquid electrolyte which helps the ions transportation. Nevertheless, there is a chance of leakage of the electrolyte and therefore safety issues. So far, liquid electrolytes in Li-ion batteries use a Li salt in organic solvents. However, organic solvents have many disadvantages such as their easy decomposition, volatility and flammability. In addition, they are not benign for the environment. In consequence, a lot of research has been done in order to replace the use of organic solvents as electrolytes and to counteract their drawbacks. Hereupon, ionic liquids (ILs) resulted as being a good solution as electrolytes or additives for the batteries. (3)

ILs, or room temperature molten salts, composed of large organic cations and organic/inorganic anions, have melting point lower than 100 ℃ in liquid state. (4) They have several unique character such as low volatility, good thermal stability, high electrochemical stability, near zero vapor pressure, wide electrochemical window and other tuneable properties like polarity and solvent miscibility, etc. (5) These properties endowed ionic liquids more possibilities for electrochemical energy storage. Ionic liquids are usually used to modify electrolyte to improve the interfacial architectures and properties. (6)

1.2.Existing theory and knowledge in this field

Iron-ion battery is a new type of battery trying to replace the lithium-ion one. The first patent for a rechargeable iron-iron battery dates from July 2018 in Norway. (2) In later years, a lot of research has been done in the field of batteries in order to achieve a new type of battery which can overcome all the disadvantages that the lithium-ion battery has. However, few studies have been focused on the research of the iron-ion battery.

Furthermore, ILs are rather new in the battery technology developments and are currently being introduced to electrolyte solutions on an attempt to improve the battery performance. There are a large number of ILs since these can be made using different cations and anions. Nevertheless, it would be impossible to synthesize each different type of IL and test it. This is the reason why each group of research tries to focus their study on a group of ILs. Moreover, ILs are often mixed with other solvents to counteract the properties such as the high viscosity. Some of the most important studies regarding ILs are reviewed in section "2.4. Current development in ILs and batteries" in this thesis. However, it should be noted that none of the studies showed in this section are implemented on iron-ion batteries.

In recent years, some studies have focused on ILs based on imidazolium cation. Additionally, certain of them have focused on the IL containing 1-butyl-3-methylimidazolium (Bmim). Nevertheless, very little research has been done so far in the study of the IL $BmimFeCl_4$ which is the one this thesis focuses on. Hence, it can be stated that it is a present-day topic where the existing theory has to be extrapolated to the new field of the iron-ion batteries.

1.3. Problem description and goal

The research on iron-ion batteries is very new and there is not much data available. However, iron-ion batteries have a lot of advantages with regard to the lithium ones. Therefore, a thorough study of the iron-ion batteries trying to maximize their performance is needed. The electrolyte of a battery plays an important role in its working operation. Thus, finding a suitable electrolyte for an iron-ion battery is required. Due to the major advantages that ILs have, their addition in the electrolytes for iron-ion batteries could considerably enhance their efficiency. If this is achieved, iron-ion batteries could replace the market of lithium ones in a near future, thereby providing further benefits.

The goal of this thesis is to find an electrolyte containing an IL which maximizes the performance of an iron-ion battery. Different ILs will be prepared and tested as an electrolyte. In addition, the ILs will be mixed with other solvents such as DMC and EC in order to see how this can affect the electrolyte properties, and consequently, the battery performance. All the solutions will be studied to determine their physical properties as their density, viscosity, and conductivity. A deep study of the latter properties will be done in an attempt to find the optimal electrolyte which has high density, low viscosity and high ionic conductivity.

Furthermore, to study the charge-discharge speed, the specific capacity and the efficiency of the battery, the electrolyte will be added in an iron-ion battery and it will be tested on a charge/discharge battery testing system and in a cyclic voltammetry test. By interpreting all this data, it will be easy to understand which IL solution is more suitable to use as an electrolyte for an iron-ion battery.

2. Theory

2.1. What is an ionic liquid?

ILs are low-temperature molten salts that consist of a cation and an anion which can delocalize the negative charge. They have peculiar physicochemical properties such as a melting point lower than 100 ℃, near zero vapor pressure, low viscosity, good thermal stability, high electrochemical stability, wide electrochemical window and other tuneable properties as solubility and polarity. That's why ILs are seen as green solvents suitable to replace the commonly used volatile organic solvents. (7)

In addition, ILs can be synthesized in many ways depending on particular features for a specific application. ILs are a combination of organic cations (typically imidazolium, pyridinium and pyrrolidinium) and organic or inorganic anions (for instance Cl^-, NO_3^-, COO^- or BF_4^-). In *Figure 1* and *Figure 2* it can be seen some of the cations and anions that are often utilized to synthesize an ionic liquid, respectively.

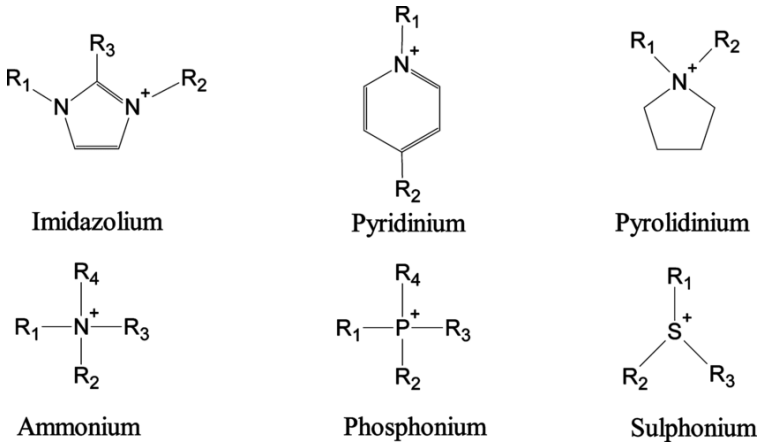

Figure 1. Cations of six families of ionic liquids.

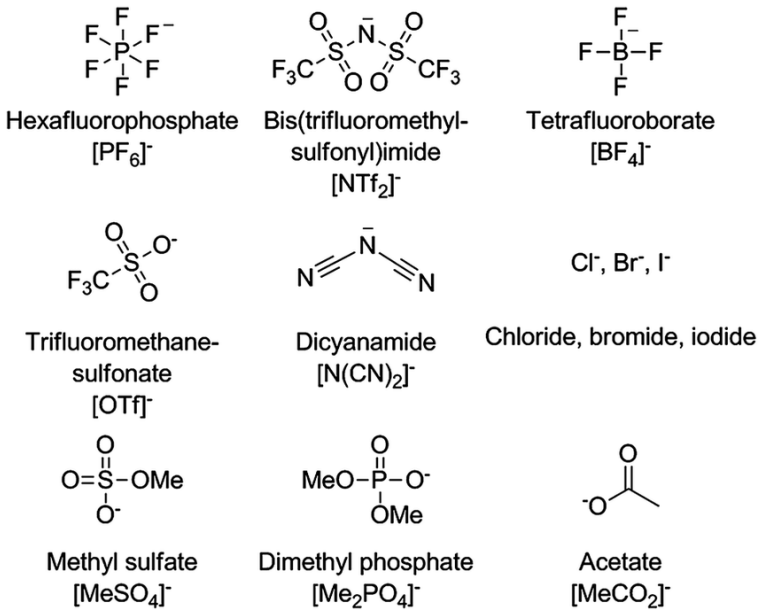

Figure 2. Some common anions used in ionic liquids and their abbreviations.

The first IL found in the literature dates from 1914 when Paul Walden synthesized the ethylammonium nitrate. However, ILs have gained attention since the past two decades. Thus, a few papers were written before 1996 in comparison with the >5000 at present. A multidisciplinary research is being done on ILs to use in chemistry, materials science, chemical engineering and environmental engineering amongst all the fields. In fact, ILs can be utilized in many different applications as they can designed combining cations and anions to meet the requirements needed for a specific process. (8)

ILs are considered green solvents because of the following characteristics:

- ILs have very low vapour pressure (near-zero) at ambient conditions and that is the reason why they are non-volatile compounds.
- They have a wide liquid range of temperature and therefore they remain in liquid state.
- ILs can be tuned to have a specific acidity or basicity.
- They have very low viscosity.
- ILs are perfect lubricants and have excellent hydraulic properties.
- They can be tuned to be hydrophobic or hydrophilic.
- ILs have high thermal stability and are non-flammable.
- ILs have a wide electrochemical window.
- They are soluble in a wide range of conditions due to their tuneable combination of anions and cations.

- ILs can take in and release gases.
- They have microwave absorbing characteristics. (7) (9)

2.2. Physical Properties

In this thesis, several physical properties of the pure ILs and different solutions of ILs have been measured to determine how beneficial they will be as an electrolyte in the application of battery technology. These properties and their purpose will be further explained below.

- Density:

Density is a measurement of the mass per unit of volume. The most common units for density are g/cm^3 or specific gravity, which is dimensionless. However, the modern SI units of kg/m^3 are increasingly common. (10)

$$\rho = \frac{m}{V}$$

Where ρ is density, m is mass and V is volume.

This parameter not only can give information about the floatability of a compound when is in contact with another material, but it can also show how much space it will take in a specific volume. (11) The latter information is of interest in our thesis as we want to have a high density ionic liquid in order that the electrolyte takes less space with the same mass.

In order to use the density of the different samples in this thesis, a densimeter similar as DMA 5000 M provided by Anton Paar Products shown in *Figure 3* has been utilized. (12)

Figure 3. Densimeter DMA 5000 M. (12)

- Viscosity:

Viscosity is the ratio of the shearing stress to the velocity gradient in a fluid and it is calculated as showed in the following equation.

$$\eta = \frac{F/A}{dv_x/d_z}$$

Where η is viscosity, F/A is the shearing stress and dv_x/d_z is the velocity gradient.

The SI unit of viscosity is the pascal second (Pa s). Nevertheless, this unit is rarely used in the scientific field and instead it is used the unit poise (P). The name poise was given by Jean Poiseuille (1799-1869) to represent the dyne second per square centimetre (dyne s/cm^2). The ratio to convert poise to pascal second is 10:1. (13)

There are two types of viscosity: dynamic viscosity and cinematic viscosity. Dynamic viscosity it is also named absolute viscosity, though it is normally just called viscosity. This one is represented and defined as mentioned above and informally characterizes a fluid's resistance to flow. On the other hand, kinematic viscosity is the viscosity of a fluid divided by its density as represented below.

$$\nu = \frac{\eta}{\rho}$$

Where ν is kinematic viscosity, η is dynamic viscosity and ρ is density.

This property measures the resistive flow of a fluid under the influence of the gravity.

The SI unit of kinematic viscosity is the square meter per second (m^2/s) although the common unit is the square centimetre per second (cm^2/s) named as stoke (St) by the mathematician and physicist George Stokes (1819-1903). (14)

In this thesis the viscosity of different percentages of IL in solvents will be measured utilising a machine similar to the Rolling-ball viscometer Lovis 2000 M/ME provided by Anton Paar Products shown in *Figure 4*. (15)

Figure 4. Rolling-ball viscometer Lovis 2000 M/ME. (15)

This apparatus measures both dynamic and kinematic viscosity. However, only dynamic viscosity results will be shown as the most important property is having a low viscosity for faster transportation of ions in the liquid.

- Conductivity:

Electrical conductivity is the current, in other words the movement of charge, due to the presence of an electric field. Consequently, ionic conductivity is the movement of ions from one part to another through defects of the crystal lattice of a solid or aqueous solution. The ionic conductivity is often represented by the Greek letter σ and the following equation shows its calculation. (16)

$$\sigma = q \cdot n \cdot b$$

Where q is the carrier charge, n is the concentration of the sample and b is the mobility of ions in response to an electric field.

The conductivity of the different samples of electrolytes will be measured with the conductivity meter Mettler Toledo Seven Compact S230 shown in *Figure 5*. (17)

Figure 5. Seven Compact S230 Conductivity meter by Mettler Toledo. (17)

The ionic conductivity of an electrolyte gives information of how fast and easy the ions can move through the aqueous solution. Consequently, it can be known how long a cell will take to be charged or discharged. (18) Additionally, it is usually claimed that the lower viscosity a solution has, the higher conductivity will present since ions can move easily.

2.3.Battery working principles

There is a wide variety of batteries that have been studied. Nonetheless, most of them follow the same working principle. A battery is a device where it can be stored electrical energy due to the electrochemical reactions that take place. To understand the performance of a battery it is important firstly to know the three main components of it: the anode, the cathode and the electrolyte. The negative electrode is the anode and it is made with a different material from the positive electrode, in other words the cathode. Between anode and cathode there is a separator immersed in an electrolyte solution that allows ions to pass through it. In addition, the anode and the cathode are connected to an external circuit that allows the circulation of electrons. (19)

During the discharge process the positive ions flow from the anode to the cathode through the electrolyte. Conversely, the negative ions move in the opposite way. A cell voltage appears since the anode is accumulating negative charge and the cathode is accumulating positive charge. Hence, the electrons move through the external circuit from the anode to the cathode, and that is what creates an electric current in the contrary way. (20)

During the charging process, the reversed operation takes place. Therefore, an oxidation reaction occurs when the cathode's material liberates positive ions which flow through the electrolyte. Meanwhile, in the positive electrode a reduction reaction takes place as it consumes electrons by transferring positive ions from the electrolyte. (20)

The charging and discharging processes above explained can be schematically represented by *Figure 6.*

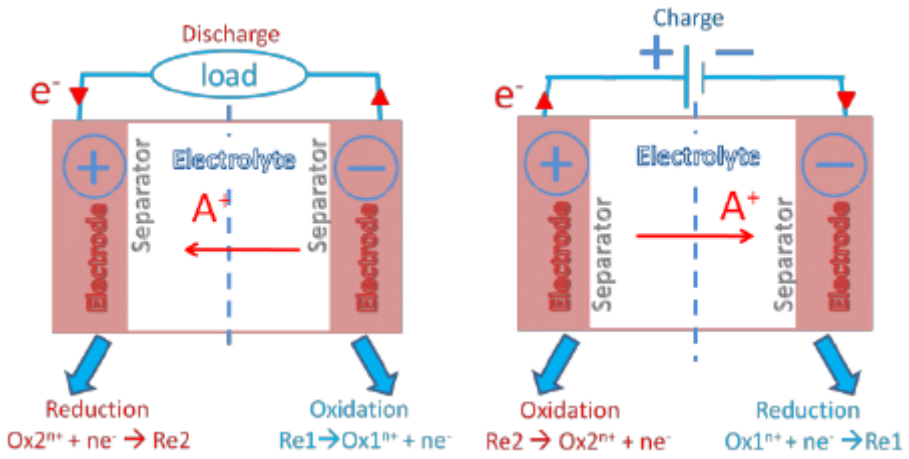

Figure 6. Charging and discharging processes in a usual battery. (21)

2.4. Current development in ILs and batteries

Due to the growing environment pollution and shortage of fossil fuels, electrical energy storage devices such as batteries and supercapacitors has attracted ever-increasing attention from all over the world. Lithium-ion batteries (LIBs) have improved significantly and dominated the mobile market over the last decade owing to their advantages in terms of high energy density, long cycle life and so on. However, researchers are still researching and designing more powerful Li-ion batteries to meet the requirements of different scenarios such as high/low temperature conditions, automotive, etc. Meanwhile, lithium-sulphur (Li-S) and lithium-oxygen/air (Li-O_2/air) batteries, employ lithium metal which is an attractive material attributed to it´s high theoretical energy density up to 2600 W h kg^{-1} as anodes, have also draw great attention in recent years. (22) Sulphur is a cathode material of Li-S batteries, undergoes a conversion reaction (S_8+16Li→8Li_2S) and has a high theoretical capacity of 1672 mAh g^{-1}. (23)-(30) Moreover, sulphur is naturally abundant, inexpensive and environment benign. Similarly, Oxygen/air is a cathode material of Li-O_2/air batteries which can perform a reversible electrochemical reaction with Li metal and it can be drawn directly from the ambient

atmosphere. (31) Besides, because of the lower cost and more abundant sources than Li, which can meet the requirements for large-scale energy storage systems, other type batteries such as sodium (Na)-ion batteries (NIBs) have received significant attention as well. (32)-(34) Recently, replacing the traditional liquid electrolytes with solid electrolytes have become a very active research, as all-solid-state batteries can both improve the electrochemical window and make the batteries safer. (35) (36) Supercapacitors are generally classified into pseudocapacitors and electric double-layer capacitors (EDLCs). (37) (38) They store the charge in a physical way without redox reaction heat, have high specific capacitance, high rate capacity for fast charging/discharging, long cycle life and they are safe, on account of which attracted many attentions. (39)-(42)

Despite of the charming prospect of the electrochemical energy storage, there are still many problems of different type of batteries and supercapacitors which limited them to achieve enhanced battery safety and improved electrochemical performance. Ionic liquids (ILs), or room temperature molten salts, composed of large organic cations and organic/inorganic anions, have melting point less than 100 ℃ in liquid state. (43) (44) (45) They have several unique properties, such as low volatility, good thermal stability (-81-280℃), high electrochemical stability, near zero vapor pressure, wide electrochemical window, and other tuneable properties like polarity and solvent miscibility, etc. (46) These properties endowed ionic liquids more possibilities for electrochemical energy storage to improve the properties in different ways. The composition and structure of electrode materials can be modified through ionic liquids to gain better electrochemical performance. And ionic liquids are also usually used as electrolyte directly or as electrolyte additive to improve safety greatly and enhance the interfacial architectures and properties. (47) Therefore, the application of ionic liquids in the electrochemical energy storage synthesize and design has been extensively studied.

2.4.1. Lithium-based batteries

2.4.1.1. Li-ion batteries

Li-ion batteries (LIBs) are nowadays the power source of choice for application and dominate energy storage devices market such as portable electronics and electric vehicles (EVs), which attributed to light weight, high energy, and good cycle life. Despite this, to adapt the market demand, higher energy density, more stable electrochemical properties

and safer LIBs need to be improved as soon as possible. State-of-the-art LIBs typically consisting of a metal oxides cathode, a graphite anode, and an organic electrolyte.

IL-assisted synthesis of electrode materials have received widespread interest, which benefit superior properties of ILs to optimize chemical particle, architecture, composition and so on. IL as reaction medium to synthesize carbon-metal-oxide nanocomposites is helpful to restrict the particle size and intimate coupled interface. Cheng et al. reported TiO_2-carbon hybrid nanostructures through simple one-step IL-assisted approach which employ an IL (1-ally-3-methylimidazolium chloride, AmimCl) as reaction medium. (48) The IL AmimCl can recover the graphitic structure of carbon without extra reducing agent. What's more, the direct growth of TiO_2 on CNTs or graphene shows more open porous and robust structures than pure TiO_2 nanoparticles because of the incorporation of carbon supports, which ensure the strong coupling between TiO_2 nanoparticles and carbon support. As a result, the TiO_2-carbon hybrid nanocomposites exhibited high specific capacity, long cycle life and superior rate capability for lithium-ion batteries.

Attributed to the unique properties of ILs such as wide electrochemical windows, stable thermodynamic properties and low vapor pressures, electrodeposition to synthesis nanostructured materials from ILs has also been extensively studied. (49)-(51) Recently, Liu et al. designed a Ge-coated 3D porous carbon (3D-Void/Ge@C) via ionic liquid electrodeposition approach. (51) Ge nanoparticles were electrodeposition from 0.1mol/L $GeCl_4$/[EMIm]Tf_2N ionic liquid system. After that, the samples were annealed at low temperature (600 °C) (*Figure 7*). By a 3D micro-nano void structure and porous carbon layer networks, the volume changes can be suppressed significantly and ensure the contact areas between the electrode and electrolyte. The obtained electrode displayed a discharge specific capacity more than 990 mAh g^{-1} after 100 cycles at 0.1A g^{-1} and superior rate performance.

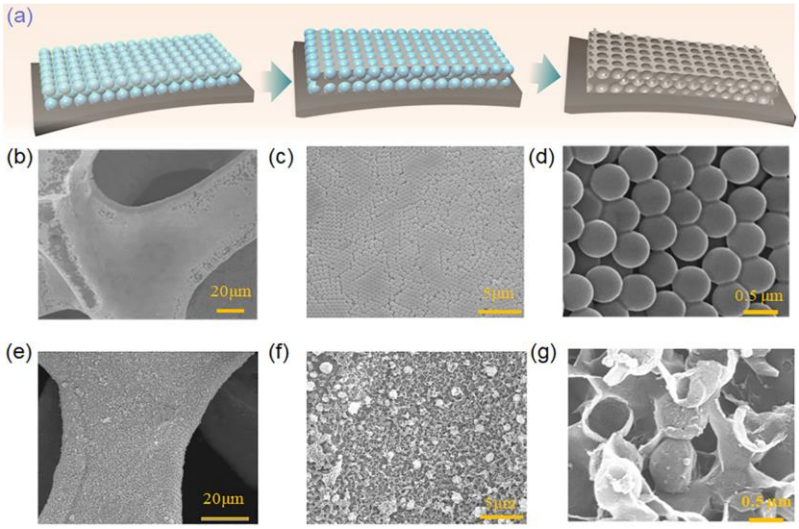

Figure 7. (a) A schematic illustration of the preparation for 3D-Void/Ge@C; (b–d) SEM images of the 3D-Void/Ge@C sample; (e, f) TEM images of the 3D-Void/Ge@C sample. (51)

As one of the most components of electrode, electrolyte has the function of ionic conduction and electron insulation which determines the properties of cells in stability, safety, cycle life and so on. (46) The commercial electrolytes are mostly based on organic carbonates such as ethylene carbonate (EC) and diethyl carbonate (DEC), yet the issues especially, safety problems, are making people looking for alternatives urgently. The non-flammability, ultralow vapor pressure, chemical and electrochemical stability, and non-toxicity of ionic liquids made it a promising candidate of electrolyte and additives, especially at high voltage and high temperature. Imidazolium, pyrrolidinium, pyridinium, piperidinium and quaternary ammonium have been the most used cations of ionic liquid electrolyte. Tetrafluoroborate (BF_4^-), bis(trifluoromethansulfonyl)imide (TFSI-) and bis(fluorosulfonyl)imide (FSI-) have been the most investigated anions. Through designing the chemical structures of ionic liquids and employing them as electrolytes and additives, have positive effect on the LIBs. Sun et al. designed a series of ionic liquids, a bicyclic imidazolium ionic liquid [ETMIm][TFSI], and reference ionic liquids [EMIm][TFSI], [DMBIm][TFSI] were act as solvent for LIBs (Figure 1). (52) The special chemical structure of bicyclic [ETMIm][TFSI] displays relatively stable SEI formation ability on the surface of graphite anodes and exhibits reversible capacity of 330mA h g^{-1} and 250 mA h g^{-1} even at 50 ℃. Cao et al. selected two LiTFSI/pyrrolidinium bis(tri fluoromethane sulfonyl)imide RTIL based electrolytes, PyrTFSI and MMMPyrTFSI, in high-voltage $LiNi_{0.5}Mn_{1.5}O_4$(LNMO)/$Li_4Ti_5O_{12}$(LTO) (*Figure 8*). (53) The traditional electrolytes show severe decomposition and side reactions take place at 60ºC ascribe to

the unstable of traditional solvent-based electrolytes. In contrast, the electrode used PyrTFSI and MMMPyrTFSI based electrolytes which exhibits higher lithium utilization, higher specific capacity and better capacity retention at even 60ºC.

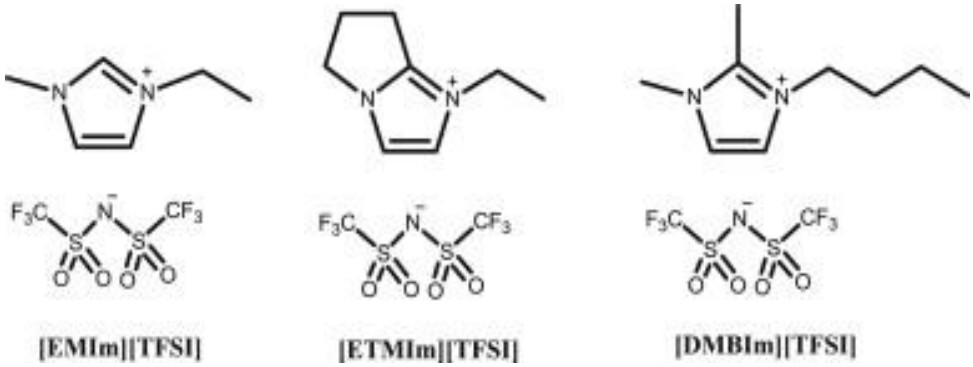

Figure 8. Structures of ionic liquids [ETMIm][TFSI], [EMIm][TFSI] and [DMBIm][TFSI]. (52)

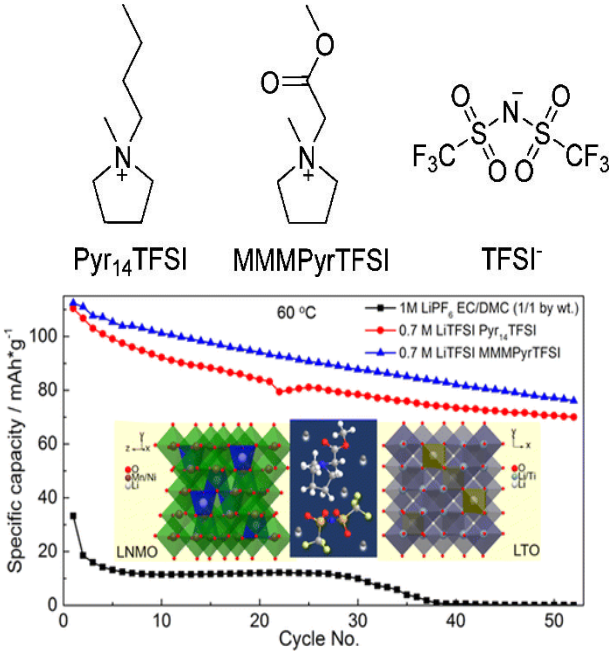

Figure 9. Left: Chemical structures of the selected TFSI–-based ionic liquids and the TFSI– anion. Right: cycle performance at 60 °C at 0.5C after 2 formation cycles at 0.2C of LNMO/LTO full cells. (53)

2.4.1.2. Li-S batteries

Li-S battery act as a promising candidate for energy storage, employs sulphur as cathode and lithium metal as anode, possesses higher theoretical capacity and energy than Li-ion battery, and it has several attractive advantages such as high energy density, low cost, environment friendliness. (54) However, there are still many challenges such as the low conductivity of sulphur and lithium sulphide, shuttle effect of polysulfides, the

non/uniform solid electrolyte interphase (SEI) of lithium metal anode and the lithium dendrite growth impede Li-S battery from practical applications. (23) The performance of Li−S batteries continues to suffer from low Coulombic efficiency and capacity fade because of the low utilization of elemental sulphur which arises from the dissolution of Li_2Sm when the system is in conjunction with a nonaqueous liquid electrolyte.

Researchers use IL to solve these problems in different ways. ILs are most commonly used to modify electrolyte to improve the interfacial architectures and properties. The formation of a passivation layer on the Li metal anode using ether-based mixture electrolyte containing $LiNO_3$ as an additive is a widely utilized way, can lead slower diffusion speed of polysulfides and less polysulfide dissolution. Wang et al. reported an effective approach to solve the self-discharge of Li-S battery via optimizing a room temperature IL of N-methyl-N-propylpiperidinium bis(trifluoromethanesulfonyl)imide (PP13TFSI)-based electrolytes with the $LiNO_3$ additive. (55) They found the PP13TFSI is beneficial to hinder the solubility and mobility of Li_2S_x (*Figure 10*). Moreover, when working with $LiNO_3$ additive, Li-S battery exhibits even better zero self-discharge. In addition, simply hybrid ILs with commonly used liquid electrolytes is an effective method. Shruti et al. systematically investigated the role of different cations of ILs through hybrid these cations with commonly used liquid electrolytes as electrolyte. They consider that the MPP-4 hybrid electrolyte can suppress the dendrite formation, polysulfide shuttling and SEI growth effectively, and thus exhibited an improved cycling performance. (24)

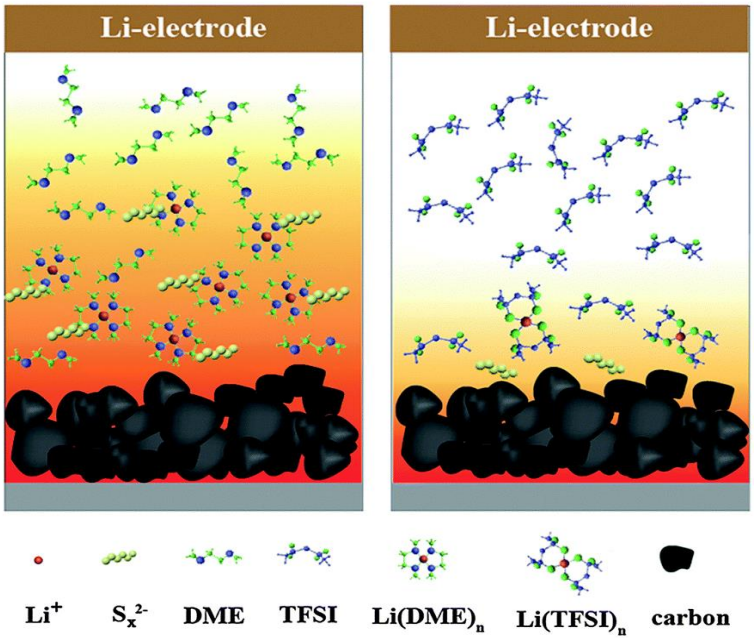

Figure 10. Schematic illustration of the function mechanism of polysulfide dissolution and diffusion in ether (left) or PP13TFSI-based (right) solvent. (55)

Modification of sulphur cathodes with polymer coating is also an effective way. Suo et al. employ a novel high fluid IL (1-Ethyl-3-methylimidazolium dicyanamide) as a carbon precursor to coat a dense carbon cage on Li_2S nanoclusters uniformly. (56) The electrode they designed shows higher Li_2S utilization and low charge transfer. What's more, ionic liquid carbon precursor is beneficial to improve the stability of electrode for long term cycling through entangle the lithium polysulfide within the carbon cage. At the same time, a high capacity of 826 mAh g^{-1} at 0.1C and high capacity retention of 82% at 1C.

Attributed to the volume changes (80%) that occurs when Li_2S is formed, designing an ionic liquid polymer as binder for sulphur cathode has also been explored. Alen et al. investigated five different polymer ionic liquids (PILs) which have different chemical structure and polymer backbones, and they were used as sulphur cathode binders. (26)

2.4.1.3. Li-O_2/air batteries

Lithium oxygen (Li-O_2) batteries combining the advantage of lithium metal (light weight) and oxygen (natural abundance) as the active materials, possesses the superhigh theoretical energy density of (>3400 Wh kg^{-1}) among all possible battery technologies. (40) (57)-(63) However, the practical realization of lithium-oxygen batteries has been limited due to the high overpotential, low energy efficiency, the degradation of electrolyte and insufficient reversibility of the electrochemical reaction ($2Li + O_2 \rightarrow Li_2O_2$). (64)

To solve the problems above-mentioned, many attempts were made. Early as 2011, Mizuno et al. reported that a PP13TFSA-based ionic liquid shows improved cycle performance at 60ºC which attributed to the O_2 radical stability of ionic liquid-based electrolyte. (65) Asadi et al. reported a lithium oxygen battery system using an ionic liquid-based $EMMIBF_4$/DMSO (25%/75%) electrolyte. (66) The mixed ionic liquid electrolyte offers the maximum oxygen reduction and evolution in a three-electrode cell. They also use an initio molecular dynamics simulations to better understand the relationship between CO_2 and water molecules on a Li_2O_2 surface in the $EMMIBF_4$/DMSO electrolytes (*Figure 11*). The results exhibit that the electrolyte/Li_2O_2 interface shows no specific preference for CO_2 or water to adsorb on the Li_2O_2 surface or electrolytes.

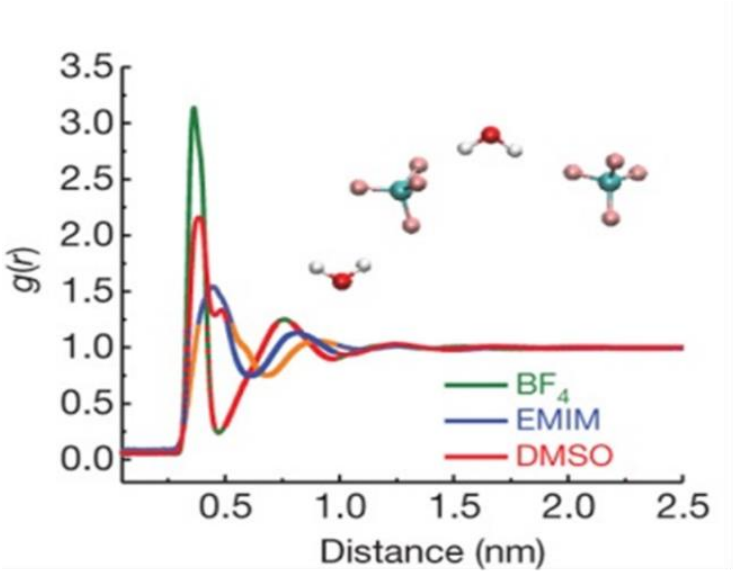

Figure 11. Classical molecular dynamics radial distribution function showing the interaction of water with $BF4^-$, $EMIM^+$ and DMSO, calculated from the trajectory of a system at 2 mol% water. (66)

Appropriate redox mediators, which is a soluble electrocatalysts, are applied to facilitate the oxidation of Li_2O_2 upon charging, reduce the overvoltage of oxygen reduction and evolution, and hence improve the energy efficiency and stability of Li-O_2 batteries. (67) Nevertheless, its addition may cause various side reactions such as shuttle reactions and detrimental interaction with the Li-metal anodes. (63) Zhang et al. reported an ionic liquid containing the redox active 2,2,6,6-tetramethyl-1-piperidinyloxy moiety (TEMPOImIL) which exhibited highly reversible redox reactions at 3.0V and 3.75V, and served as redox mediator, oxygen shuttle and lithium anode protector (*Figure 12*). (68) In the meantime, the TEMPOImIL is beneficial to facilitate the formation of a stable SEI to decrease the side reactions and promotes the smooth lithium plating/stripping on the anode. As a result, the cycle life was improved to more than 200 cycles. Subsequently, they synthesized two families of new TEMPOImILs and found that when n=4, 5; R=H, the TEMPOImILs show the most effective result in Li- O_2 batteries. (69)

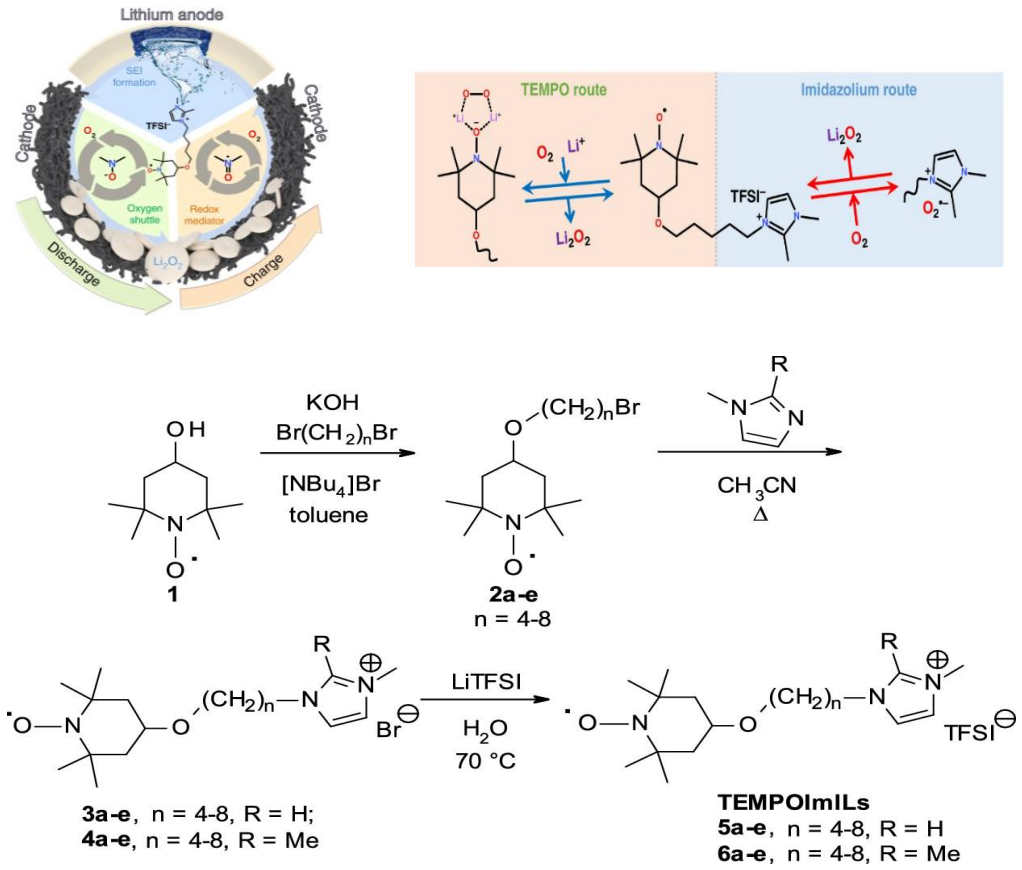

Figure 12. Left: Schematic illustration of the TEMPOImIL facilitating the performance of Li–O_2 batteries. Right: The mechanism of the discharge facilitation using TEMPOImIL. Both routes involve the formation of intermediates with the oxygen species. (68) Upper: Synthesis of two families of TEMPOImILs. (69)

2.4.2. Sodium-based batteries

Due to the increasing energy demand, it is necessary to develop new storage technologies and materials that are suitable for high performance devices which are truly sustainable. Within the last two decades, rechargeable batteries have proven to be an important tool in the modern society – and in particular lithium-ion batteries. (70) Even though lithium-ion batteries have been the most utilized battery in the market the last decades, they still have their downsides. From the perspective of availability and cost, and the overall energy demand, lithium-ion batteries might not be the best solution. One foreseen sustainable and low-cost alternative could be sodium-ion batteries. Sodium-ion batteries are a promising candidate to lithium-ion batteries because of its many similar alkali metal chemistries of lithium. (71) This means that sodium-ion batteries have the same working principle and cell construction as lithium-ion batteries, but instead of

lithium compounds they utilize sodium compounds. The similar working principles makes it possible for sodium-ion batteries to replace the lithium-ion batteries not only in terms of application, but also during the production process because of the same manufacturing protocols. (71) It will therefore be inexpensive to replace lithium with sodium when it comes to developing the batteries.

Not only is sodium inexpensive, it is also much more abundant than lithium. Sodium is widely distributed in the earth and can be found in numerous minerals as well as in rather high concentrations in the ocean. (70) The cost of developing a sodium-ion battery is therefore very low if the cathode and anode is based on earth-abundant elements as well.

In order for a sodium-ion battery to obtain the best performance, it has to contain the right combination of electrodes and electrolytes. The difference between the majority of the sodium-ion electrolytes properties from the lithium-ion batteries electrolytes is the difference in cation sizes, affection ion solvation and transport. The electrolyte is an important component in all sodium-ion batteries, and it plays a critical role in balancing and transferring ions between the electrodes. It is necessary to design appropriate electrolyte compositions to minimize harmful interface side reactions and improve the electrochemical performance and safety for sodium-ion batteries. (70) Sodium-based electrolytes can be based on solutions of salts in mixtures of organic solvents, polymers or ionic liquids. IL have many properties of interest for safer and in some cases environmentally friendly batteries, such as non-volatility and non-flammability. As electrolytes, ammonium-based ILs attract a wide range attention and extensive research for many researches. (71)

2.4.3. Solid-state batteries

Due to the challenges faced by modern storage systems, mainly Li-ion batteries, solid-state batteries are being deeply studied. Conventional batteries normally use a liquid electrolyte which helps the ions transportation. Nevertheless, there is a chance of leakage of the electrolyte and therefore safety issues. Another important drawback of the generalised Li-ion battery is the formation of dendrites of Li which make it prone to explosion. Loss of battery quality after several cycles and dissolution of the electrolyte are others important concerns to overcome. In order to solve these problems, the main principle of solid-state batteries has been studied. This is, using a solid electrolyte

between electrodes. This type of battery is advantageous not only because of the reduction in the net weight and volume of the battery, but also because it has an excellent energy output and greater efficiency due to the easy transfer of Li ions. The advantages lie in the very small self-discharge of the solid-state batteries, minimal wear and tear, and yield of a more uniform output voltage. However, solid-state batteries also have some drawbacks as their relatively lower power density, high ionic resistance at room temperature, and manufacturing cost. (72)

Thermal properties, chemical and electrochemical stabilities, and mechanical strength of solid-state electrolytes are in general better than those of liquid electrolytes. Figure 13 sums up the most benign characteristics that are required for a solid-state electrolyte. Solid-state electrolytes lead ions to a uniform electrodeposition that play a key role in stable cycling and high performance of the high-energy metal-based batteries. Therefore, replacing liquid electrolytes with a solid electrolyte can overcome the persistent problems of liquid electrolytes as well as offer possibilities for developing new battery architectures. However, more scientific research must be done in order to cope with the ionic conductivity, interfacial properties, mechanical strength and fabrication process. (73)

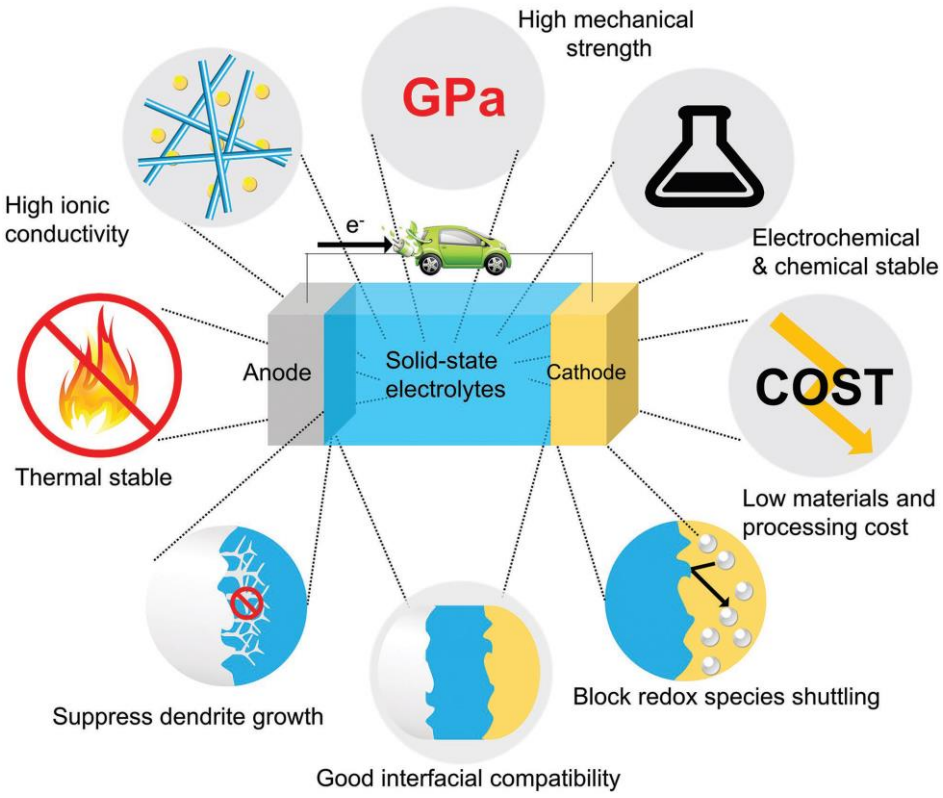

Figure 13. Specifications that should have a solid-state electrolyte. (73)

The major advantages that have attracted researchers to deeply study solid-state electrolytes are the safety, the durability, the energy density and the power density. (74)

On the one hand, the risk of explosion and fire in conventional batteries is a huge challenge. Thus, lithium-ion batteries use organic solvent electrolytes that may cause leakage issues, and therefore, serious safety concerns. Thereupon, using solid electrolytes which are non-flammable this hazardous problem can be defeated. (75)

On the other hand, the better durability of solid-state batteries can also be easily explained. The principal factor that affects batteries' lifetime is side reactions, for instance, electrolyte decomposition. While Li-ion batteries are prone to decompose the electrolyte chemically as they store high energy by combining highly oxidizing cathodes and highly reducing anodes, solid electrolytes supress side reactions. In the solid batteries only lithium ions are in movement, so no other compounds diffuse or undergo charge transfer at electrode surface. In consequence, solid-state electrolytes restrain side reactions, thus providing high durability. (75)

Apart from these benefits, using solid electrolytes have some possibilities to increase the energy densities as they allow us to use others electrode materials which increase the theoretical energy densities. In addition, the high density can be increased since solid-state batteries do not need as many safeguards as the liquid ones. Solid-state electrolytes can not only simplify the battery system, but they can also simplify the module structure in large battery systems. Hence, a serial connection is achievable in solid systems by stacking bipolar electrodes and electrolytes layers alternatively in a single battery case. This reduces the weight and volume of the battery cases to increase the gravimetric and volumetric energy density. (75)

Finally, solid-state electrolytes can achieve high power density if they have conductivities higher than 10^{-3} S cm^{-1}. Liquid electrolytes have diffusion limitation as there is an important concentration gradient in the electrolyte due to the transportation of both anions and lithium ions. Conversely, in solid-state batteries this phenomenon is unlikely to happen since only lithium ions are in movement. (75)

A solid-state battery has the same structure as a liquid electrolyte battery except from the type of electrolyte positioned between anode and cathode. It has been proved that replacing a liquid electrolyte by a solid one can improve the storage capacity and the battery is less hazardous and less flammable. Furthermore, solid-state electrolytes tend to

last longer and can operate within a larger temperature range, up to about 200 ºC. Despite this, some disadvantages must be faced such as the bad performance in low and ambient temperatures conditions and the lower current output. (72)

A lithium based solid state battery is made by an anode attached to copper foil, a cathode with high ionic conductivity and a solid electrolyte which must also have a high ionic conductivity and very low electronic conductivity. Both cathode and electrolyte should exhibit a high degree of chemical stability as they supply the necessary ions during the charging and discharging process. (72)

During the charging cycle, there is movement of the Li ions of the $LiCoO_2$ crystal toward the electrolyte interface. As a result, the Li ions cross over to the carbon layers in the anode through the electrolyte. During the discharging cycle, the reverse process takes place, and the Li ions travel via the electrolyte toward the $LiCoO_2$ particles. Figure 14 illustrates the charging and discharging process in a solid-state lithium battery. (72)

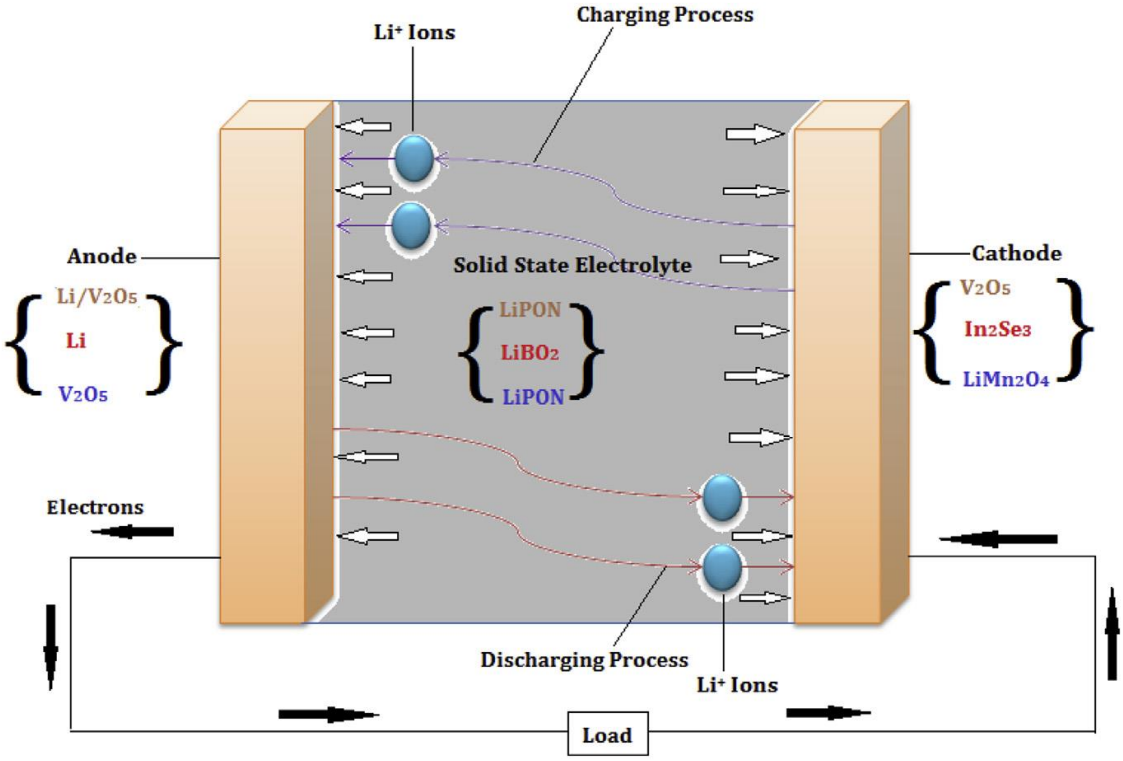

Figure 14. A schematic representation of a representative lithium based solid state battery, showing the direction of ion movement and some of the possible anode, electrolyte, and cathode combinations. (72)

Cathodes are usually made by lithium-based oxides as they are structurally stable during these processes and they also present a good ionic conductivity. Vanadium based

oxides have also been examined due to their similar layered structures that help during the lithiation/delithiation process. Nevertheless, they have some drawbacks as they produce low output voltages. Indeed, further research on the cathode materials is required in order to cope with the low capacity they perform in solid state batteries. (72)

Anodes must show great capacity to store Li/Li^+ because here is where the lithiation takes place during the charging process. Pure lithium metal, lithium-based metal oxides, graphite as well as carbon and carbon-based materials are commonly used in anode materials in solid state batteries. Soft carbon, metallic alloy-based and silicon- and carbon-based composite anodes have also been tested. All these materials have their pros and cons, however, in Figure 15 it can be seen the different solid-state battery systems with their application and respective capacities. (72)

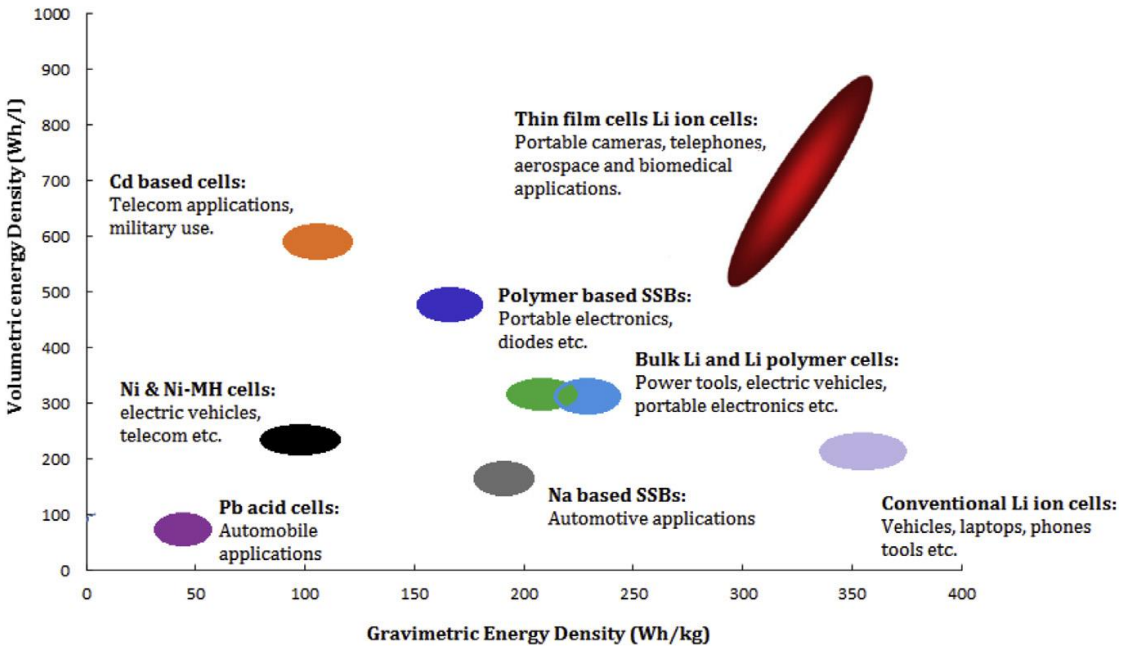

Figure 15. The capacities of different types of batteries and their respective applications. (72)

Figure 15 shows that thin film Li ion based on solid state batteries provide some of the best properties in terms of both gravimetric energy density and volumetric energy density.

It is difficult to find the desirable electrolyte that combines all the properties shown in Figure 13 and can maintain them after several cycles. However, solid-state electrolytes

could be a good solution. Comparing fundamental parameters of conventional liquid electrolytes and solid-state ones as shown in Figure 16, it can be stated that solid-state electrolytes have better mechanical and thermal stabilities. Moreover, they are electrochemically more stable. Other advantages of solid-state electrolytes are that they delay the electrode/electrolyte interfacial deformation and avoid the dendrite growth.

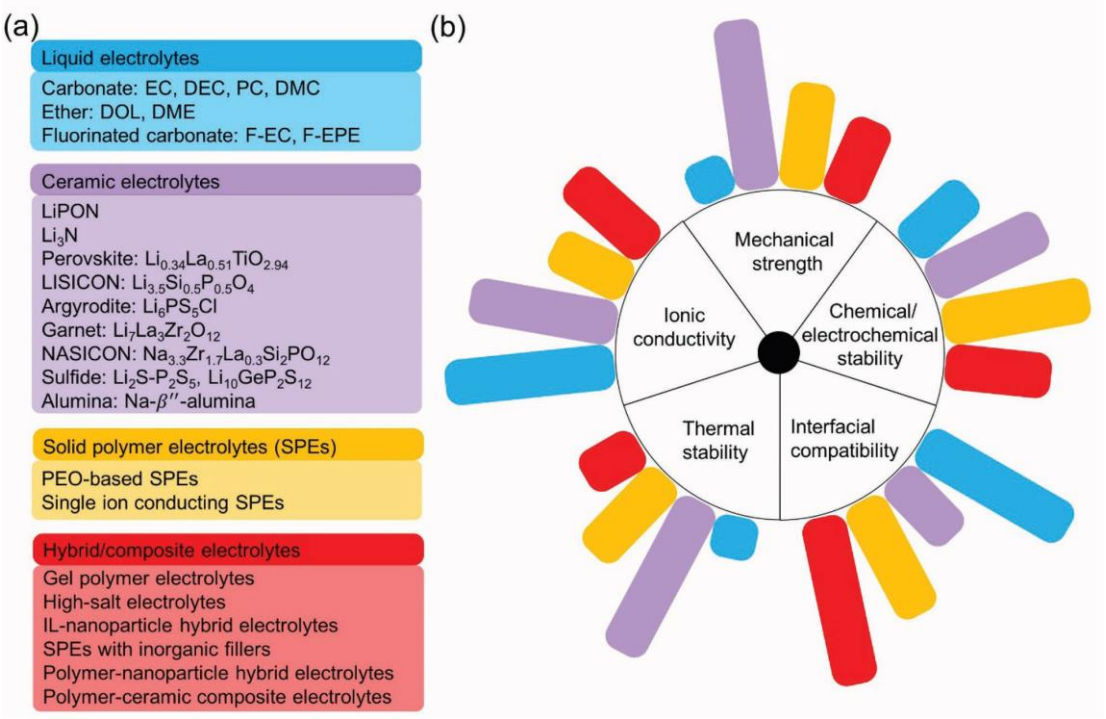

Figure 16. a) Summarization of common electrolyte systems for liquid, ceramic, solid polymer, and quasi-solid-state electrolytes. b) Different physical and electrochemical characteristics of liquid, ceramic, solid polymer, and hybrid/composite electrolytes. The height of the rectangle represents the capability of the performance. (73)

According to the chemical and physical properties, solid-state electrolytes can be divided into ceramic electrolytes, solid polymer electrolytes, and hybrid/composite electrolytes. Ceramic electrolytes own many attractive physical and electrochemical properties including high elastic modulus, high thermal stability, wide electrochemical stability windows, and favoured lithium-ion transference number. Nonetheless, they also have weak points: (1) some solid inorganic electrolytes can react directly with Li causing safety dangers; (2) numerous solid ceramic electrolytes present low chemical stability as they are not stable in contact with moisture and CO_2; (3) the high interfacial resistance between electrolyte and metal electrode due to their poor electrical contact; (4) the processing difficulties and high cost. (73)

Conversely, solid polymer electrolytes exhibit better flexibility to overcome the poor interfacial resistance and is more cost-effective compared with ceramic electrolytes. Despite this, the main drawback for solid polymer electrolytes is the poor ionic conductivity. In fact, the complexity of the polymer system and lack of simple structure-properties correlations prevent researchers from understanding the mechanism of ion transport. (73)

Due to the inconveniences that ceramic and polymers electrolytes must face hybrid or composite solid-state electrolytes are being studied in order to combine the advantages of ceramics, polymers and even liquids electrolytes.

Notwithstanding all the advantages that solid-state batteries can achieve in comparison with the liquid ones, poor ionic conductivity at room temperature and the decrease of mechanical properties at higher temperatures prevent their market entry. One approach is adding aprotic solvents, although this solution also leads to problems as a reaction with the lithium metal anode. Thereupon, this is where the introduction of ionic liquids comes into play. It has been stated that utilizing room temperature ionic liquids (RTILs) the long-term stability of the lithium metal electrodes can be enhanced. Moreover, when adding RTILs in the matrix/solid electrolyte the ions can move easily through a created path, hence improving the ionic conductivity. The solid electrolyte's wettability with the RTILs enhance the interfacial properties electrolyte/electrodes. (74) (75) However, it is highly important to study and select the proper RTIL for batteries. The reason is that when introducing an IL made of 1-ethyl-3-methylimidazolium cation certain characteristics may be appealing like the low viscosity, high ionic conductivity and wider electrochemical stability window, although the poor stability with a lithium metal electrode prevent its use in battery applications. (76) Conversely, ILs consisting of N-alkyl-N-methylpyrrolidinium cations show also an excellent ionic conductivity and a wide electrochemical stability window but no drawbacks. (77)

Shin J. et al studied the addition of N-methyl-N-propylpyrrolidinium bis/trifluoromethanesulfonyl)imide (PYR13TFSI) RTIL in a solid-sate Li/$LiFePO_4$ polymer electrolyte battery. The experiment was run at 40 ºC and some excellent results as an ionic conductivity of $6 \cdot 10^{-4}$ S cm^{-1} or a discharge capability at currents reaching 1.52 mA cm^{-2} were recorded. (74)

González F. et al. reported a thermoplastic polymer electrolyte containing polyethylene oxide, surface modified sepiolite (TPGS-S), lithium bis(trifluoromethanesulfonyl)imide (LiTFSI), and 1-Butyl-1-methylpyrrolidinium bis(trifluoromethanesulfonyl)imide (PYR14TFSI) with good properties. These included a conductivity of 0.5 $S \cdot cm^{-1}$ at 60 ºC, a stability up to 4.2 V vs Li/Li^{+} and a perfect compatibility with the electrodes during more than 1600 hours cycling under conditions such as 1 $mA \cdot cm^{-2}$ and 2 $mAh \cdot cm^{-2}$. However, it has a limit of 4.0 V. (75)

2.4.4. Beyond Li and Na batteries

2.4.4.1. Potassium batteries

Potassium ion batteries have gained more attention last years due to their low-cost, the abundance of potassium on earth's crust and the similar properties with lithium. In fact, the potassium is the 7th element most abundant on the earth's crust so it could be used for many applications during many years. Regarding its properties, it stands out potassium's low reduction potential (-2.93 V), being close to the lithium's one (-3.04 V) and even lower than sodium's reduction potential (-2.70 V). (78) Another important advantage is the better conductivity and quantity of solvated potassium ions than lithium and sodium ions. This is due to the weak Lewis acidity of potassium ion. Moreover, the chemical diffusion of potassium ions is higher than the lithium's one. (79)

Notwithstanding the advantages of potassium as a suitable material, further research must be done in order to understand the structural and electrochemical properties of possible electrodes for potassium ion batteries. This difficulty is due to the large radius of potassium ion (0.138 nm) that leads to a different performance during the charge/discharge process. (80) In addition, safe electrolytes still need to be studied because potassium is extremely active with oxygen and water. (81)

ILs are seen as a good electrolyte that allow cathode materials to remain stable under high-voltage conditions for Li-, Na-, Mg and Al-ion batteries. However, there has not been a lot of research in ILs electrolytes containing potassium salts. (82) (83) Yamamoto et al. prepared an IL electrolyte containing potassium bis(fluorosulfonyl)amide (KSFA) in 1-methyl-1-propylpyrrolidinium bis(trifluoromethanesulfonyl)amide (PYR13FSA) for high-voltage K-ion battery. The latter showed an electrochemical window of >5.72 V with a good ionic conductivity. (84) Beltrop et al. reported the first potassium ion-based dual-graphite battery using an IL consisting of potassium

bis(trifluoromethanesulfonyl)amide (KTFSA) in 1-butyl-1-methylpyrrolidinium bis(trifluoromethanesulfonyl)amide (PYR14TFSA). This battery demonstrated an excellent electrochemical performance when used with graphite electrodes. (85) Finally, Yoshii K et al. discovered that ILs consisting of KFSA salt in 1-propyl-1-methylpyrrolidinium TFSA (PYR13TFSA) are stable when joint with high-voltage layered oxides. Furthermore, this IL electrolyte presented a lower redox potential than the lithium- and sodium- batteries, hence exhibiting a wide electrochemical window of around 6.0 V. Thereupon, high-voltage K-ion batteries can be reached utilising an electrolyte made of KTFSA salt and high-voltage layered cathode materials. However, additional research on the layered cathodes and the cost-effectiveness of ILs remain to be deeply studied to allow K-ion batteries in the current market. (82)

2.4.4.2. Magnesium batteries

Magnesium batteries are a good alternative to lithium batteries as magnesium has a low reduction potential (-2.37 V), high volumetric capacity (3832 mA h/cm versus 2062 mA h/cm for lithium), low cost (as it's one of the most abundant elements on earth's crust) and safety (as it is an non-dendritic element). (86) (87)

However, suitable electrolytes must be further studied in order to achieve a reversible redox process of Mg since this metal is prone to form passivation films in all types of electrolyte solution. (88) After some research done on different electrolyte solutions based on Grignard reagents, the addition of ILs in electrolytes to overcome the irreversible electrodeposition of Mg has gained much attention. Vardar et al. studied the performance of electrolyte solutions based on various Mg salts, IL solvents (BMIM-Tf_2N, PP13-Tf_2N, DEME-BF_4) and organic cosolvents on Pt working electrodes, reporting contrary results of previous studies where the Mg reversible electrochemical deposition took place. As a conclusion, they suggested that electrolytes containing Tf_2N^- and BF_4^- have strong Coulombic attraction to the Mg^{2+} cation resulting in a not Mg plating. (89) Sato et al. then reported that DEME-based ILs have high conductivity, wide potential window and perfect stability and cycle durability. (90) Yoshimoto et al. prepared a new electrolyte system based on a Grignard reagent (ethylmagnesiumbromide in THF, EtMgBg/THF) and an IL of quaternary ammonium salt (DEMETFSI) for Mg batteries in room temperature. In a 3:1 ratio of the latter mixture a high ionic conductivity of 7.44 mS cm^{-1} at 25 ºC was achieved. Moreover, the ionic liquid DEMETFSI resulted on being a

good electrolyte in order to allow a reversible process of cathodic deposition and anodic dissolution of Mg. (91) Later, Yashimoto et al. continued their research in ILs for Mg batteries doing a research in order to optimize the structure of ILs based on imidazolium cations. It was stated that the addition of a methyl group at the 2-position of 1-ethyl-2-methyl imidazolium bis (trifluoromethanesulfonyl)imide: C_1C_2ImTFSI) (the most well-known IL used in electrochemistry) mixed with MeMgBr and dissolved in TFH suppressed an unwanted reaction that took place when using the latter IL mixture without any modification. Moreover, adding an allyl or alkylether group in position 1 and 3 enhanced the conductivity. (92) Finally, Yashimoto et al. reported the excellent performance of the MeMgBr/THF/IL ternary electrolyte system (being the IL a binary system made of $[DEME^+][TFSI^-]_n[FSI^-]_{1-n}$ (n=0,1) in different molar ratios) for rechargeable Mg batteries. (93)

2.4.4.3. Calcium batteries

To understand the attention given to Calcium ion batteries it is necessary to highlight that calcium is the 5th most abundant element on earth's crust and it has a high volumetric capacity of 2073 mA h mL^{-1}. Another important characteristic to have into account is that calcium ion has a low reduction potential around -2.87 V and the its radius' size is a bit larger than that of the lithium ion. (79) (94)

However, calcium ion batteries must overcome some important drawbacks in order to replace lithium's ones. The major issue to study is the poor intercalation and diffusion of the calcium cations. Padigi et al. studied the addition of water to an electrolyte to enhance calcium ion batteries and their experiment stated that with 17% of water in acetonitrile-based electrolyte increases the redox activity and the energy capacity of calcium ions. (94) The difficulty to obtain a suitable electrolyte which enables the reversible reaction of plating/stripping of calcium and a suitable cathode material for a quick Ca^{2+} insertion have led to an open field to study. (95) ILs were studied as a possible solution although at the end it was stated that many typical ions in ILs are unstable due to the fact that calcium has a low potential. And so then, electrolytes with calcium chloride and imidazolium-based ILs could not overcome the irreversible electrodeposition of calcium. Recently, an IL has been presented as a feasible electrolyte in order to enable the redox activity in calcium batteries. (96) Nevertheless, further scientific research

focused on the electrode materials and the electrolyte is required to reach a viable calcium battery.

2.4.4.4. Zinc ion batteries

Zinc ion batteries have been proved to be a perfect energy-storage device due to their high capacity, fast charge-discharge capability, low cost, eco-friendly beneficence, and safety. For instance, Xu et al. prepared a zinc ion battery with high capacity which could be charged or discharged within 30 seconds. (97) This was made with MnO_2 as cathode, Zn as anode and nontoxic, noncorrosive, and mild electrolyte, all of these low-cost materials. Furthermore, Zn is also an abundant material on earth and has a low reduction potential (-2.20 V).

Nonetheless, this type of battery also has some issues to be solved. The major problem is to find a suitable material for the cathode that allows the reversible insertion of divalent Zn^{2+}. Short cycle life and deficient discharge capacity are also drawbacks to overcome. (79) Another important problem to be solved is the growth of dendrites during the charging process due to the intrinsic properties of zinc. A lot of studies have tried many different aqueous and organic electrolytes to solve the latter issue. However, the results demonstrated that these solutions could not solve the problem.

In view of the many advantages that ILs have, some researchers started to investigate the application of this type of molten salts as electrolyte. By designing a suitable cation-anion IL, the physical and chemical properties of the electrolyte can be optimized to achieve the features wanted in the Zn battery. Zhen Liu et al. stated that using $Zn(TfO)_2$ in 1-butyl-1-methylpyrrolidinium trifluoromethylsulphonate ([PYR14]TfO) the Zn ions were deposited in a nanocrystalline structure. However, using 1-ethyl-3-methylimidazolium trifluoromethylsulfonate ([EMIm]TfO) the Zn ions were deposited in a microcrystalline structure. (98) In another study, Zhen Liu et al. demonstrated that an electrolyte based on ($Zn(TfO)_2$ + ZnO)/[EIm]TfO can supress the dendritic growth in Zn electrodes. Furthermore, the Zn battery show a stable voltage when is exposed to a long charge-discharge test. (99) Many other types of ILs have been studied to face the Zn battery challenges. If researchers continue studying in this direction a feasible Zn battery could be a good solution to replace Li ones.

2.4.4.5. Aluminium batteries

In light of the great abundance of aluminium (Al), as it is the most abundant metal in the Earth's crust, and the three-electron redox properties, Al-ion batteries have gained attention in the last decade. (100) Furthermore, this type of battery has been proved to have low-flammability, high capacity and low-cost. (79) Another important advantage is that an aqueous solution can be used as an electrolyte in the Al-ion battery. (101)

Despite the advantages mentioned above, there are still challenges for Al-ion batteries to overcome. Al^{3+} has a large radius, which has an impact on the insertion of ions into the crystalline structure. Al^{3+} is also very susceptible to corrosion and is prone to side reactions that take place between the electrolyte and the cathode. (102)

Several studies stated that using $AlCl_3$ with imidazolium ionic liquids ($AlCl_3$/[BMIM]Br, $AlCl_3$/[BMIM]Cl, $AlCl_3$/[EMIM]Cl) as electrolyte in Al batteries had a stable electrochemical performance. (103)-(105) Zhu et al. studied a new class of ILs using $AlCl_3$ with 1-methyl-1-propylpyrrolidinium chloride (PYR13Cl). They compared the results with other studies using 1-ethyl-3-methylimidazolium chloride (EMIC-$AlCl_3$) ILs stating that the first one had higher viscosity, and lower density and conductivity than the second one. (106) Nevertheless, further research has to be done in order to understand the effect that the ions in ILs can have in the electrochemical properties of an Al battery. Therefore, more research focusing on a suitable material for the electrodes and the electrolyte is required to enhance Al-ion batteries' properties such as the specific capacity and cycle life.

2.5. Battery testing

- Cyclic voltammetry test:

Cyclic voltammetry (CV) is an electrochemical technique commonly used for obtaining information about the reduction and oxidation processes of compounds and interfacial structures. In order to obtain this information, an electrochemical cell is subjected to a cycling potential and the resulting current is measured. This data is represented in a graphic showing the current-voltage curves called voltammograms.

Therefore, to be able to do the CV test the electrolysis cell (in this case, Fe-ion battery) must comprise a working electrode (WE), a counter electrode (CE), a reference electrode (RE) and an electrolytic solution.

On the one hand, the working electrode is where the varying potential is applied to. Hence, it must be made with a material inert to redox reactions. Changing the type of WE, it can be known the potential window or the ability the surface material has to interact with the species in the solution.

On the other hand, the aim of the counter electrode is to complete the electrical circuit since current start flowing when a reduction/oxidation reaction is taking place at the WE. The CE must also be designed in order to be inert to redox reactions as when examining the oxidation happening in the WE, the reduction is taking place in the CE.

A reference electrode with a well-known and stable equilibrium potential must be included to be the reference point against which the WE potential is measured. In this thesis a silver wire was used as a RE. In order to avoid the leakage of Ag^+ into the rest of the analyte solution, a separator wet with the analyte is inserted between the RE and the other electrodes.

Finally, an electrolyte solution must be inserted between the WE and CE to help the ions migrate from one electrode to another so that the charge balance can be achieved.

Once the cell is made the potential of the WE is measured against the stable potential of the RE. In a forward scan, a chosen starting potential E_1 will be applied to the WE and with the scan rate number inserted in the program the system will keep increasing the number of mV chosen per second until reaching a selected final potential E_2. From E_1 to E_2 the oxidation/ reduction potential should have happened. In this moment, the reverse scan will occur. This cycle will be applied as many times as we select. Meanwhile, the current at the WE is being recorded and studied with the potential applied in that exact moment.

- Charge-Discharge Test:

Landt CT2001 series Battery Test Systems (showed in Figure 17) is used for energy storage materials research and different battery tests. The apparatus has eight channels where independent batteries can be connected and programmed to run automatic charge-discharge test and cycle life test. The charge-discharge test is custom-built as current ranges from 1mA to 5 A and voltage ranges from 5 V to 15 V. At the same time, the software shows the results with different plots for specified cycles (Voltage & Current vs. Time, Cell voltage vs. Capacity, Charge/Discharge capacity vs. Cycle, etc) and the

detailed data for each cycle steps. Thus, this data can be easily interpreted while the battery testing system is working. (107)

Figure 17. Landt CT2001 series Battery Test System. (107)

Using this software, it can be known if the battery works properly if the response to the charge-discharge test corresponds to the method implemented. Each battery can be tested infinite times as the method can be changed by modifying the parameters of voltage and current. Thus, each battery can be set as Constant-Current (CC) Discharge, Constant-Current (CC) Charge, Constant-Voltage Charge, etc.

3. Materials and methods

3.1.Materials

Instruments:

- Densitometer DMA 5000 M
- Rolling-ball viscometer Lovis 2000 M/ME
- Mettler Toledo Seven Compact S230 Conductivity
- Cyclic Voltammetric Test
- Landt CT2001 series Battery Test Systems
- Rotary evaporator

Equipment:

- Iron battery shaped like a "T" comprising of: a hollow exterior housing made with a conductive alloy in "T" shape, three conductive metal solid cylinders, a conductive round metal piece, a spring, a plastic piece, three plastic coupling pieces and three metal coupling torque.
- PP plastic foil
- Separator
- Nickel foil
- Copper foil
- Aluminium foil
- Doctor blade
- 50 mL glass containers with lids
- 50 mL plastic containers with lids
- Automatic pipettes
- Disposable pipettes
- Magnetic stirrer and stirring bars
- Sandpaper
- Scissors
- Cutting machine into round pieces
- A thin silver stick
- Torque wrench
- Insulating tape

- Laboratory spoons-spatulas
- Integrated precision scale
- Beakers

Chemicals:

- BmimCl, $C_8H_{15}ClN_2$ (1-Butyl-3-methylimidazolium Chloride)
- $FeCl_3 \cdot 6\ H_2O$ (Iron (III) chloride hexahydrate)
- $BmimFeCl_4$, $C_8H_{15}Cl_4FeN_2$ (1-Butyl-3-methylimidazolium Tetrachloroferrate)
- Ferric phosphate, $FePO_4$
- Dimethyl carbonate (DMC), $OC(OCH_3)_2$
- Ethylene carbonate (EC), $(CH_2O)_2CO$
- Carboxymethyl cellulose (CMC), R_nOCH_2-COOH
- Powder graphite
- C45 (medium carbon steel)
- Iron (II,III) oxide, Fe_3O_4
- Carbon black
- Mettler Toledo 1413 μS/cm Conductivity standard [Mettler Toledo, Sigma Aldrich]
- Methanol for cleaning
- Distilled water

Solutions:

- 5%, 10%, 15%, 20%, 30%, 40%, 50% and 60% $BmimFeCl_4$ in DMC
- 5%, 10%, 15%, 20%, 30%, 40%, 50% and 60% $BmimFeCl_4$ in DMC+EC (ratio 1:1)
- 1M $FeCl_3 \cdot 6H_2O$ in DMC+EC (1:1)
- 1M $FePO_4$ in DMC+EC (1:1)
- 1M $Fe(CH_3COO)_3$ in DMC+EC (1:1)

3.2. Details for the chemicals utilized in the electrolyte

The aim of this section is to provide information about the most important properties of the chemicals utilized to produce an electrolyte for Fe-ion batteries in order to understand their performance. In addition, the level of hazard of the chemicals will be

known due to the Globally Harmonized System for the Classification and Labelling of Chemicals (GHS). Furthermore, the warning symbols as well as the hazards and precautionary statements will be reflected in Appendix 1.

- BmimCl:

BmimCl: 1-Butyl-3-methylimidazolium Chloride

Molecular Formula: $C_8H_{15}ClN_2$

M_w: 174.67 g/mol

M_p: 70 ºC

Density: 1.068 g/cm^3 at 20 ºC

Flash point: 192 ºC

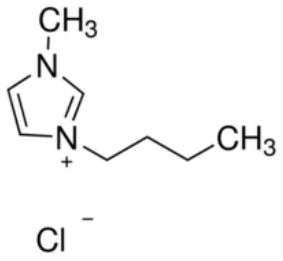

Figure 18. Chemical structure of the BmimCl.

BmimCl is a light-yellow solid at room temperature often utilized as a reagent in anionic reactions to prepare ionic liquids at room temperature. It is soluble, inter alia, with acetone, isopropyl alcohol, and water at room temperature. However, it is not miscible with hexane and toluene. Moreover, while preparing solutions it has be found that almost always the density increases when increasing the concentration of BmimCl. When adding organic solvents to an ionic liquid comprising BmimCl, there is a free mobility of ions due to the disruption of the interactions within mixtures. Hence, this leads to an improvement of the conductivity and the decreasing of viscosity. (108)

- $FeCl_3 \cdot 6\ H_2O$:

$FeCl_3 \cdot 6\ H_2O$: Iron (III) chloride hexahydrate

Molecular Formula: $Cl_3FeH_{12}O_6$

M_w: 270.29 g/mol

M_p: 37 ºC

Density: 1.82 g/cm^3

Flash point: Not applicable.

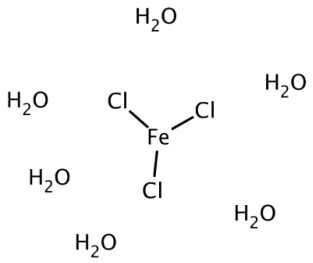

Figure 19. Chemical structure of Iron (III) chloride hexahydrate.

Iron chloride hexahydrate used was in a yellow-red powder with lumps. It is the hexahydrate form of iron chloride and its utilized as an astringent and Lewis acid. In addition, it is also used as a catalyst in a medium of the ionic liquid $BmimFeCl_4$ in order to prepare cycloalkanones in a greener way. (109) In this thesis the iron chloride hexahydrate has been utilized to react with BmimCl to prepare the ionic liquid $BmimFeCl_4$.

- $BmimFeCl_4$:

$BmimFeCl_4$: 1-Butyl-3-methylimidazolium tetrachloroferrate

Molecular Formula: $C_8H_{15}Cl_4FeN_2$

M_w: 336.87 g/mol

M_p: < Room Temperature

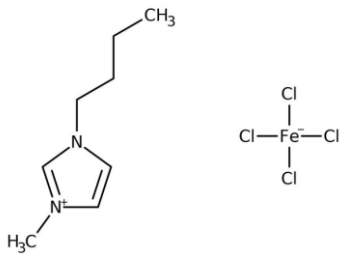

Figure 20. Chemical structure of the ionic liquid $BmimFeCl_4$.

$BmimFeCl_4$ is an ionic liquid with magnetic properties due to the presence of the $FeCl_4^-$. It is a dark brown liquid that has low water solubility. Some research done with this ionic liquid has proved to be a promising solvent in order to extract and to separate aromatic and aliphatic hydrocarbons. (110) Other studies show the good performance of $BmimFeCl_4$ as a catalyst in a multicomponent synthetic strategy. (111) In this thesis the $BmimFeCl_4$ is synthesised in the laboratory in order to utilize it as an electrolyte, pure and in solution with other solvents, in the rechargeable iron-ion batteries prepared.

- $FePO_4$:

$FePO_4$: Ferric phosphate

Molecular Formula: $FePO_4$

M_w: 150.82 g/mol

M_p: 37 ºC

Density: 1.82 g/cm^3

Flash point: Not applicable.

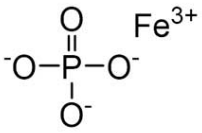

Figure 21. Chemical structure of $FePO_4$.

Iron phosphate combines phosphorous and oxygen with iron. It is a light brown solid formulated as granules and with a high level of toxicity to slugs and snails. This is the reason why this compound is often used as a pesticide. (112) In this thesis it has been tried to dissolve iron phosphate in DMC+EC in order to utilize it as an electrolyte. This idea was followed by the fact that the lithium iron phosphate has a really good performance in lithium-ion batteries. Nevertheless, it was stated that 1M of iron phosphate cannot be dissolved in DMC+EC.

- $Fe(CH_3COO)_3$:

$Fe(CH_3COO)_3$: Iron (III) acetate

Molecular formula: $C_{14}H_{27}Fe_3O_{18}$

M_w: 232.98 g/mol

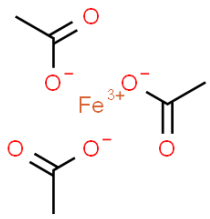

Figure 22. Chemical structure of $Fe(CH_3COO)_3$. (113)

Ferric acetate is the acetate salt of the coordination complex $[Fe_3O(CH_3CO_2^-)6(H_2O)_3]^+$. It has a brownish-red colour in solution. (114) This chemical was used to prepare a solution of 1 M ferric (III) acetate in EC+DMC in a ratio 1:1. The idea was to achieve an electrolyte containing iron ions. However, this solution was not dissolved and could not be used as an electrolyte for the batteries.

- Dimethyl carbonate (DMC):

Molecular Formula: $C_3H_6O_3$

M_w: 90.08 g/mol

M_p: 2 - 4 ºC

Density: 1.069 g/cm^3 at 25 ºC

Flash point: 16 ºC – closed cup

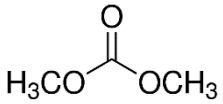

Figure 22. Chemical structure of DMC.

DMC is a highly flammable transparent liquid and vapor which smells like ethanol. It is considered a nonpolar aprotic solvent with a complete miscibility with organic solvents and full solubility with water. DMC is known as a green solvent due to its safety, health and environmental criteria. That is the reason why one of its application is replacing other noxious solvents. In addition, DMC is often used as electrolyte in Li-ion batteries since Li salts are soluble in this solvent. Therefore, the batteries show high conductivity. Long-term stability, low viscosity and good resistance to oxidation and

reduction are other attractive properties of this solvent. (115) Moreover, some studies have proved the extraordinary enhancement of Li-batteries while using a DMC solution with graphite electrodes. (116)

- Ethylene carbonate (EC):

Molecular Formula: $C_3H_4O_3$

M_w: 88.06 g/mol

M_p: 35 – 38 ºC

Density: 1.321 g/cm^3 at 25 ºC

Flash point: 143 ºC – closed cup

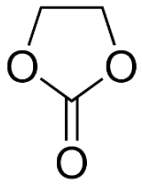

Figure 24. Chemical structure of EC.

EC is a colourless crystalline solvent which is highly polar. Its features include low toxicity, no odour and the ability to dissolve multiple electrolytes. (117) It is mainly used as a mixture solvent in electrolytes for LIBs due to its high dielectric constant. (118) Nevertheless, EC decomposes at high voltage which prevents improving the LIBs' energy density. (119)

3.3.Methods

In this section the methods used during the thesis are further explained below.

- <u>Method for preparation of the IL:</u>

In order to prepare the IL $BmimFeCl_4$ the following reaction must take place:

$$BmimCl + FeCl_3 \cdot 6H_2O \rightarrow BmimFeCl_4 + 6\ H_2O$$

To achieve 30 g of $BmimFeCl_4$, the reagents BmimCl and $FeCl_3 \cdot 6H_2O$ are weigh in a laboratory balance (15.56 g and 24g, respectively). These two reagents are added in a 3-neck bottle with a stirrer. In 1 neck of the bottle the water refrigerator system is connected to cool the sample. The other two necks of the bottle are closed with plugs and the sample

is stirring for 4 hours. After this time, the sample is poured into a separating tunnel and after waiting for some minutes two clear separate layers can be observed. The dark layer in the bottom part is the IL which has more density than the water which remains in the upper part. The IL is separate it carefully from the water and it is put in a vacuum system for two hours in order to evaporate any small drop of water and obtain pure IL.

- Method for preparation of the electrolyte:

Firstly, different electrolytes were prepared mixing different proportions of the IL obtained before ($BmimFeCl_4$) with DMC. The following samples were prepared considering the density of the DMC and that a sample of 10 ml of each percentage of electrolyte was wanted. Therefore, first the amount of IL was weighed in a small glass bottle and then the DMC was added until the total amount of electrolyte was 10.7 g.

% $BmimFeCl_4$ in DMC	$BmimFeCl_4$ (g)	DMC (g)
5%	0.535	10.165
10%	1.070	9.630
15%	1.605	9.095
20%	2.140	8.56
30%	3.210	7.49
40%	4.280	6.42
50%	5.35	5.35
60%	6.42	4.28

Table 1. Amounts to prepare different percentages of $BmimFeCl_4$ in DMC.

Then, other types of electrolytes were prepared mixing the $BmimFeCl_4$ with the solvents EC+DMC in a ratio of 1:1. Hence, considering the density of the latter two organic solvents 100 ml of the solution EC:DMC=1:1 was prepared mixing 107 g of EC and 107 g of DMC. Later, different samples of 10 ml of electrolyte weighing 11.96 g were obtained, as it can be seen on Table 2, mixing different amounts of $BmimFeCl_4$ with the EC+DMC solution.

% $BmimFeCl_4$ in EC+DMC	$BmimFeCl_4$ (g)	EC+DMC (g)
5%	0.598	11.362
10%	1.196	10.764
15%	1.794	10.166
20%	2.392	9.568
30%	3.588	8.372
40%	4.784	7.176
50%	5.980	5.980
60%	7.176	4.784

Table 2. Amounts to prepare different percentages of $BmimFeCl_4$ in EC+DMC.

Finally, two other types of electrolytes were prepared using different ILs. The aim was to obtain 1 M ILs in EC+DMC. Hence, 0.302 g $FePO_4$ were mixed and stirred with 2 ml of EC+DMC=1:1 but at the end it was stated that $FePO_4$ could not be dissolved being 1 M in the latter mixture of solvents. Then, the same test was done for $FeCl_3 \cdot 6H_2O$. In this case, 0.541 g $FeCl_3 \cdot 6H_2O$ was stirred with 2 ml of EC+DMC and after some time the mixture was completely dissolved.

- Method for measuring density and viscosity:

Density and viscosity of each sample mentioned above were measured using a combined Densitometer DMA 5000 M and Rolling-ball viscometer Lovis 2000 M/ME. Firstly, and appropriate apparatus method was chosen, and the syringe was cleaned with ethanol and water. Then, the fan was turned on until any drop of ethanol or water was observed. This process was repeated each time before inserting the syringe in the 10 ml electrolyte's bottle glass. When each test was finished (around 1h30min after the start) the syringe was inserted into a waste bottle in order to start the cleaning program. Once started, the machine inserted ethanol and water several times through all the syringe. Finally, when the syringe was filled with air the cleaning process had finished and it was ready to measure another sample. After all the samples were measured the data was collected in a pen drive to interpret the results.

- Method for measuring conductivity:

Conductivity of samples was measured using conductivity meter Mettler Toledo Seven Compact S230 Conductivity. In the first place, it was made sure that the conductivity meter was adjusted to the standard potential of the electrode. Then, the electrode was calibrated using a 1413 µS/cm conductivity standard. Once calibrated, the electrode was inserted into a tube filled with the electrolyte until the signal was stabilized. The conductivity was noted, and the electrode was removed, rinsed with ethanol and dried carefully with a paper. This process was repeated until all the samples were measured.

- Method for assembling the batteries:

In order to assemble a battery a PP plastic film cut in a square of 44x45 mm is inserted in the principle hole of the iron battery. Then, a round iron piece is inserted followed by the cathode (previously cut in a 11 mm circle or in a 11x11 mm square and weighed). After that, a separator (previously cut in a circle of 12 mm) is inserted and it is wet with some drops of the desired electrolyte. Later, the anode (also previously cut in a 11 mm circle or in a 11x11 mm square and weighed) is inserted followed by an iron solid cylinder covered in its central part with a non-conductive material such as adhesive tape and in its upper part with two plastic pieces which will avoid short-circuits. In order to finish, the anode part must be closed using a coupling torque. Afterwards, a spring is inserted next to the round iron piece and the same process of the anode will be repeated in order to close the cathode. In the central hole of the T shaped iron battery another PP plastic film is inserted followed by another separator wet with the same electrolyte. Then, a round plastic piece which has a silver stick which passes through it is inserted and the closing process is repeated.

- Method for performing the Open Circuit Potential and Cyclic Voltammetry test:

In order to run an Open Circuit Potential test the red crocodile clip is connected to the anode, the green one to the cathode and the white one to the reference electrode. Then, the Open Circuit Potential technique is chosen in the program and it is implemented selecting the desired parameters of time, higher and lower voltage, and scanning rate. By doing this test, it can be known if the electrolyte in the battery is stable. Later, the Cyclic Voltammetry test can be selected in the program and implemented by choosing the same previous parameters. While running the test the voltammogram can be observed with the results.

- Method for performing Landt Battery Testing System:

The Landt Battery Testing System has 8 channels whereby 8 batteries can be connected at the same time. The two red crocodiles clips are connected to the anode and the two black ones are connected to the cathode. Then, a method in the computer program is chosen and the test starts running. The 8 batteries are checked after some time to see if there has been a short-circuit or they are delivering too much/low voltage, current or capcity. In order to check if they are running correctly, we must make sure that the method of charge/discharge implemented in the program is taking place since a plot of time-current and time-voltage will be recorded as well as all the numerical data. Other methods can be implemented to the batteries changing the parameters for charging and discharging the battery.

4. Results and discussion

In this section all the data collected during the experiments performed throughout the thesis will be presented. Moreover, the results will be discussed in order to reach a conclusion.

4.1. Ionic Liquids physical properties

The conductivity, density and viscosity of the ILs solution were measured in order to know which amount of ILs in the electrolyte show better properties and how to optimize them by changing the percentage of ILs and organic solvents.

4.1.1. Conductivity

Firstly, the conductivity of the solutions based on different amount of $BmimFeCl_4$ in DMC were measured at 24.2 ºC. The results are shown in Table 3. Later, other solutions based on different quantities of $BmimFeCl_4$ and EC+DMC in a ratio 1:1 were prepared. The conductivity of the latter was also measured at 24.2 ºC as it is shown in Table 4.

% $BminFeCl_4$ in DMC	Conductivity (µS/cm)
0 %	0
5 %	413
10 %	1942
15 %	3660
20 %	5570
30 %	12940
40 %	17310
50 %	19690
60 %	19310
100%	7.8

Table 3. Conductivity of different % of $BmimFeCl_4$ in DMC at 24.2 ºC.

% $BmimFeCl_4$ in EC + DMC	Conductivity (µS/cm)
0 %	7.41
5 %	5180
10 %	9260
15 %	12140
20 %	15140
30 %	18290
40 %	19150
50 %	19540
60 %	18600
100 %	7.8

Table 4. Conductivity of different % of $BmimFeCl_4$ in EC+DMC at 24.2 ºC.

The best electrolyte for the battery will be the one which has higher ionic conductivity. Hence, from Table 3 and Table 4 it can be stated that the 50% solution in both cases is the best one as it has the higher ionic conductivity. However, from Table 3 it can be seen that the conductivity for the 50% and 60% solution is almost the same. Similarly, from Table 4 it can be affirmed that the conductivity for the 40% and 50% solution is practically invariable. These conclusions can be better seen in Figure 25 and Figure 26 based on the results in Table 3 and Table 4. Additionally, in Figure 27 is shown the conductivity measures for the solutions of IL in DMC and of IL in EC+DMC in the same graphic in order to be compared.

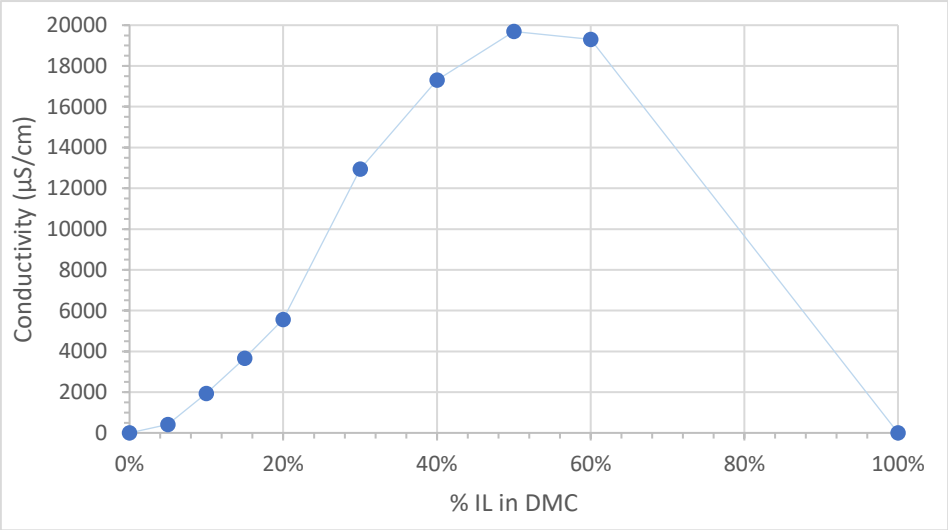

Figure 25. Conductivity of various concentration of $BmimFeCl_4$ in DMC at 24.2 ºC. Values obtained from Table 3.

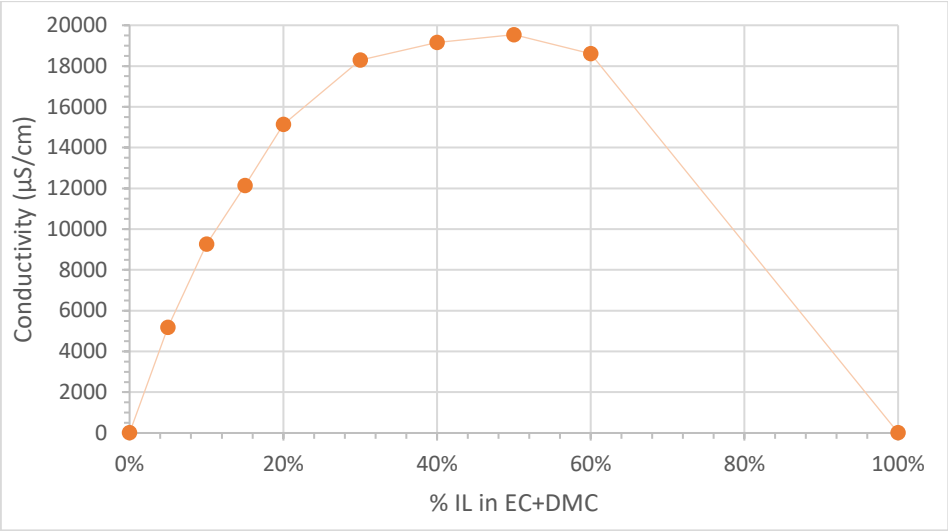

Figure 26. Conductivity of various concentration of $BmimFeCl_4$ in EC+DMC at 24.2 ºC. Values obtained from Table 4.

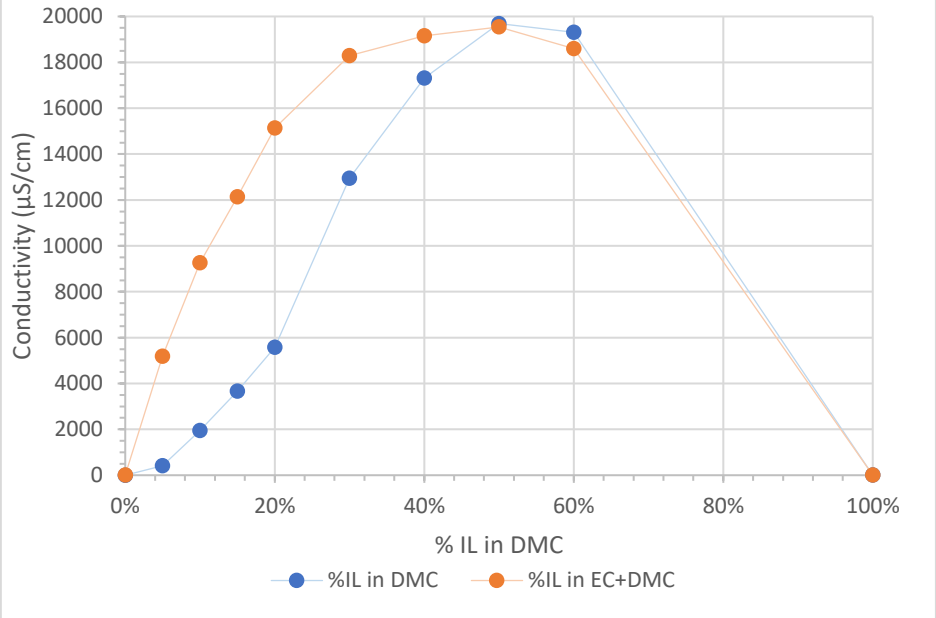

Figure 27. Comparison of the conductivity of the two electrolytes based on various concentration of $BmimFeCl_4$ in DMC and in EC+DMC at 24.2 ºC.

From Figure 25 and 26, it can be stated that the conductivity increases when the amount of $BmimFeCl_4$ added in the solvent increases until reaching a certain point. Thus, in both cases for the solutions from 5% until 50% it can be observed how the conductivity rises while increasing the percentage of IL. Once it is added more than 50% $BmimFeCl_4$ in the solvent, the conductivity starts decreasing.

Taking Figure 25 a step further, it can be observed how the conductivity from 5% until 20% IL in DMC increases linearly. Nevertheless, when the percentage of IL in DMC is between 20% and 40% the conductivity raises significantly. Thus, the conductivity of 40% IL in DMC is more than three times higher than the one of 20%. It can be stated that the electrolyte has a good conductivity when the percentage of IL in DMC is around 50%. Adding more than 50% IL in DMC makes no sense when trying to optimize the conductivity since this is slightly lower for 60% than for 50%.

When studying the conductivity of the different percentages of IL in EC+DMC from Figure 26, it can be said that this type of electrolyte achieves a great conductivity when it has 30% IL in EC+DMC or higher. As happened for the other electrolyte, adding more than 50% IL in EC+DMC turns conductivity to lower values.

Furthermore, from Figure 27, it is noted that while the conductivity of 50% solution in both cases reaches almost the same number, the conductivity for the solutions of $BmimFeCl_4$ in DMC is lower for the lowest percentages. As a result, 30% $BmimFeCl_4$ in EC+DMC has higher conductivity than 40% $BmimFeCl_4$ in DMC. In the same way, for low percentages of IL the conductivity for the solutions made with EC+DMC is much higher than the ones made with only DMC.

In conclusion, the aim of studying the conductivity of an electrolyte is to choose the one which has high ionic conductivity. A higher conductivity means that the ions move faster between the electrodes and consequently the charge/discharge rate is quicker and smoother. Hence, it can be claimed that in general the electrolyte consisting of IL in EC+DMC is better in terms of conductivity than the one which only consists of IL in DMC. Moreover, when the percentage of IL in EC+DMC is around 30% the conductivity is considerably good, reaching its highest point at around 50%.

4.1.2. Density

The density of the solutions based on different amounts of $BmimFeCl_4$ in DMC were measured at different temperatures using the Densitometer DMA 5000 M. The results are shown in Table 5. Later, the solutions based on different quantities of $BmimFeCl_4$ in EC+DMC in a ratio 1:1 were measured obtaining the results in Table 6.

Density (g/cm^3)										
T (°C)	0%	5%	10%	15%	20%	30%	40%	50%	60%	100%
20	1,0698	1,0838	1,0975	1,1117	1,1262	1,1463	1,1844	1,2121	1,2432	1,3679
25	1,0633	1,0775	1,0913	1,1057	1,1203	1,1403	1,1791	1,2070	1,2384	1,3637
30	1,0567	1,0711	1,0851	1,0996	1,1143	1,1336	1,1738	1,2018	1,2335	1,3596
35	1,05	1,0646	1,0787	1,0934	1,1084	1,1270	1,1684	1,1967	1,2286	1,3554
40	1,0433	1,0581	1,0724	1,0873	1,1024	1,1193	1,1630	1,1915	1,2238	1,3513
45	1,0366	1,0516	1,066	1,0811	1,0964	1,1103	1,1576	1,1863	1,2189	1,3472
50	1,0299	1,045	1,0597	1,0749	1,0903	1,0973	1,1523	1,1812	1,2141	1,3432
55	1,0231	1,0384	1,0533	1,0687	1,0843	1,0849	1,1469	1,1761	1,2092	1,3391
60	1,0163	1,0318	1,0468	1,0625	1,0782	1,0734	1,1415	1,1709	1,2044	1,3351

Table 5. Density of different concentrations of $BmimFeCl_4$ in DMC at various temperature.

Density (g/cm^3)										
T (°C)	0%	5%	10%	15%	20%	30%	40%	50%	60%	100%
20	1,2042	1,2103	1,2179	1,2260	1,2339	1,2494	1,2654	1,2821	1,2985	1,3679
25	1,1983	1,2044	1,2122	1,2204	1,2284	1,2441	1,2603	1,2772	1,2938	1,3637
30	1,1923	1,1986	1,2065	1,2148	1,2228	1,2388	1,2551	1,2722	1,2890	1,3596
35	1,1863	1,1927	1,2007	1,2091	1,2173	1,2334	1,2500	1,2672	1,2842	1,3554
40	1,1804	1,1868	1,1949	1,2034	1,2117	1,2281	1,2448	1,2623	1,2794	1,3513
45	1,1744	1,1809	1,1892	1,1978	1,2062	1,2227	1,2397	1,2573	1,2747	1,3472
50	1,1684	1,1750	1,1834	1,1921	1,2006	1,2174	1,2346	1,2524	1,2699	1,3432
55	1,1623	1,1691	1,1776	1,1864	1,1951	1,2121	1,2294	1,2475	1,2652	1,3391
60	1,1563	1,1632	1,1718	1,1808	1,1895	1,2067	1,2243	1,2425	1,2605	1,3351

Table 6. Density of different concentrations of $BmimFeCl_4$ in EC+DMC at various temperature.

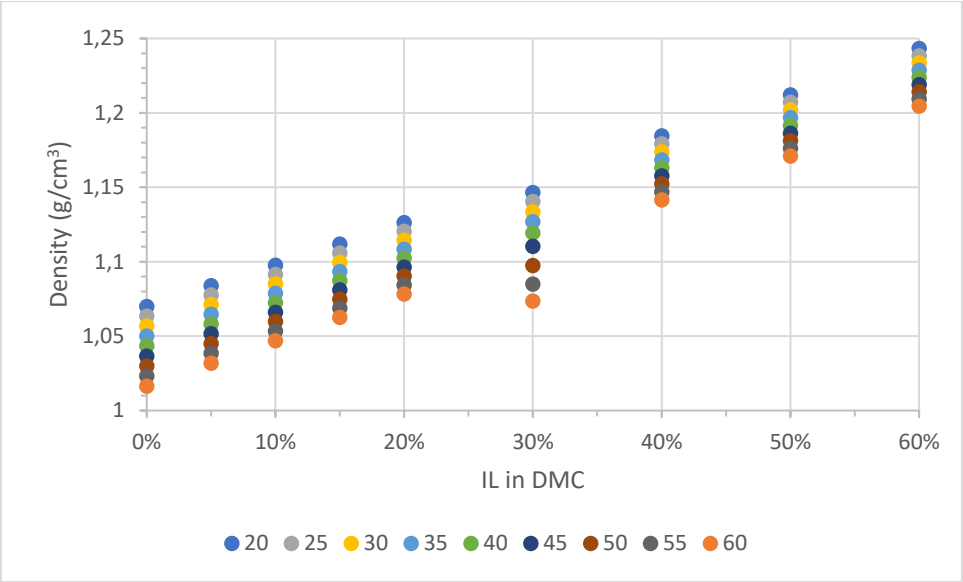

Figure 28. Density of different concentrations of $BmimFeCl_4$ in DMC at the temperatures in ºC shown in the caption. Values obtained from Table 5.

From Figure 28, it can be stated that the density results obtained from different percentages of $BmimFeCl_4$ in DMC measured in a range of temperatures show a direct correlation. Hence, as the ionic liquid has higher density than the DMC, the density of the samples is higher when the percentage of ionic liquids in DMC in the sample is higher too. However, the density of a sample is higher when the temperature is lower.

The aim is to have an electrolyte with high density since this will take smaller space with the same mass. In this way, the electrolyte based on $BmimFeCl_4$ in DMC is better when it has high percentage of IL and low temperature. To better see this correlation in Figure 29 and Figure 30 is represented how the density varies depending on the percentage of IL and on the temperature of the sample, respectively.

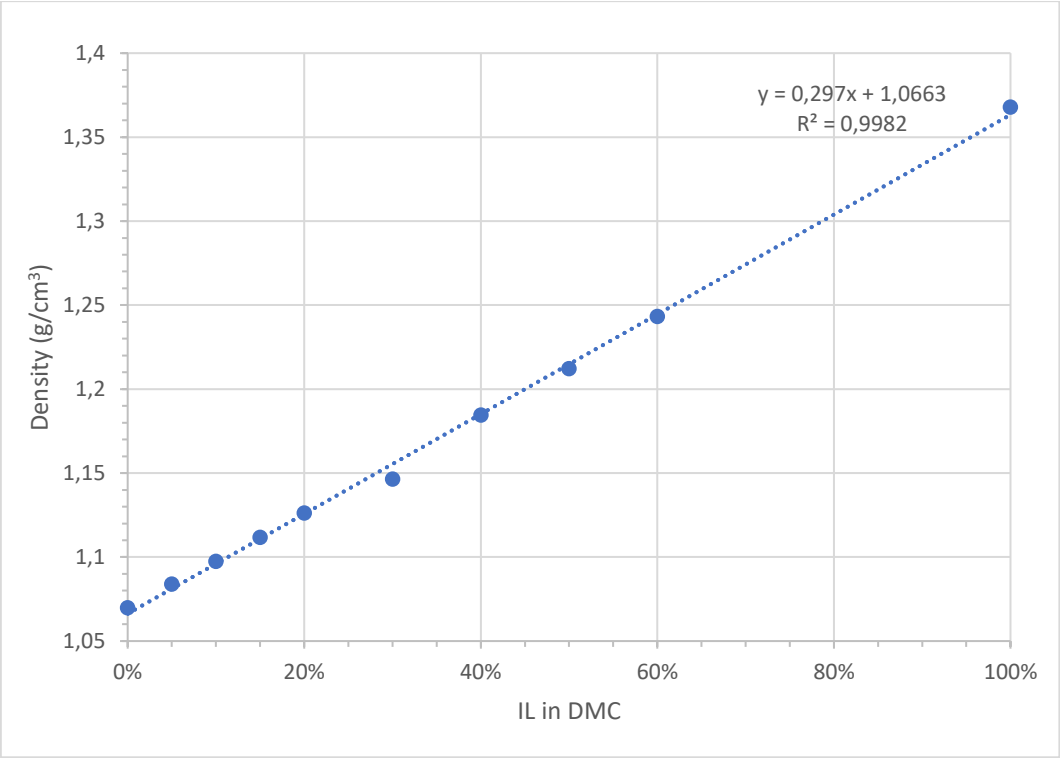

Figure 29. Density of different concentrations of $BmimFeCl_4$ in DMC at 20 ºC. Values obtained from Table 5.

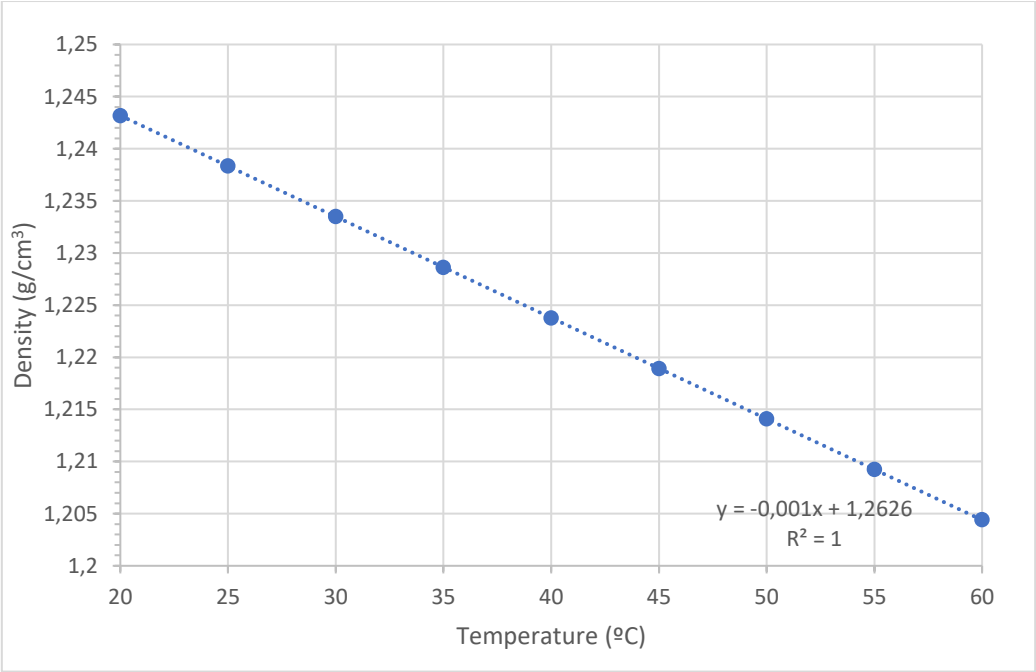

Figure 30. Density of 60 % $BmimFeCl_4$ in DMC at different temperatures. Values obtained from Table 5.

From Figure 29 it can be seen how the percentage of $BmimFeCl_4$ in the electrolyte and the density is directly proportional with a correlation of 0.9982 when the temperature in the sample remains at constant at 20 ºC. The slope of the line is 0.297 meaning that for each 10 % of ionic liquids added to the electrolyte, the density will increase 0.0297 g/cm^3.

In Figure 30 the density measurements are represented in relation to the temperature of the 60% $BmimFeCl_4$ in DMC sample. An inverse proportion between density and temperature is proved as the correlation number is 1. Furthermore, the slope of the line is -0.001 so when the sample is 10 ºC higher, the density is 0.01 g/cm^3 lower in the range between 20 and 60 ºC.

To sum up, regarding all the electrolytes prepared consisting of $BmimFeCl_4$ in DMC the best one in terms of density is the electrolyte which has higher percentage of IL, therefore, this is the sample of 60% $BmimFeCl_4$ in DMC. Moreover, this sample will have higher density at lower temperatures.

Similarly, density measurements obtained for different percentages of $BmimFeCl_4$ in DMC+EC at different temperatures is shown in Figure 31. The same conclusion is drawn. Hence, the electrolyte based on $BmimFeCl_4$ in DMC+EC will have higher density when it has high percentage of IL and low temperature. This direct and inverse relation is shown in Figure 32 and Figure 33, respectively.

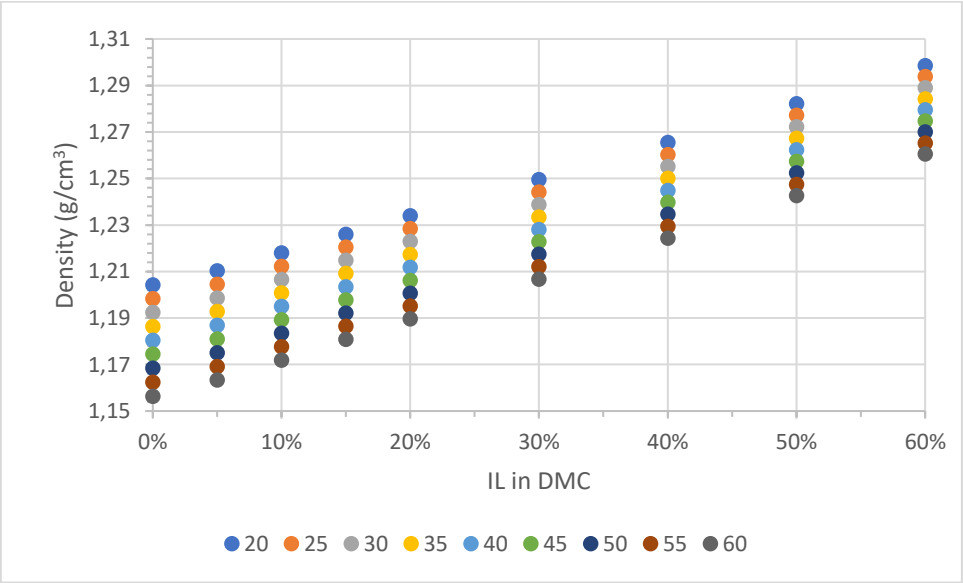

Figure 31. Density of different concentrations of $BmimFeCl_4$ in DMC+EC at the temperatures in ºC shown in the caption. Values obtained from Table 6.

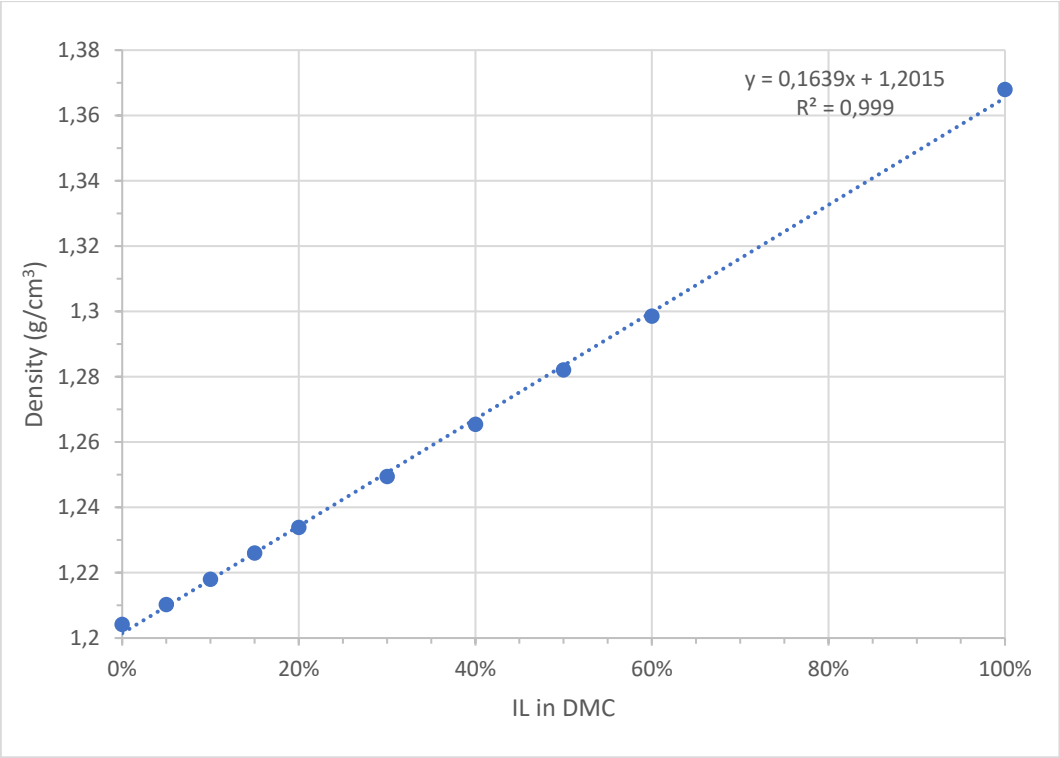

Figure 32. Density of different concentrations of $BmimFeCl_4$ in DMC+EC at 20 ºC. Values obtained from Table 6.

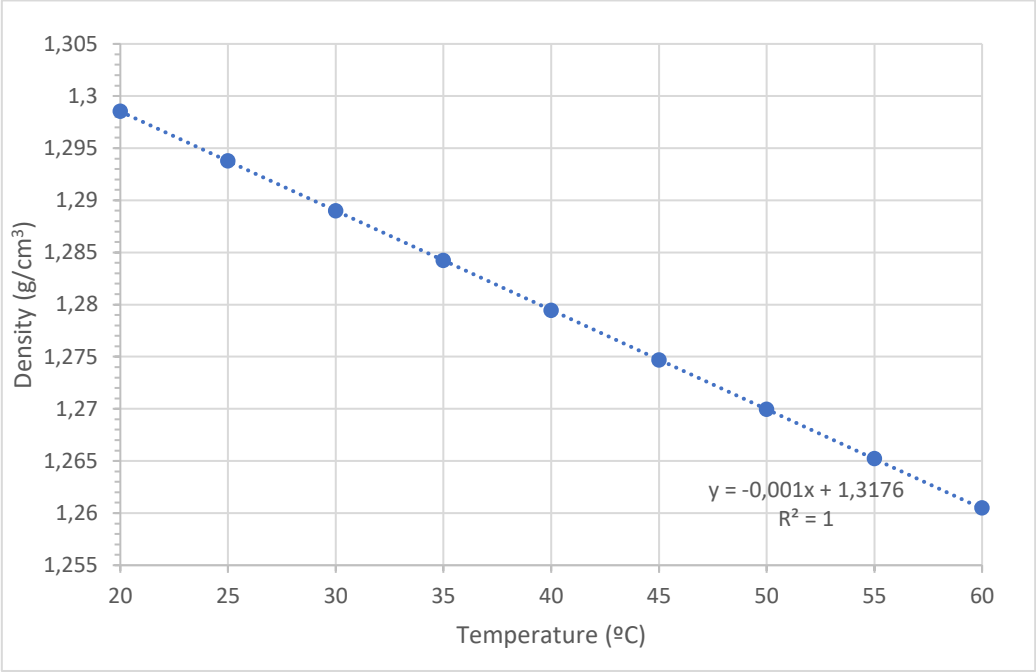

Figure 33. Density of 60 % $BmimFeCl_4$ in DMC+EC at different temperatures. Values obtained from Table 5.

From Figure 32, it can be determined that the relation between density and percentage of $BmimFeCl_4$ in DMC+EC is directly proportional with a correlation number of almost

1 and a slope of 0.1639. Conversely, the inverse relation is drawn from Figure 33 with a correlation number of 1 and a slope of -0.001. As concluded previously, regarding all the samples tested based on $BmimFeCl_4$ in DMC+EC the best electrolyte is the one which has 60 % $BmimFeCl_4$ in DMC+EC and low temperature.

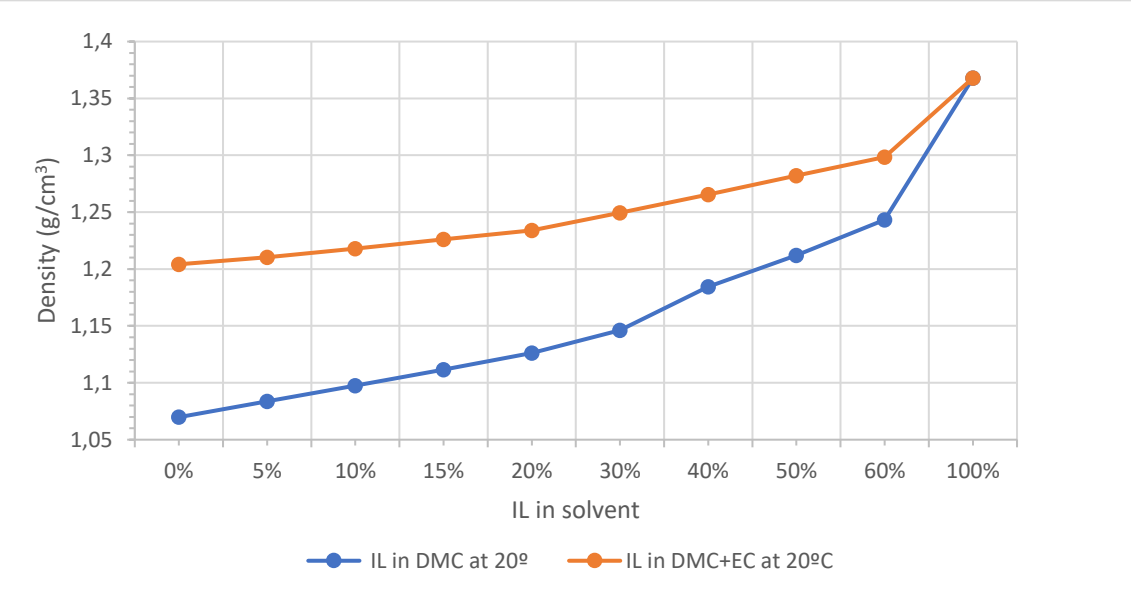

Figure 34. Density of different concentrations of $BmimFeCl_4$ in DMC (blue line) and in DMC+EC (orange line) at 20 ºC.

Finally, from Figure 34 both types of electrolytes can be compared. From this figure it can be seen that the density for the electrolyte using DMC+EC as solvent is higher than the one using only DMC. Thus, the electrolyte based on DMC+EC is better as it will take less space in the same mass.

4.1.3. Viscosity

The viscosity was measured at the same time as the density since the apparatus has incorporated a Rolling-ball viscometer Lovis 2000 M/ME. The data obtained for the samples are shown in Table 6 and Table 7.

Viscosity (mPa·s)									
T (°C)	0%	5%	10%	15%	20%	30%	40%	50%	60%
20	0,803	0,98	1,166	1,309	1,498	2,195	2,815	4,540	6,026
25	0,754	0,9	1,054	1,217	1,387	1,898	2,557	3,727	5,354
30	0,71	0,837	0,974	1,132	1,291	1,759	2,345	3,380	4,829
35	0,67	0,786	0,91	1,058	1,204	1,636	2,156	3,104	4,349
40	0,634	0,741	0,855	0,991	1,128	1,523	1,997	2,827	3,953
45	0,601	0,7	0,805	0,933	1,06	1,427	1,886	2,607	3,608
50	0,572	0,663	0,761	0,879	0,996	1,338	1,761	2,425	3,291
55	0,544	0,628	0,72	0,83	0,94	1,261	1,646	2,255	3,044
60	0,519	0,598	0,681	0,786	0,89	1,189	1,541	2,095	2,827

Table 7. Viscosity of different concentrations of $BmimFeCl_4$ in DMC at various temperature.

Viscosity (mPa·s)									
T (°C)	0%	5%	10%	15%	20%	30%	40%	50%	60%
20	1,725	1,895	2,274	2,546	2,754	3,182	4,119	5,338	---
25	1,585	1,747	1,911	2,104	2,302	2,919	3,703	4,773	6,419
30	1,467	1,625	1,753	1,954	2,106	2,925	3,346	4,363	5,766
35	1,365	1,510	1,627	1,810	1,961	2,758	3,245	3,838	5,196
40	1,277	1,405	1,514	1,682	1,817	2,243	2,792	3,499	4,707
45	1,197	1,321	1,416	1,569	1,693	2,061	2,572	3,127	4,284
50	1,128	1,244	1,325	1,467	1,581	1,951	2,379	2,911	3,923
55	1,064	1,162	1,246	1,375	1,484	1,822	2,210	2,721	3,611
60	1,007	1,102	1,176	1,294	1,396	1,711	2,059	2,546	3,323

Table 8. Viscosity of different concentrations of $BmimFeCl_4$ in DMC+EC at various temperature.

The purpose of the viscosity test is to know the relation between the percentage of $BmimFeCl_4$ in the solvent and the viscosity as well as the correlation between temperature and viscosity. The electrolyte will be better if it has a low viscosity within the operable

temperature range of the battery since this allows a faster transportation of ions in the liquid.

From Table 7 and Table 8, it follows that the viscosity is higher when adding more percentage of IL in the solvent and when the temperature is lower. $BmimFeCl_4$ has a high viscosity (as it is usual in the ILs), consequently there is a direct correlation between amount of IL and viscosity. This may lead to a problem since in order to have a high conductivity in the electrolyte the percentage of IL must be high too. Consequently, a balance between conductivity and viscosity must be found to optimize the electrolyte performance. Besides that, there is an inverse correlation between temperature and viscosity. Thus, the electrolyte will have faster diffusion and ion cycling while working at lower temperatures than if it does it at high temperatures.

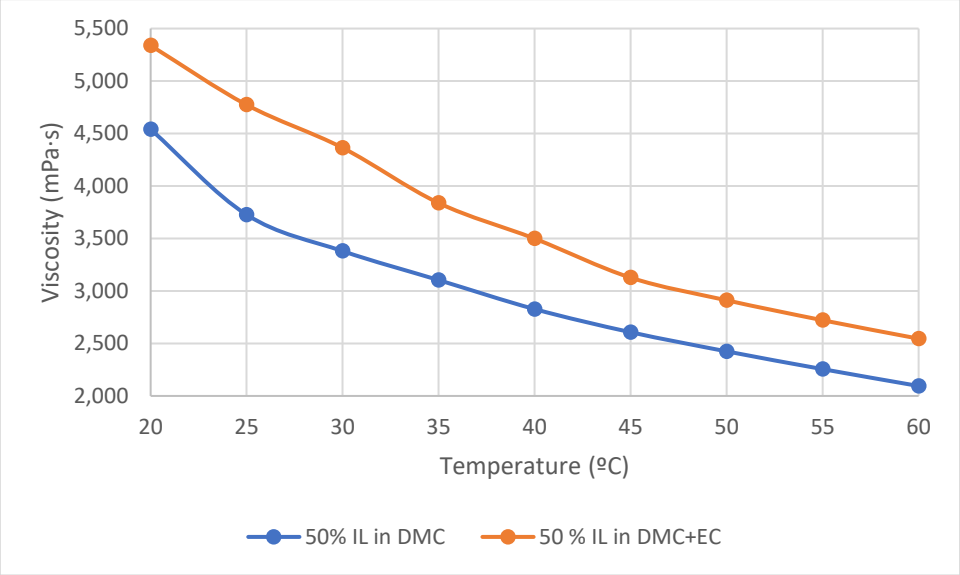

Figure 35. Comparison of the viscosity of the 50 % $BmimFeCl_4$ in DMC and in DMC+EC.

Additionally, in Figure 35 the viscosity of the 50 % $BmimFeCl_4$ in DMC and in DMC+EC is compared. The viscosity is lower when the solvent used in the electrolyte is only DMC. The difference between both types of electrolytes is around 0.7 mPa·s. Thus, it could be stated that the electrolyte based on $BmimFeCl_4$ in DMC is a bit better in terms of viscosity than the one which uses DMC+EC as solvent. Nevertheless, the electrolyte using DMC+EC has higher conductivity and density. In consequence, a balance must be found between these properties.

4.2.Other electrolytes

Apart from the IL $BmimFeCl_4$, other electrolytes were prepared. A solution based on 1 M $FeCl_3 \cdot 6H_2O$ in DMC+EC in a ratio 1:1 was prepared mixing 0.5407 g $FeCl_3 \cdot 6H_2O$ with 2 ml of DMC+EC. This sample was stirred and after being completely dissolved it was dried using $CaCO_3$. Then, this electrolyte was tested in some batteries. Results are exposed in the section "4.4.battery performance" below.

Furthermore, an electrolyte consisting of 1 M $FePO_4$ in DMC+EC in a ratio 1:1 was made adding 0.3014 g $FePO_4$ in 2 ml of DMC+EC. This sample was stirred during a long period, but it could not be dissolved. Similarly, a solution of 1 M $Fe(CH_3COO)_3$ in DMC+EC=1:1 was prepared. The latter could not be dissolved either. From Figure 36, it can be seen how the left and right sample are unclear solution meaning that they are not dissolved. Hence, these electrolytes could not be tested in the batteries.

Figure 36. Electrolytes based on 1 M $Fe(CH_3COO)_3$, $FeCl_3$ and $FePO_4$ in DMC+EC, respectively from left to right.

4.3.Corrosion test

A corrosion test was performed in order to know which material is more suitable for the electrodes and it is not corroded by the electrolyte containing $BmimFeCl_4$. Different types of foils (aluminium-, nickel- and copper-foil) are tested and results are compared for the different solutions (5 %, 10 %, 15 %, 20 %, 30 %, 40%, 50 %, 60 % and 100 % $BmimFeCl_4$ in DMC and in EC+DMC) and periods of time (0 h, 24 h, 72 h and 1 week).

Firstly, some pictures were taken during the corrosion test in order to see the progress of the different foils immersed in the 5%, 10%, 15%, 20% and 100% $BmimFeCl_4$ in DMC. It was used a nickel-foil, an aluminium-foil and a copper-foil. The photos were taken at 0 h, 24 h, 72 h and 1 week. In Figure 37, it can be seen the starting point of the corrosion test.

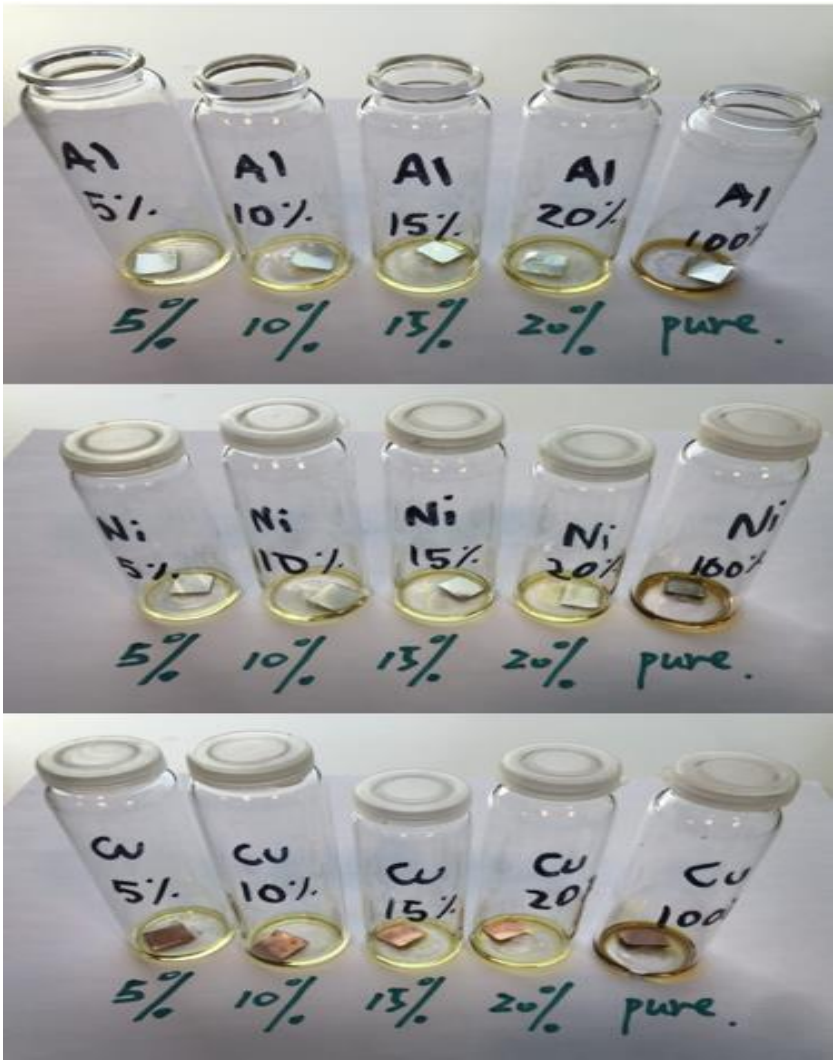

Figure 37. Corrosion test for various concentrations of $BmimFeCl_4$ in DMC at 0 h.

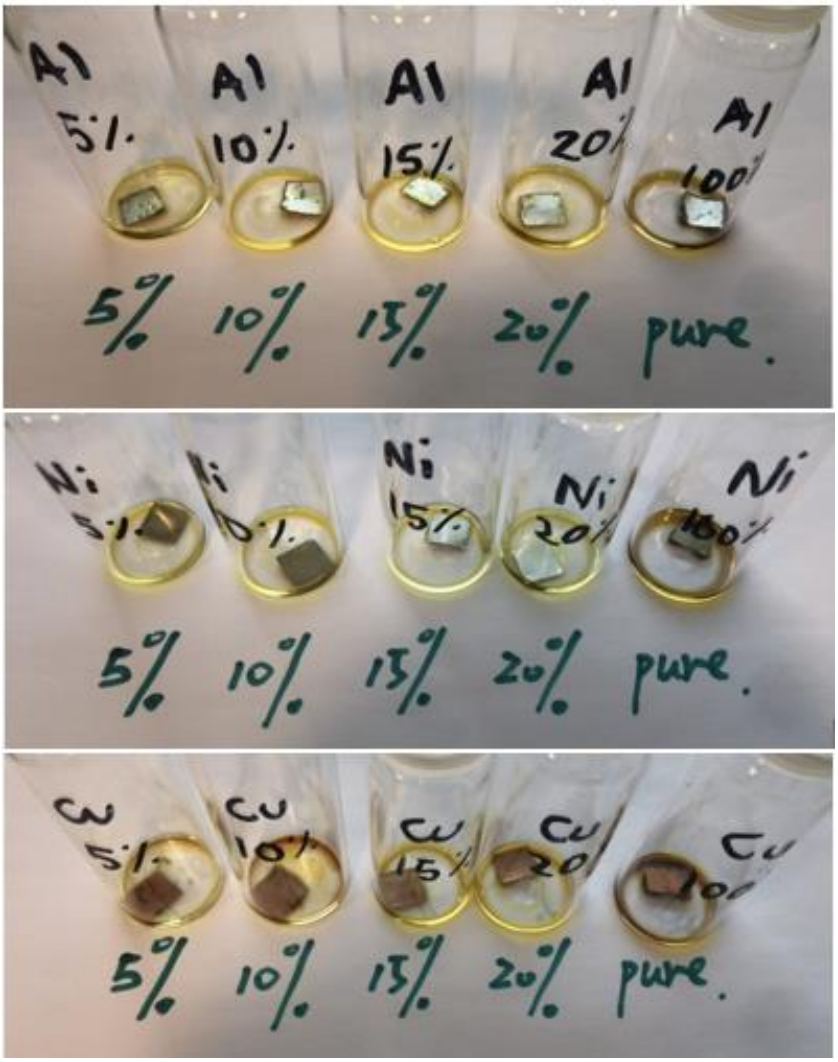

Figure 38. Corrosion test for various concentrations of $BmimFeCl_4$ in DMC after 24 h.

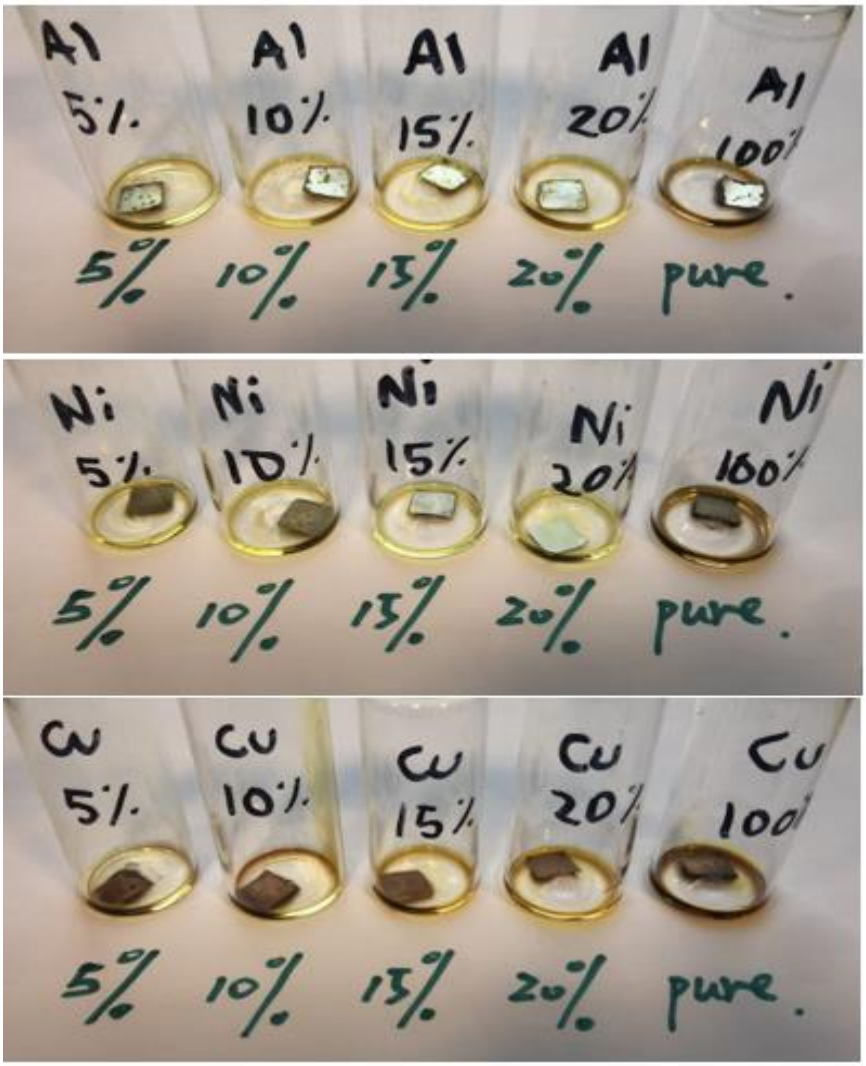

Figure 39. Corrosion test for various concentrations of $BmimFeCl_4$ in DMC after 72 h.

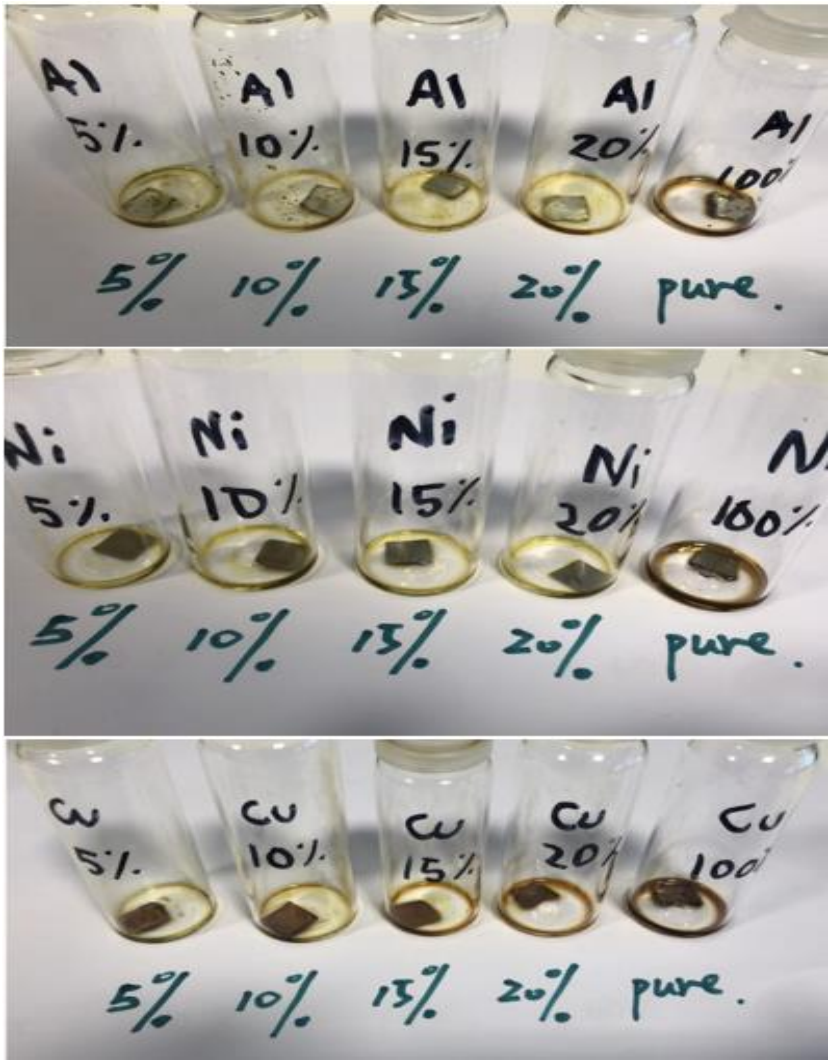

Figure 40. Corrosion test for various concentrations of $BmimFeCl_4$ in DMC after 1 week.

From Figure 38, it can be observed after 24 hours of corrosion test some foils start revealing some signs of corrosion. Specifically, all the samples containing aluminium-foil are already corroded after 24 hours. Moreover, 100 % IL in DMC solution has start corroding the nickel-foil and copper-foil. In addition, the first corrosion indications for 5 % and 10 % solutions in nickel-foil and copper-foil can be detected. These first indications can be confirmed after 72 hours, since from Figure 39 it can be seen how 5 % and 10 % $BmimFeCl_4$ in DMC has corroded, changing therefore the colour of the nickel- and copper-foil. Furthermore, the sample containing 15 % and 20 % IL in DMC has started corroding the copper-foil. On the other hand, some small signs start to appear after 72 hours in the nickel-foil immersed with 15 % solution. Hence, at this point of the test (after 72 hours) it can be claimed that the nickel-foil immersed with 20 % $BmimFeCl_4$ in DMC is the only one that does not present any corrosion signs.

Finally, as seen from Figure 40, after 1 week even 15 % and 20 % samples containing nickel- and copper-foil have been noticeably corroded. Thus, all the foils have been corroded by the different solutions of $BmimFeCl_4$ in DMC after 1 week. However, it can be concluded that the aluminium-foil is not suitable for using in solutions based on $BmimFeCl_4$ in DMC as after the first 24 hours of the test the aluminium-foils had been already corroded. Conversely, it has been proved that the nickel-foil is the most corrosion resistant when it is immersed in a solution of 20 % $BmimFeCl_4$ in DMC. The copper-foil immersed in the latter solution also shows some resistance to corrosion.

After the latter conclusions, further experiments regarding corrosion by more concentrated solutions were done. Results using 30 %, 40 %, 50 % and 60 % $BmimFeCl_4$ in DMC with aluminium-foil, nickel-foil and copper-foil are shown in Figure 41, Figure 42 and Figure 43, respectively.

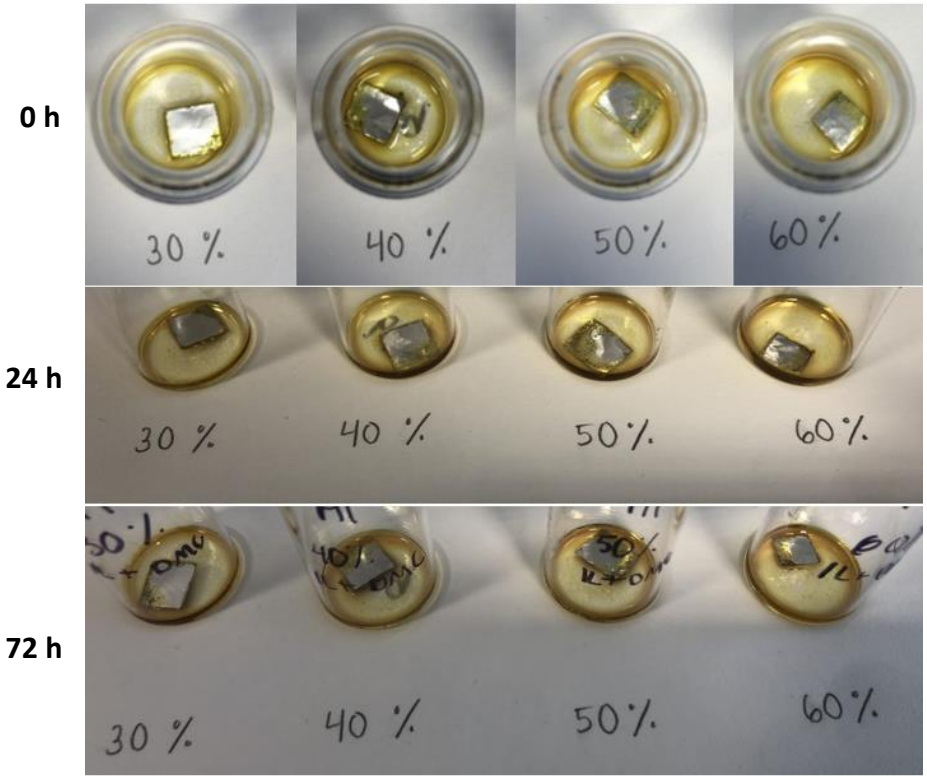

Figure 41. Corrosion test for additional concentrations of $BmimFeCl_4$ in DMC with Al-foil.

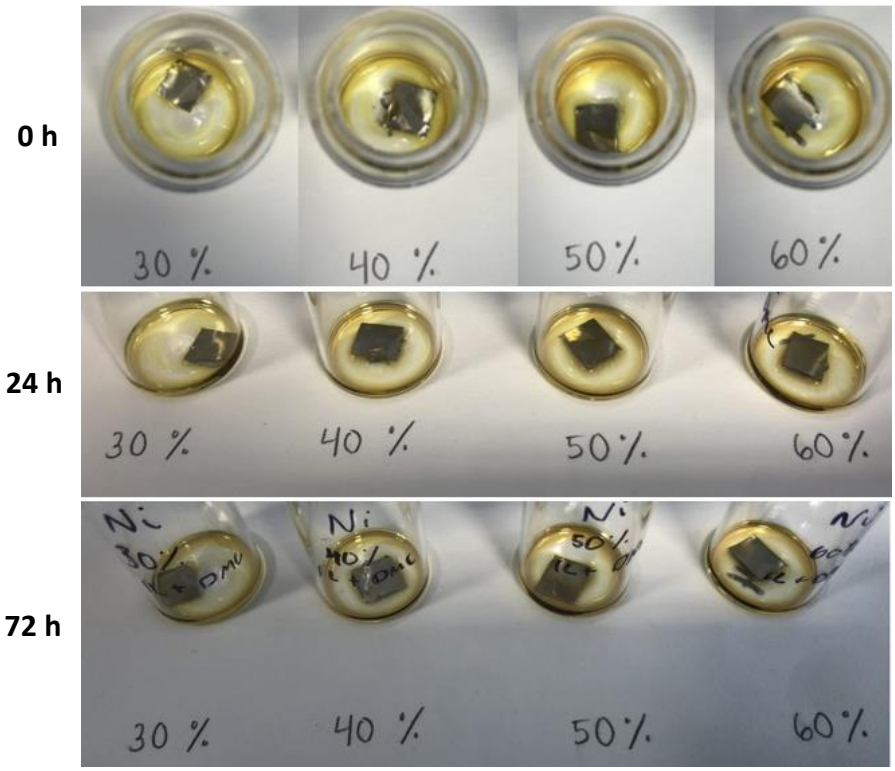

Figure 42. Corrosion test for additional concentrations of $BmimFeCl_4$ in DMC with Ni-foil.

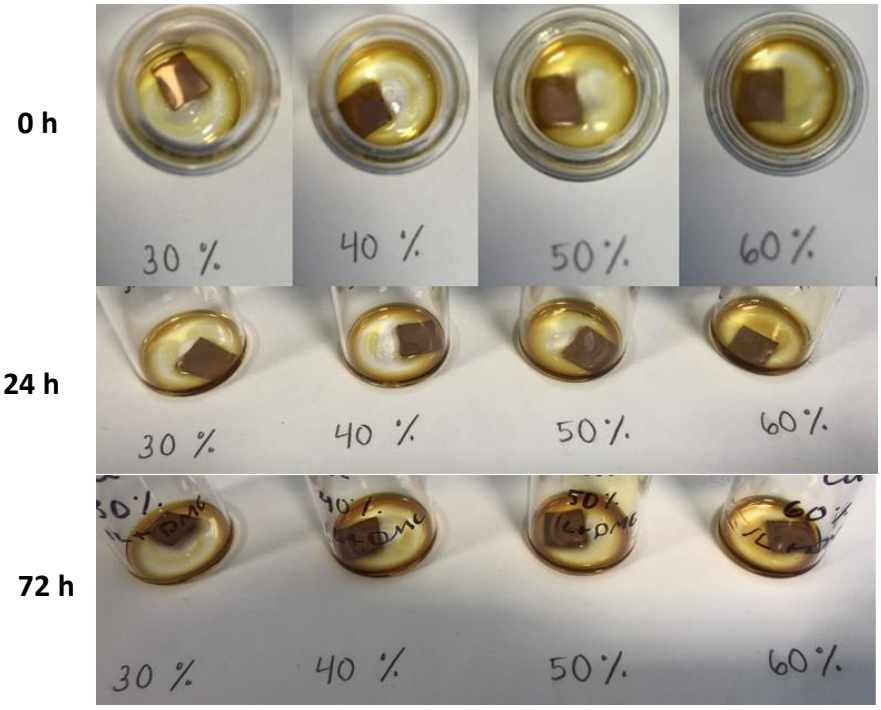

Figure 43. Corrosion test for additional concentrations of $BmimFeCl_4$ in DMC with Cu-foil.

From Figure 41, it can be seen that the aluminium-foil is corroded by the solutions after 24 hours. Some signs appear at the same time this foil is in contact with the solutions, and as the times passes the aluminium-foil gets more corroded.

From Figure 42 and Figure 43, it appears that the nickel-foil and copper-foil are not corroded by the 30 %, 40 %, 50 % and 60 % $BmimFeCl_4$ in DMC before 72 hours. This experiment should be controlled during weeks and months in order to prove that Ni-foil and Cu-foil are corrosion resistant to these solutions even as time goes by.

On the other hand, the same corrosion experiments were conducted using solutions of $BmimFeCl_4$ in EC+DMC. In Figure 44, Figure 45 and Figure 46, pictures showing the results of the corrosion test depending on the percentage of solution, waiting time and type of foil can be analysed.

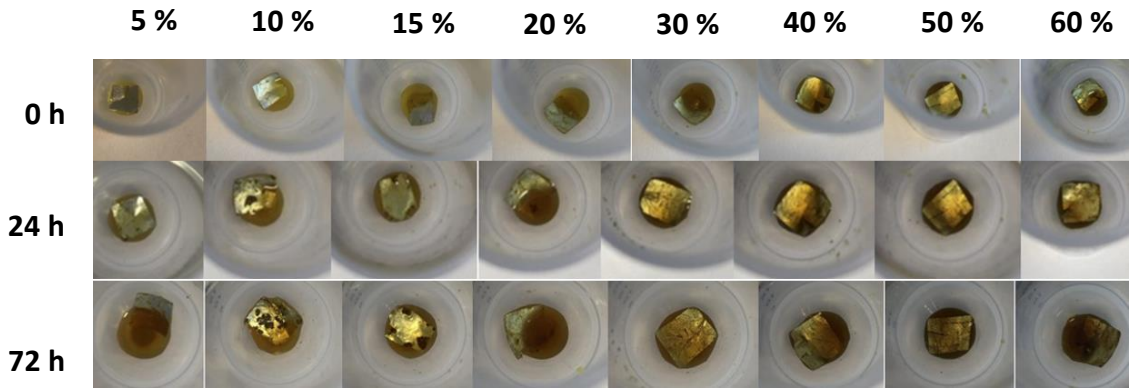

Figure 44. Corrosion test for various concentrations of $BmimFeCl_4$ in EC+DMC with Al-foil.

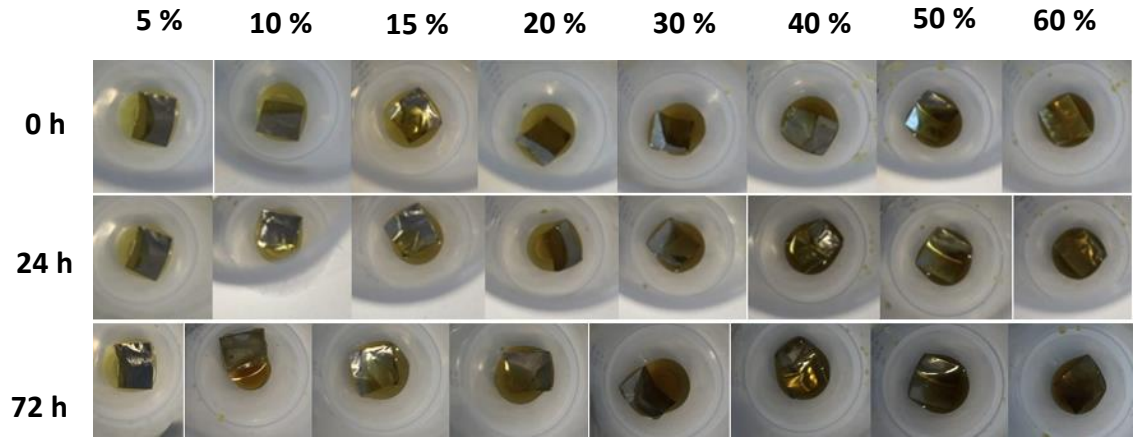

Figure 45. Corrosion test for various concentrations of $BmimFeCl_4$ in EC+DMC with Ni-foil.

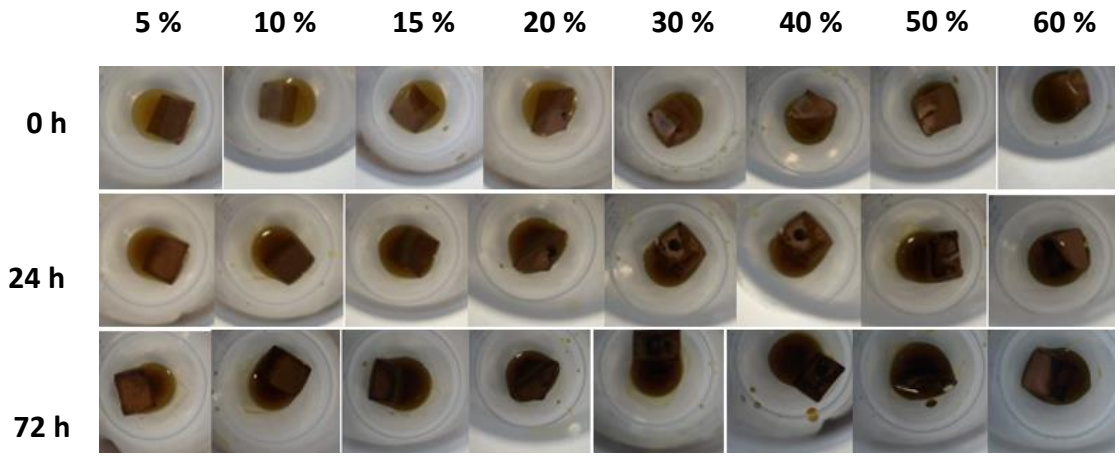

Figure 46. Corrosion test for various concentrations of $BmimFeCl_4$ in EC+DMC with Cu-foil.

From Figure 44, it can be seen how the aluminium-foil has been corroded by all the different percentages of IL in EC+DMC after 24 hours. This corrosion is stronger after 72 hours from the start of the experiment. The corrosion signs in the aluminium-foil are especially observed in the solution of 10 % and 15% $BmimFeCl_4$ in EC+DMC.

From Figure 45 and Figure 46, it can be stated that no signs of corrosion appear in nickel-foil and copper-foil before 72 hours when using different percentages of IL in EC+DMC. In order to prove that the nickel-foil and the copper-foil are corrosion resistant to these solutions further experiments should be done for longer periods of time.

To sum up, it can be claimed that the aluminium-foil is not a good material to use for the electrodes when the electrolyte is a solution based on $BmimFeCl_4$ in DMC or in EC+DMC. However, the nickel-foil seems to be corrosion resistant when using 20 % $BmimFeCl_4$ in DMC. The 15 % solution with the latter foil also shown great results. The copper-foil could also be a good material when using 15 % and 20 % IL in DMC. Moreover, the nickel-foil and copper-foil showed excellent results when these are immersed in solutions of $BmimFeCl_4$ in EC+DMC for 72 hours. Nevertheless, the latter should be controlled during weeks and months to be able to claim that they could be used in the electrodes without being corroded.

4.4.Battery performance

4.4.1. Landt Battery Testing System

Fifteen batteries were prepared with different percentage of ionic liquids in the electrolyte. All these were produced following the same method explained in "3.3.5. Method for assembling the batteries". However, the mass of the anode and cathode differ from each battery as the electrodes are prepared manually and when the active materials are added to the nickel-foil with a doctor-blade the accuracy is not 100%. In Table 9, it can be seen the mass of each electrode and type of electrolyte used is each battery.

	Mass anode (g)	Mass cathode (g)	Electrolyte (20µl)
Battery HA1-HC1	0.0232	0.0204	100% $BmimFeCl_4$
Battery HA2-HC2	0.0237	0.0211	100% $BmimFeCl_4$
Battery HA3-HC3	0.0235	0.0207	100% $BmimFeCl_4$
Battery HA4-HC4	0.0234	0.0197	100% $BmimFeCl_4$
Battery HA5-HC5	0.0233	0.0209	100% $BmimFeCl_4$
Battery HA6-HC6	0.0228	0.0203	100% $BmimFeCl_4$
Battery HA7-HC7	0.0230	0.0207	30% $BmimFeCl_4$ in DMC+EC
Battery HA8-HC8	0.0235	0.0195	30% $BmimFeCl_4$ in DMC+EC
Battery HA9-HC9	0.0235	0.0202	30% $BmimFeCl_4$ in DMC+EC
Battery HA10-HC10	0.0222	0.0192	30% $BmimFeCl_4$ in DMC+EC
Battery HA11-HC11	0.0237	0.0209	0.5 M $BmimFeCl_4$ in DMC+EC
Battery HA12-HC12	0.0233	0.0201	5% $BmimFeCl_4$ in DMC+EC
Battery HA13-HC13	0.0228	0.0204	40% $BmimFeCl_4$ in DMC+EC
Battery HA14-HC14	0.0226	0.0191	100% $FeCl_3$
Battery HA15-HC15	0.0230	0.0220	100% $FeCl_3$

Table 9. Mass of the electrodes and electrolyte for each battery prepared.

All the batteries shown in Table 9 were tested on the Landt Battery Testing System. Nevertheless, only Battery HA1-HC1, Battery HA3-HC3, Battery HA4-HC4 and Battery HA5-HC5 worked correctly. These four batteries which were working are the ones prepared with 20 µl of 100 % $BmimFeCl_4$ as electrolyte.

Different methods of charge-discharge were tested. The methods can be grouped in 3 types depending on which parameters were changed.

4.4.1.1. First method tested

Firstly, "Method 1" was implemented to each battery. This method had different conditions written in the code as it can be seen in Figure 47.

Stp	Variables	Mode	End Cond1	(And) End Cond2	GOTO	Log Cond
1		Charge CC: 1 mA	Voltage >= 2.2 V		Next Step	01:00
2		Charge CV: 2.2 V	Current <= 0.01 mA		Next Step	01:00
3		Discharge CC: 1 mA	Voltage <= 0.1 V		Next Step	01:00
4		<IF>	Cycle <= 100 Times		1	
5		<IF>			End_OK	

Figure 47. Code implemented for "Method 1".

This method means that the battery is charged at a constant current of 1 mA while the voltage of the battery is equal to or less than 2.2 V. Once the voltage of the battery is equal to or more than 2.2V, the battery is charged at a constant voltage of 2.2 V until the current decreases to a value equal to or less than 0.01 mA. When this happens, the battery is discharged at a constant current of 1 mA until the voltage is equal to or less than 0.1 V. Then, this cycle made of three steps will be repeated for 100 times.

Results obtained after implementing "Method 1" are compared for the four batteries which worked correctly. Since it has been checked that the four batteries behave similarly, only the results for Battery HA4-HC4 will be represented.

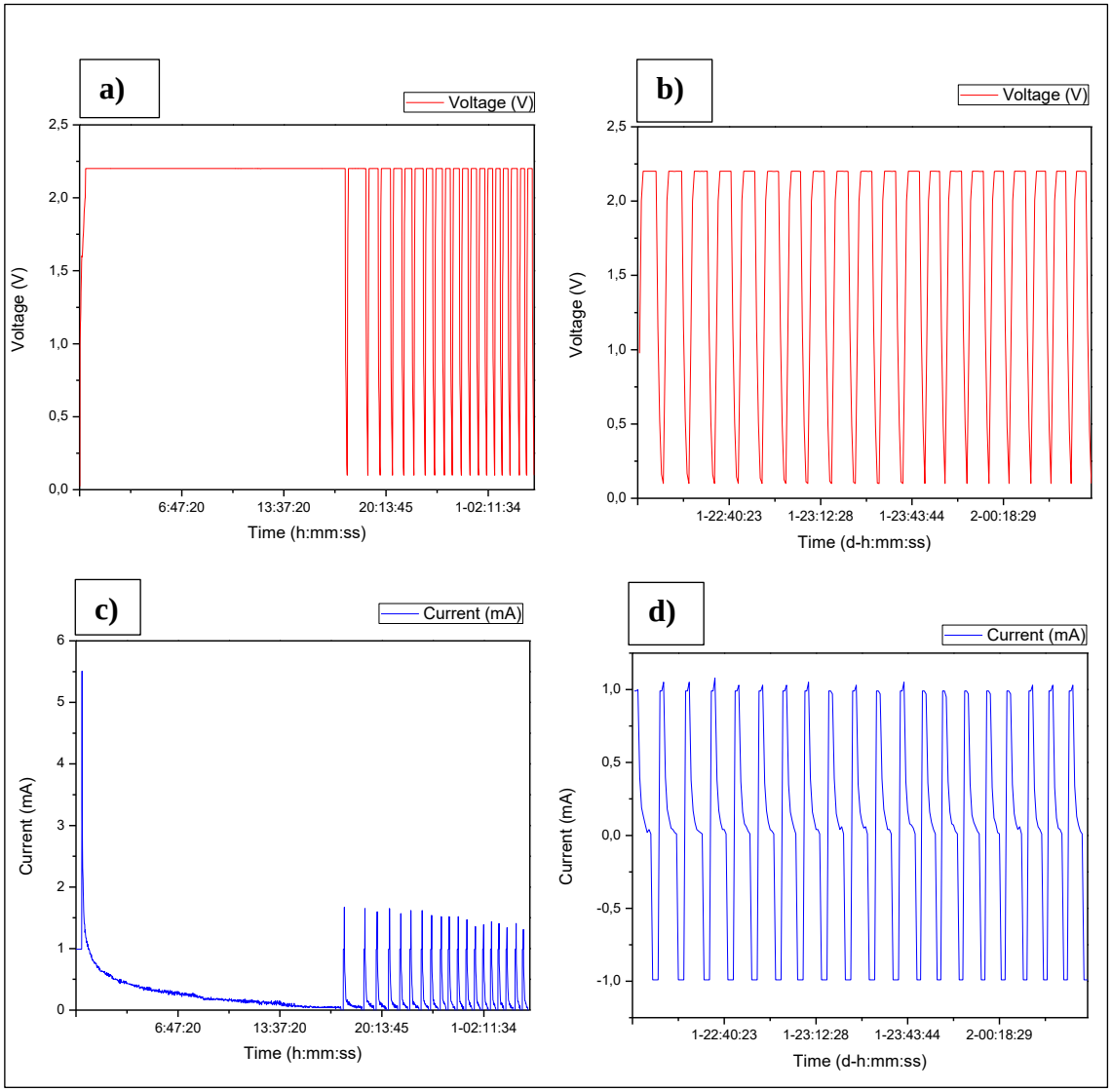

Figure 48. Plot Voltage vs. Time (a and b) and Current vs. Time (c and d) for the first 20 cycles (a and c) and for the last 20 cycles (b and d) using "Method 1" in the Battery HA4-HC4.

From Figure 48, it can be seen that the first cycle of the method takes around 17 hours while the other cycles take only 8 minutes. This is due since in the first cycle of charging and discharging a battery a chemical reaction takes place between the electrolyte and the surface of the electrodes. However, after the first cycle it can be seen how the battery behaves in the same way. Thus, in Figure 48 b and d, the last 20 cycles of the charge-discharge test of the battery are showed to prove that the data obtained is the same. Furthermore, in Figure 48, it can be stated that the battery run properly as it is following the conditions implemented in the "Method 1" explained above.

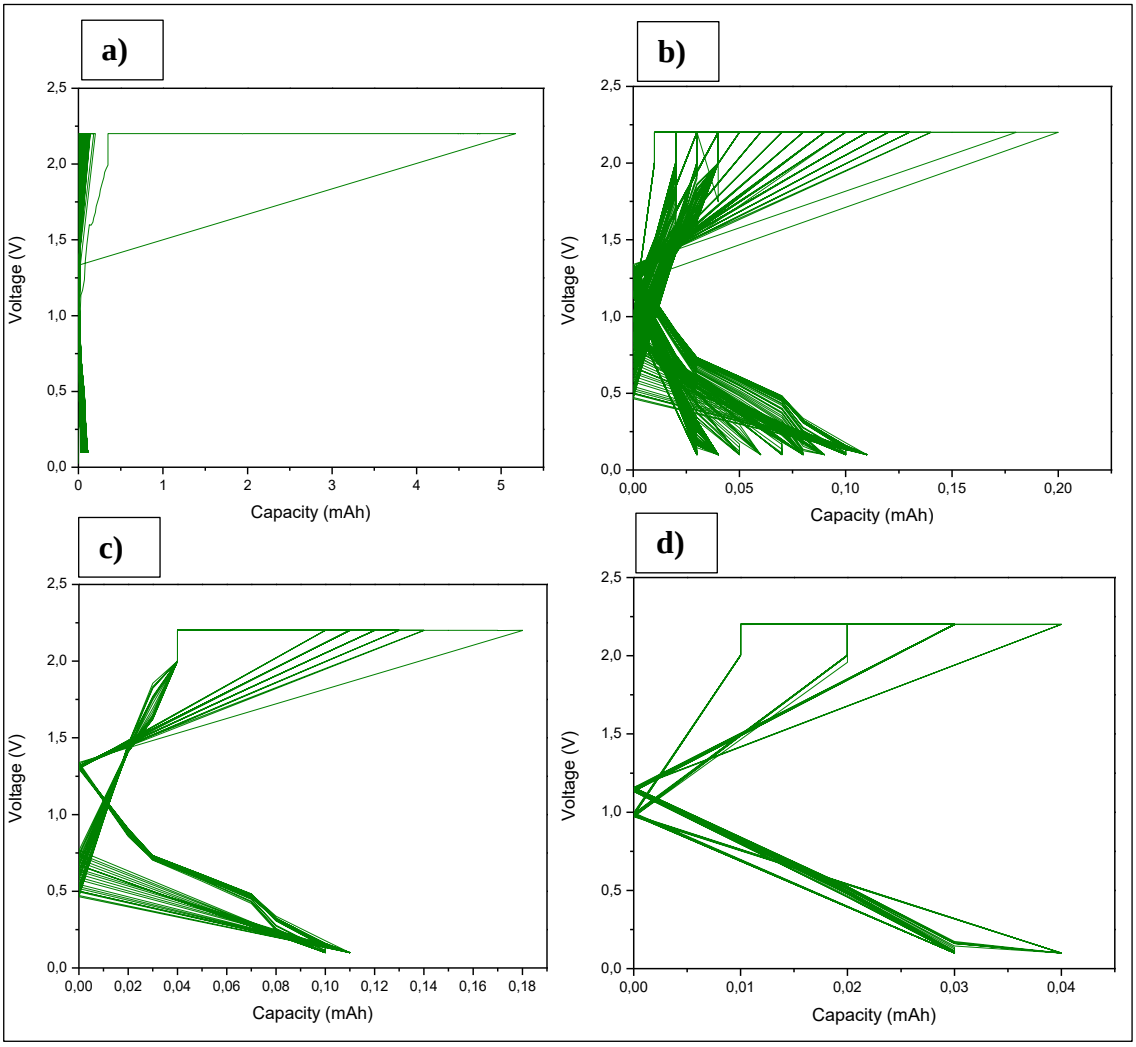

Figure 49. Plot Voltage vs. Capacity for 100 cycles (a), for 2-100 cycles (b), for 2-22 cycles (c), for 80-100 cycles (d); using the method "Method 1" in the Battery HA4-HC4.

In Figure 49 a) the capacity of the battery is plotted against the voltage for the 100 cycles that last the test. The battery reaches 5 mAh of capacity in the first cycle due to the chemical reaction that takes place. However, when the data from the first cycle is removed the result is plotted in Figure 49 b). Thus, from the 2nd cycle until the cycle 100 the battery only reaches around 0.2 mAh in one cycle and decreases for the others. Comparing from Figure 49 c) and d) it can be proved that the battery has higher capacity in the first cycles than in the latest ones. In the last 20 cycles the battery has really low capacity, achieving values around 0.02 mAh.

Another important parameter about the battery is its specific capacity. The specific capacity will be represented in the units mAh/g and it is the capacity divided by the active materials of the cathode. This is because the capacity of the cathode is less than the one of the anode since the active material of the anode is graphite which allows to have a very

high capacity of around 600 mAh. Thus, the specific capacity of the battery will be determined by the weight of the active materials of the cathode. This value is obtained for each battery when the total weight of the cathode used is subtracted from the average weight of the nickel-foil used as a current collector. This value is 18.539 mg and it was obtained from weighing 20 different 12 mm diameter nickel-foil circles. As the cathode for the Battery HA4-HC4 weighed 0.0197 g, the amount of active materials in the cathode is:

$$Active\ materials\ HC4 = 19.7 - 18.539 = 1.161\ mg$$

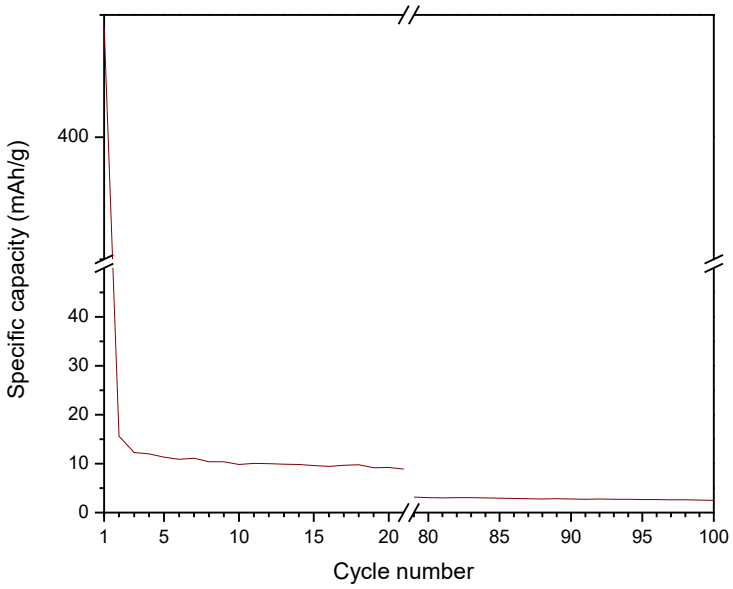

Figure 50. Specific capacity vs. Cycle number when using "Method 1" in the Battery HA4-HC4.

From Figure 50, it can be seen that the specific capacity for the Battery HA4-HC4 when "Method 1" is implemented shows one high peak in the first cycle due to the chemical reaction. After the 5^{th} cycle it remains practically constant with a slightly negative slope starting. Thus, in the 5^{th} cycle the specific capacity is around 12 mAh/g and it decreases constantly reaching a value of 2.5 mAh/g in the last cycle.

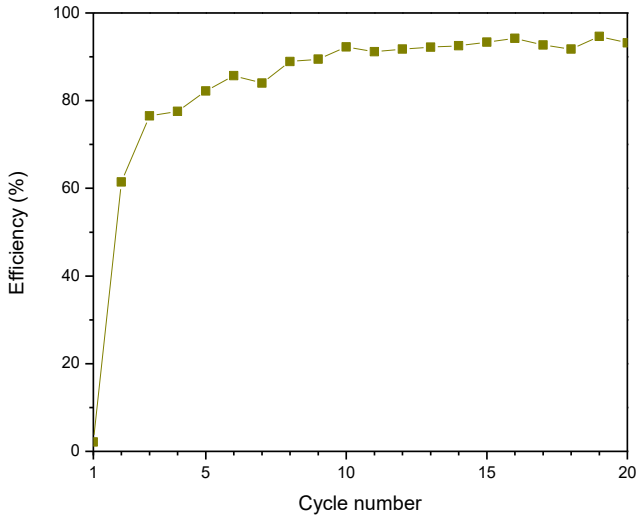

Figure 51. Efficiency (%) vs. Cycle number for the 20 first cycles of "Method 1" in the Battery HA4-HC4.

Finally, Figure 51 shows the efficiency of the Battery HA4-HC4 when using "Method 1" only for the 20 first cycles as it remains almost the same until cycle number 100. It can be observed that the efficiency increases rapidly from cycle 1 until cycle 10 and after these it remains around 90 %.

After studying all the data obtained for "Method 1" for the four batteries working (Battery HA1-HC1, Battery HA3-HC3, Battery HA4-HC4 and Battery HA5-HC5) and verifying that they all perform in the same way (all the plots are similar to the ones presented above for the Battery HA4-HC4), others tests are implemented.

4.4.1.2. Charging rate influence

A group of methods are written in the software of the Landt Battery Testing System to see how the charging rate will influence the performance of the battery. The code written for the method with highest charging rate of this group is showed in Figure 52. The yellow squares highlight the parameters that will be changed in this group of methods, these are the constant current charge and the constant current discharge.

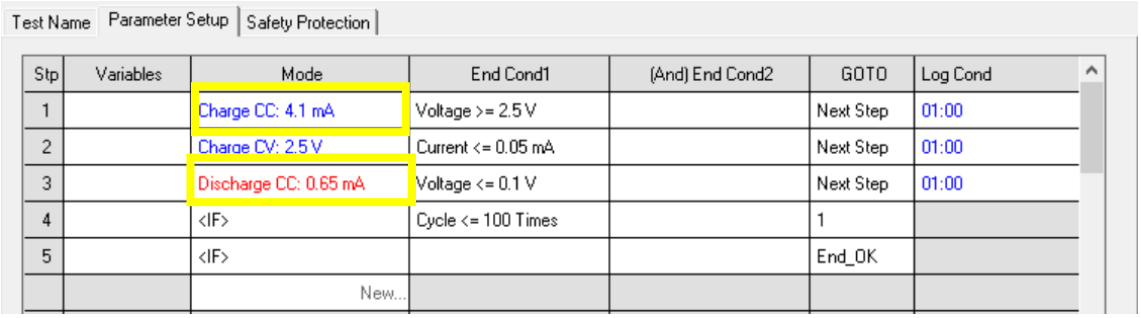

Figure 52. Code for the methods implemented changing the constant current charge and constant current discharge

The Battery HA4-HC4 showed that its highest capacity (without considering the one of the first cycle) is 0.18 mAh. This means that if we charge the battery for 1 hour it achieves its 100 % capacity. Considering the latter and that the method charges the battery at a constant current of 4.1 mA, the charging rate for this battery is:

$$\frac{4.1}{0.18} = 22.8\ \text{C}$$

Table 10 shows the methods implemented to study how the charging rate affects the data. Additionally, the values for the constant current charge and constant current discharge are also presented in Table 10. Thus, these values are the ones which are changed in the yellow boxes in Figure 52 for each method. Finally, the last column of Table 10 calculates the charging rate.

Name of method	Constant Current Charge (mA)	Constant Current Discharge (mA)	Charging rate
2.5V- 22.8 C	4.1	0.65	4.1/0.18 = 22.8
2.5V- 18.2 C	3.28	0.52	3.28/0.18 = 18.2
2.5V- 13.7 C	2.46	0.39	2.46/0.18 = 13.7
2.5V- 9.1 C	1.64	0.26	1.64/0.18 = 9.1
2.5V- 4.6 C	0.82	0.13	0.82/0.18 = 4.6
2.5V- 2.3 C	0.41	0.13	0.41/0.18 = 2.3

Table 10. Methods tested to see how the charging rate affects the performance of the batteries.

All the methods showed in Table 10 were tested on Battery HA1-HC1, Battery HA3-HC3, Battery HA4-HC4 and Battery HA5-HC5. The results obtained for each of these batteries were studied to prove that they perform the same way as they are prepared with

the same electrolyte. In the following figures the results for the Battery HA4-HC4 will be showed as an example of how these four batteries work when the methods specified in Table 10 are implemented.

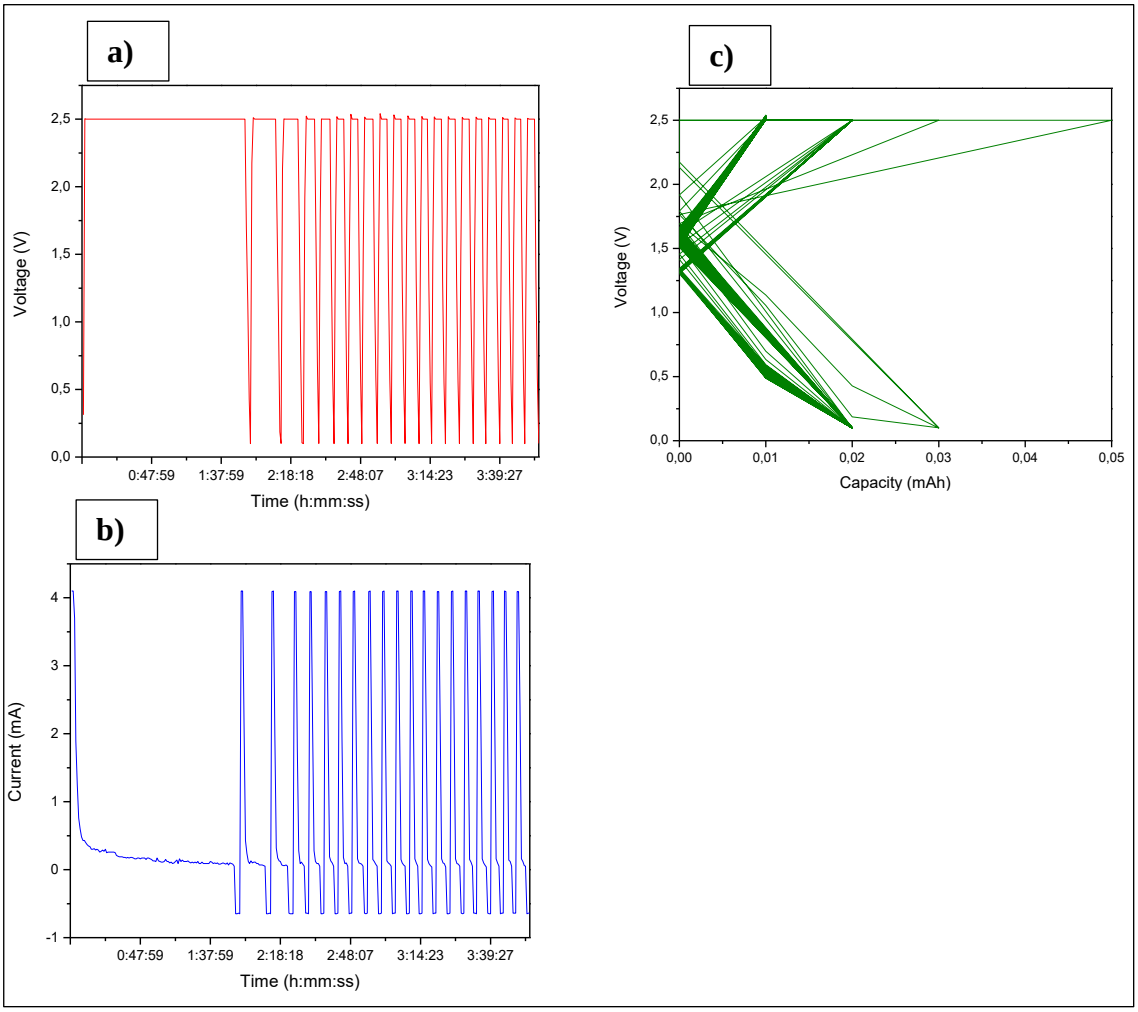

Figure 53. Plot Voltage vs. Time (a) and Current vs. Time (b) for the first 20 cycles; plot Voltage vs. Capacity for the 100 cycles (c) using the method "2.5V- 22.8 C" in the Battery HA4-HC4.

On the one hand, Figure 53 a) and b) shows that the Battery HA4-HC4 takes around 3 hours 52 minutes to complete the first 20 cycles of the method "2.5V- 22.8 C". Additionally, it takes 1 hour 57 minutes to charge and discharge the battery for the first cycle. However, once the first cycle have been completed the battery takes around 5 minutes in each of the next 99 cycles to be charged with a charge constant current of 4.1 mA and discharged with a discharge constant current of 0.65 mA until the voltage is equal to or less than 0.1 V, keeping a constant voltage of 2.5 V in the battery while the current is equal or higher than 0.05 mA.

On the other hand, Figure 53 c) shows that in the first cycle the Battery HA4-HC4 reaches a capacity of 0.05 mAh due to the chemical reaction that always takes place in the first charge-discharge cycle. However, the charge capacity of the battery starts decreasing while the number of cycles performed increases. Thus, it can be observed some peaks showing 0.03 mAh, 0.02 mAh and in the last cycles of the test the battery has 0.01mAh of capacity.

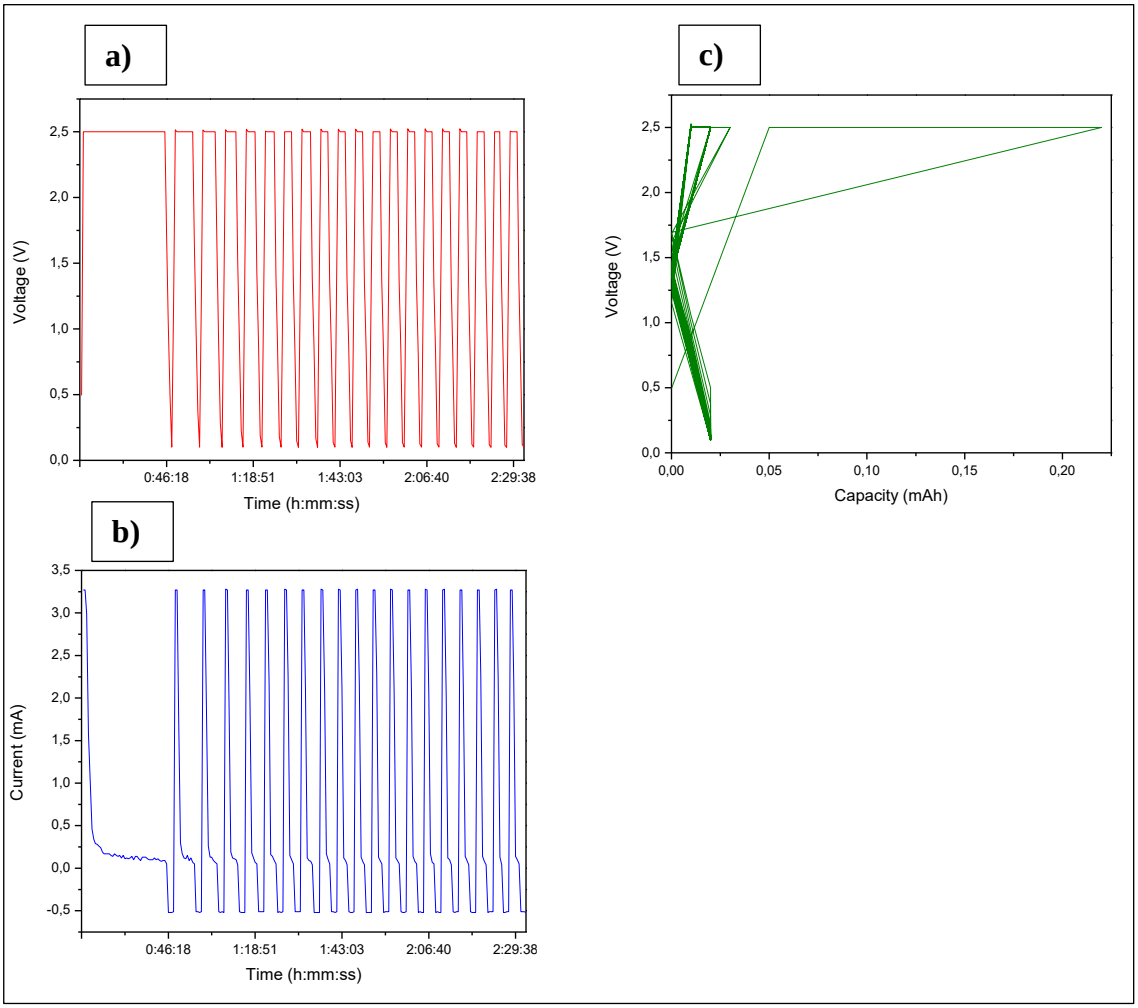

Figure 54. Plot Voltage vs. Time (a) and Current vs. Time (b) for the first 20 cycles; plot Voltage vs. Capacity for the 100 cycles (c) using the method "2.5V- 18.2 C" in the Battery HA4-HC4.

From Figure 54 a) and b), it can be seen how the Battery HA4-HC4 is being charged and discharged just like the code in the method "2.5V- 18.2 C" requires. Hence, the battery is being charged with a charge constant current of 3.28 mA and discharged with a discharge constant current of 0.52 mA keeping a constant voltage of 2.5 V in the battery while the current is equal to or higher than 0.05 mA. Using this method which has a

charging rate of 18.2 the normal capacity, the first 20 cycles takes around 2 hours 30 minutes and the first cycle is finished after 47 minutes. After the first cycle, the battery is charged and discharged in approximately 4 minutes.

Figure 54 c) shows that the Battery HA4-HC4 reaches in the first cycle a capacity of 0.22 mAh (much more higher than using the method "2.5V- 22.8 C") but the next 99 cycles the capacity of the battery reaches only 0.02 mAh when the voltage is 2.5 V and around 0.1 V. Nevertheless, when using the method "2.5V- 18.2 C" the performance Voltage vs. Capacity of the Battery HA4-HC4 is more stable than when using the method "2.5V- 22.8 C".

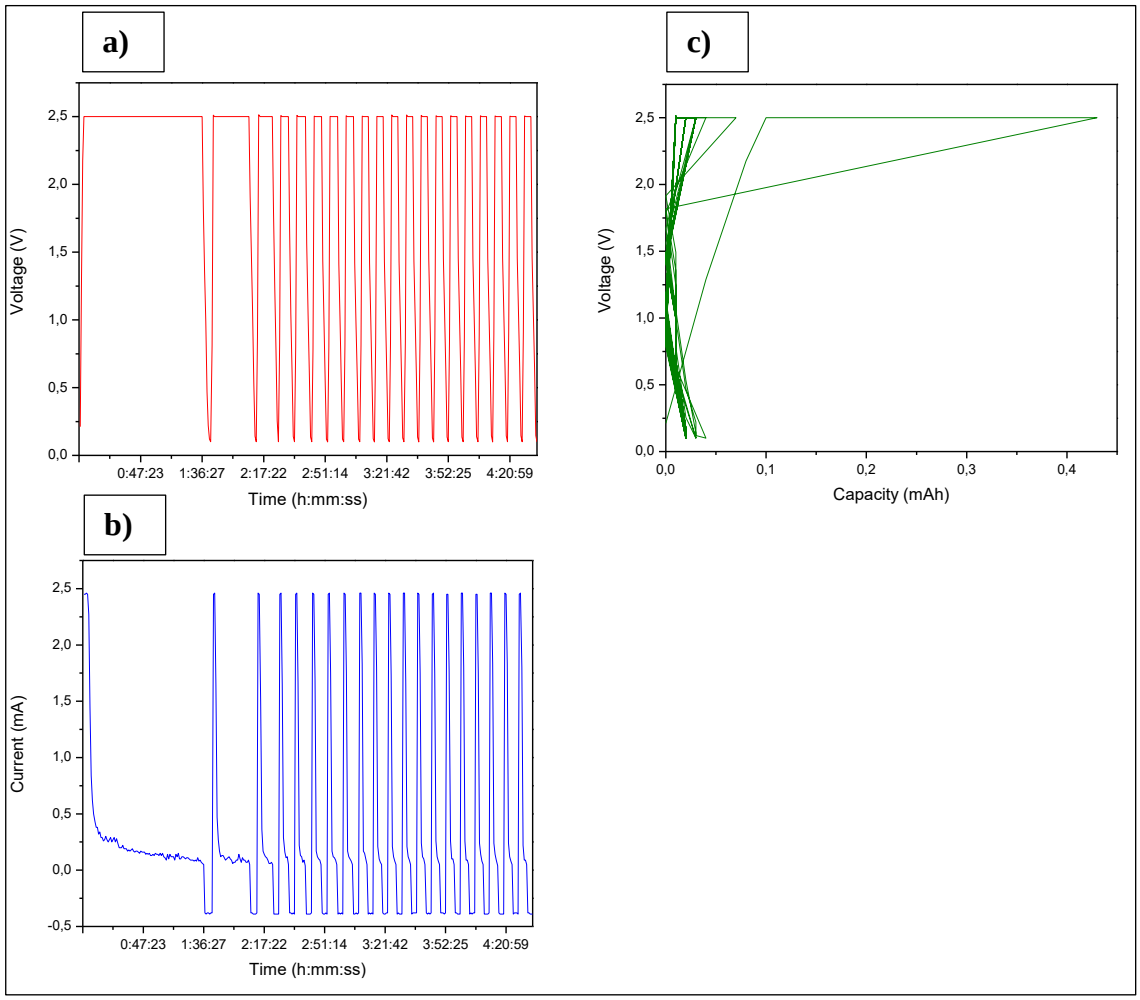

Figure 55. Plot Voltage vs. Time (a) and Current vs. Time (b) for the first 20 cycles; plot Voltage vs. Capacity for the 100 cycles (c) using the method "2.5V- 13.7 C" in the Battery HA4-HC4.

As it appears in Figure 55 a) and b), when testing the method "2.5V- 13.7 C" in the Battery HA4-HC4, the latter is charged with a charge constant current of 2.46 mA and

discharged with a discharge constant current of 0.39 mA keeping a constant voltage of 2.5 V while the current is equal to or higher than 0.05 mA. The first cycle takes around 1 hour 37 minutes to be completed while the rest ones take only 7 minutes.

Furthermore, with the method "2.5V- 13.7 C" the capacity of the Battery HA4-HC4 rises until 0.43 mAh as it can be observed from Figure 55 c). From the second cycle until the last cycle the battery shows a capacity of around 0.02 mAh.

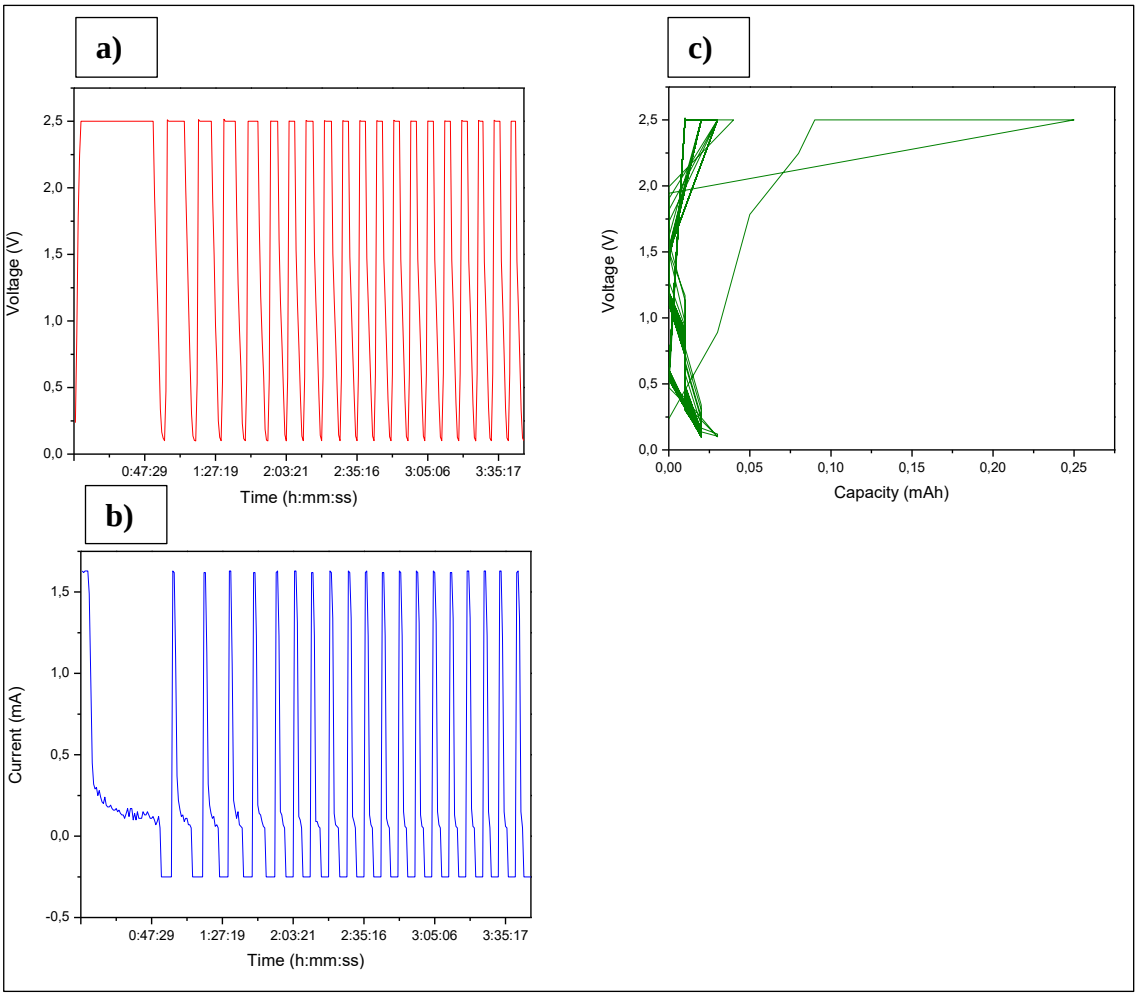

Figure 56. Plot Voltage vs. Time (a) and Current vs. Time (b) for the first 20 cycles; plot Voltage vs. Capacity for the 100 cycles (c) using the method "2.5V- 9.1 C" in the Battery HA4-HC4.

Following this sequence of methods, the Battery HA4-HC4 works just as the method "2.5V- 9.1 C" requires in its code with a charge constant current of 1.64 mA and a discharge constant current of 0.26 mA, consequently plotting the diagrams showed in Figure 56. From the latter it must be highlighted that the first charge-discharge cycle lasts 1 hour while the rest ones takes 6 minutes. In addition, the capacity increases until 0.25

mAh in the first cycle and it remains fluctuating around 0.02 mAh when the highest and lowest voltages take place. Nevertheless, the sequence voltage-capacity varies more often than in the other methods tested above.

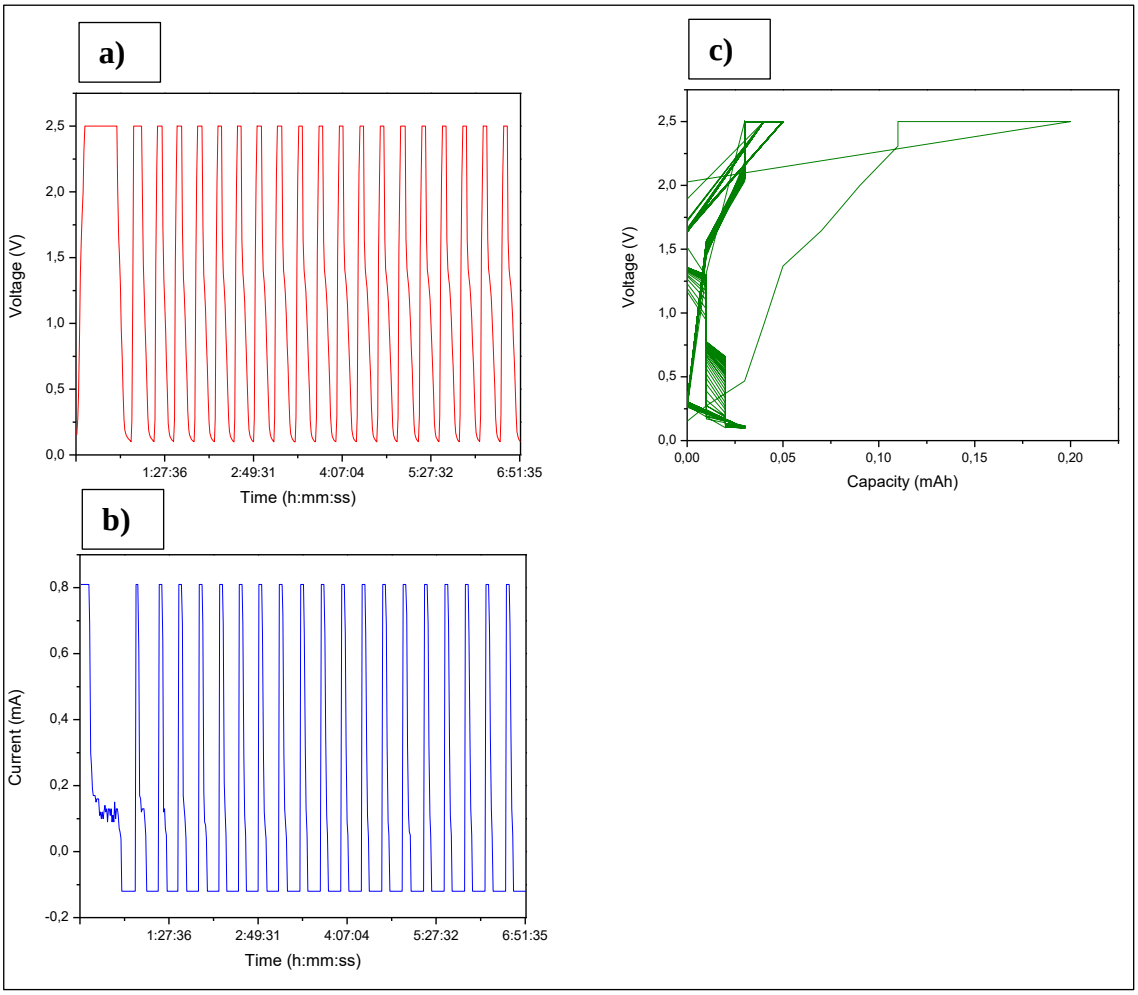

Figure 57. Plot Voltage vs. Time (a) and Current vs. Time (b) for the first 20 cycles; plot Voltage vs. Capacity for the 100 cycles (c) using the method "2.5V- 4.6 C" in the Battery HA4-HC4.

From Figure 57 a) and b), it can be seen that when testing the method "2.5V- 4.6 C" in the Battery HA4-HC4, the latter only takes 58 minutes to be charged with a constant current of 0.82 mA and discharged at 0.13 mA with a voltage of 2.5 V when the current is equal to or higher than 0.05 mA. From the second cycle until the hundred cycle each one lasts for around 15 minutes.

Similarly, from Figure 57 c), it can be seen that the Battery HA4-HC4 reaches 0.2 mAh as its highest capacity when the method "2.5V- 4.6 C" is tested. For the rest of the cycles the capacity ranges from 0.04 to 0.01 mAh.

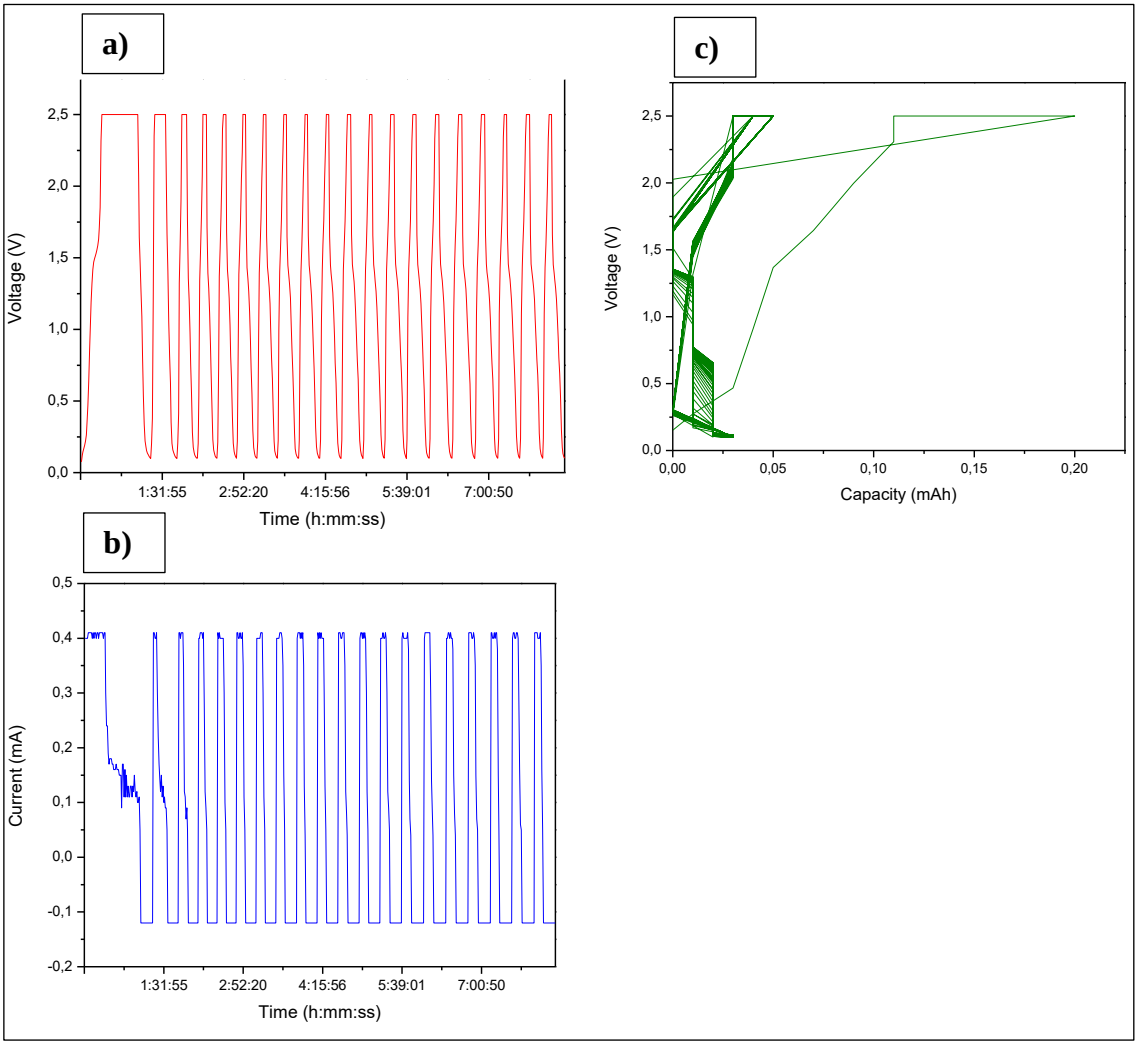

Figure 58. Plot Voltage vs. Time (a) and Current vs. Time (b) for the first 20 cycles; plot Voltage vs. Capacity for the 100 cycles (c) using the method "2.5V- 2.3 C" in the Battery HA4-HC4.

Finally, when the method with lowest charging rate is tested in the Battery HA4-HC4 (method "2.5V- 2.3 C") the results show the plots in Figure 58. The battery takes 1 hour 20 minutes to be charged with a constant current of 0.41 mA until reaching a voltage of 2.5 V and discharged with a constant current of 0.13 mA until the voltage is equal to or less than 0.1 V. For the rest of the cycles, each one lasts around 23 minutes. In this method, the battery also reaches 0.2 mAh as its highest capacity. Moreover, when comparing Figure 57 and Figure 58, it can be stated that the performance of the Battery HA4-HC4 is almost the same when using the method "2.5V- 4.6 C" and the method "2.5V- 2.3 C".

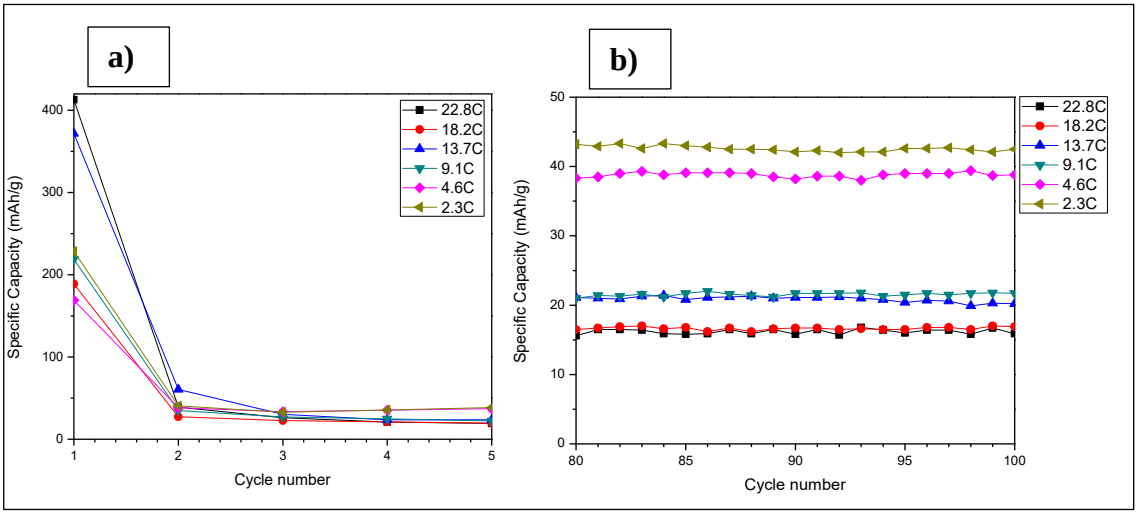

Figure 59. Plot Specific capacity vs. Cycle number for the first 5 cycles (a) and for the last 20 cycles (b) using the different methods showed in Table 10 in the Battery HA4-HC4.

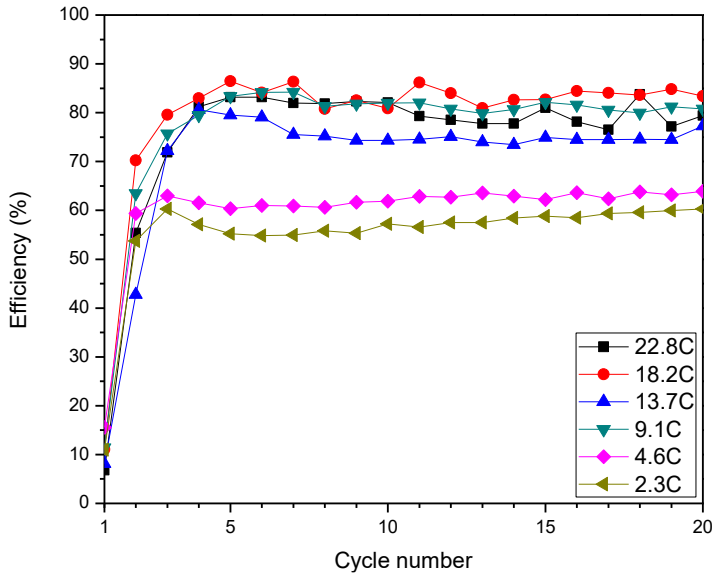

Figure 60. Plot Efficiency vs. Cycle number for the different methods showed in Table 10 in the Battery HA4-HC4.

To sum up, in order to see how the charging rate can affect the battery performance the specific capacity and efficiency of each method are plotted versus the cycle number in Figure 59 and 60, respectively.

From Figure 59, it can be stated that the specific capacity of the battery is higher when the charging rate is lower. Thus, when we use a very low charging rate, as for example in the method "2.5V-2.3C" the specific capacity is around 44 mAh/g. However, when the charging rate is high, as in the method "2.5V- 22.8 C", the specific capacity is

only 16 mAh/g. However, Figure 59 b) also shows that when the charging rate is very high the specific capacity can be almost the same when the charging rate does not differ too much between methods. Thus, the specific capacity for the method “2.5V- 22.8 C” and “2.5V- 18.2 C” is essentially the same. Equally, the method “2.5V- 13.7 C” and “2.5V- 9.1 C” show a similar specific capacity. It is known that if the charging rate is lower, the battery will be on charge for longer, but the accuracy will be better. Consequently, the specific capacity of the battery will be higher.

In Figure 60 the efficiency of the Battery HA4-HC4 is shown for the first 20 cycles as it remains practically constant until the last cycle. From this Figure, it can be seen that the efficiency of the battery is gets worser when the charging rate is very low. Thus, the efficiency when using the method “2.5V- 2.3 C” is the worser reaching only 60 % after several cycles. Additionally, the efficiency for the method “2.5V- 2.3 C” remains very low at around 65 %. Nevertheless, when the charging rate is very y high, the efficiency is high and don’t differ a lot from one method to another. That is the reason why the efficiency for the four methods which highest charging rate varies around 80 %.

4.4.1.3. Voltage influence

The voltage is another parameter that can be changed in the method to see how it influences the performance of the battery. Thus, in this group of methods the battery will be always charged and discharged at a constant current of 1 mA. However, the charging mode will stop when the voltage is equal to or higher than the voltage it has been implemented in that specific method. For instance, the method shown in Figure 61 will stop charging at 2 V. Then, the voltage of the battery will remain constant at that exact value imposed in condition 1 until the current is equal to or less than 0.05 mA. When this happens, the discharging mode will start, and the battery will be discharged at 1 mA until the voltage of the battery is equal to or less than 0.1 V.

Figure 61 shows the code implemented for this group of methods marking with the yellow squares the values that will change in each method. These are, in fact, the same value of the voltage that will stop charging the battery and it will remain constant until the current decreases breaking the second condition. In Table 11, it can be seen the different voltages that will be implemented in the yellow squares of Figure 61 generating like that 3 different methods.

Stp	Variables	Mode	End Cond1	(And) End Cond2	GOTO	Log Cond
1		Charge CC: 1 mA	Voltage >= 2 V		Next Step	01:00
2		Charge CV: 2 V	Current <= 0.05 mA		Next Step	01:00
3		Discharge CC: 1 mA	Voltage <= 0.1 V		Next Step	01:00
4		<IF>	Cycle <= 100 Times		1	
5		<IF>			End_OK	

Figure 61. Code for the methods implemented changing the constant voltage charge.

Name of method	Charge Constant Voltage (V)
1mA- 2 V	2
1mA- 2.5 V	2.5
1mA- 3 V	3

Table 11. Methods tested to see how the charging constant voltage affects the performance of the batteries.

The three methods shown in Table 11 were tested on the batteries working correctly that were Battery HA1-HC1, Battery HA3-HC3, Battery HA4-HC4 and Battery HA5-HC5. After testing the latter, the results were compared to prove that they all had a similar performance as they were the same type of battery with 100 % $BmimFeCl_4$ as electrolyte. That is why it has been plotted only the results for one battery as it will represent the behavioural pattern for the four of them. Hence, in the following figures the results of voltage vs. time, current vs. time and voltage vs. capacity obtained on Battery HA4-HC4 are shown for each method. The plots voltage vs. time and current vs. time only show the first 20 cycles as after this cycle the pattern is almost the same until cycle 100. Later, the specific capacity and efficiency of this battery are compared between methods.

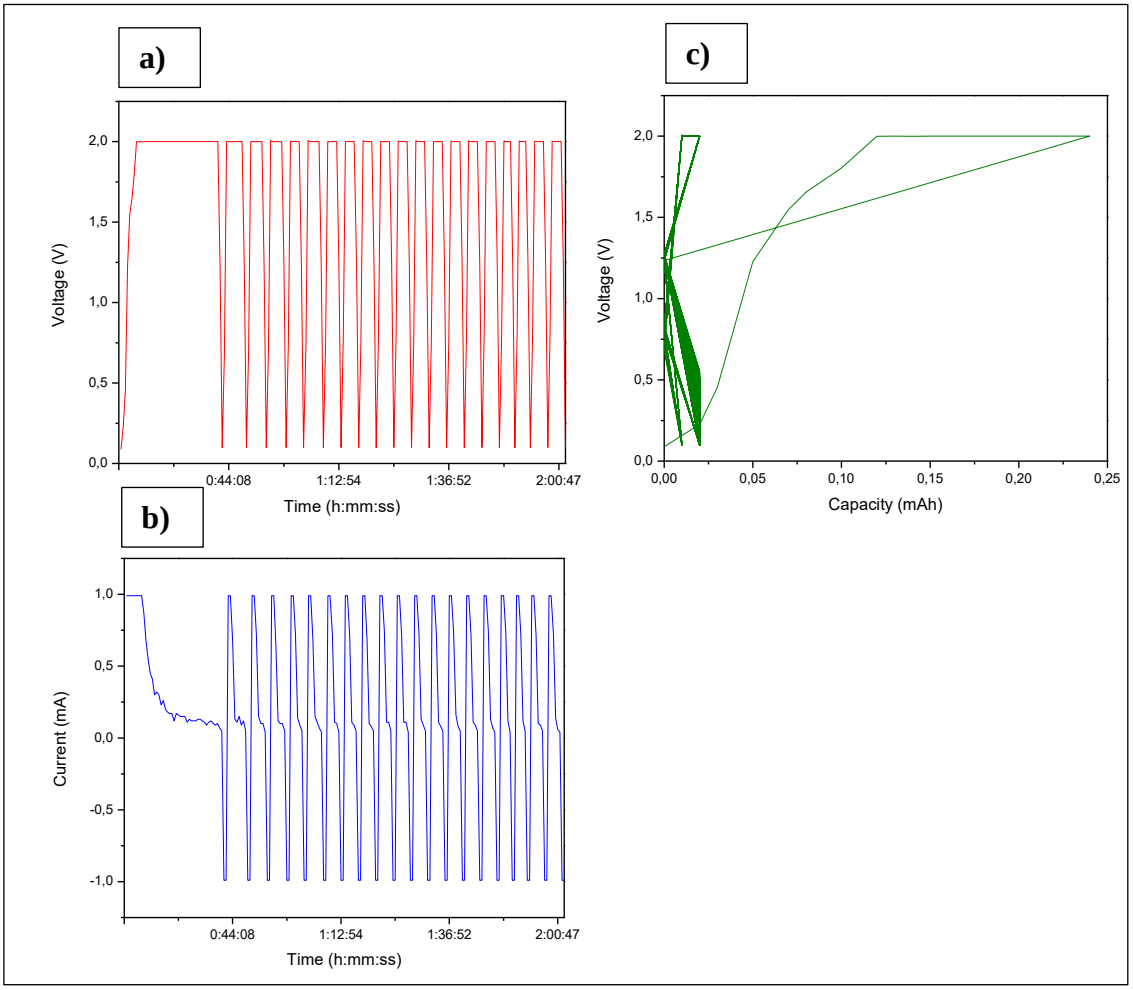

Figure 62. Plot Voltage vs. Time (a) and Current vs. Time (b) for the first 20 cycles; plot Voltage vs. Capacity for the 100 cycles (c) using the method "1mA- 2 V" in the Battery HA4-HC4.

From Figure 62 a) and b), it can be seen how the battery is being charged at 1 mA until the voltage reaches 2 V. Then, the voltage remains constant until the current is equal to or less than 0.05 mA. After this, the battery is discharged while the voltage decreases until 0.1 V. At this value, the next cycle will start again if the number of cycles ran are less than 100, and therefore, the battery will be charged at a constant current of 1 mA repeating the same cycle as before. Moreover, it can be observed than the first cycle lasts around 43 minutes while the rest ones only take 4 minutes.

Figure 62 c) shows that in the first cycle the battery reaches 0.24 mAh of capacity due to the chemical reaction that takes place. After this, in the following cycles the battery reaches a capacity of 0.02 mAh in most of the cycles and 0.01mAh in the rest ones.

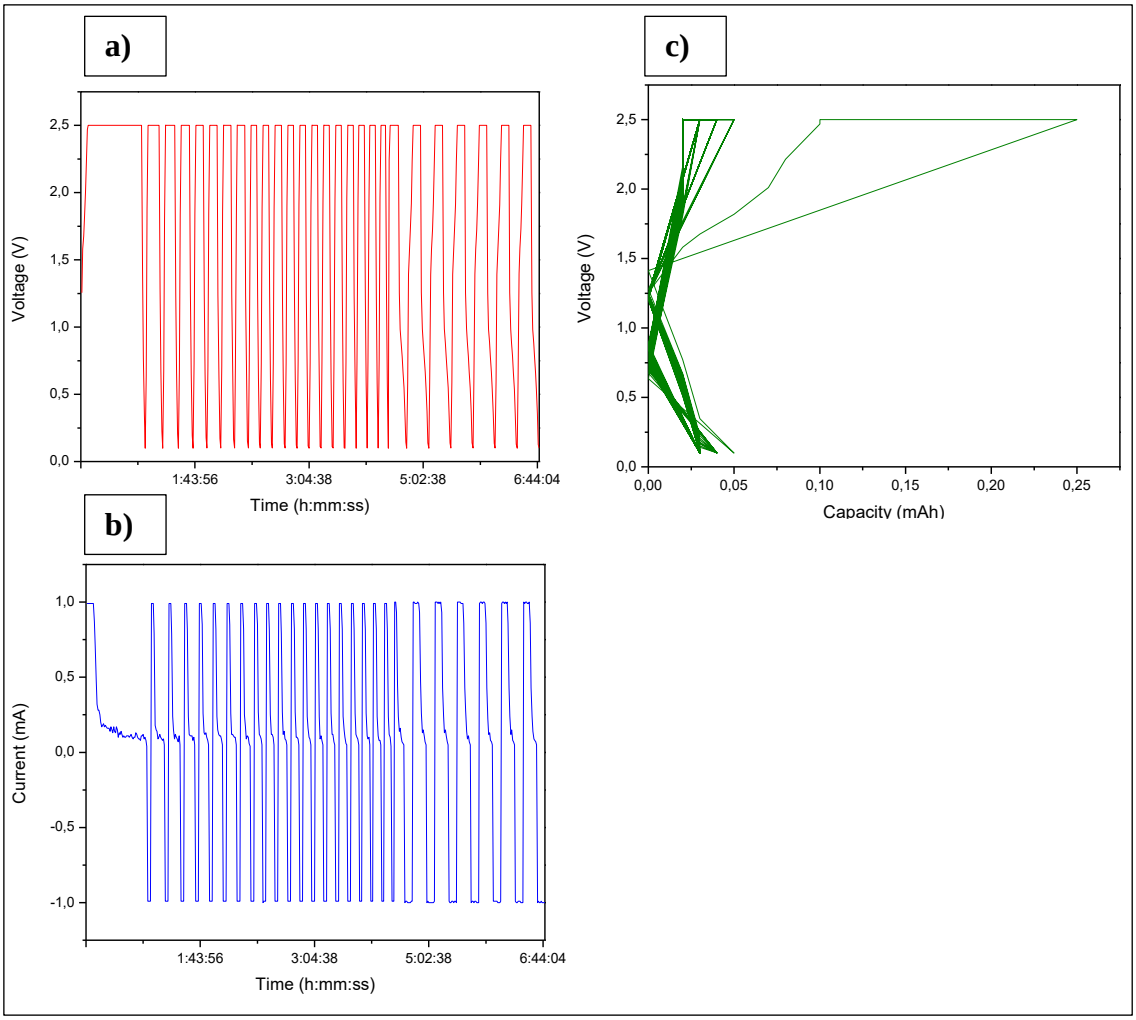

Figure 63. Plot Voltage vs. Time (a) and Current vs. Time (b) for the first 20 cycles; plot Voltage vs. Capacity for the 100 cycles (c) using the method "1mA- 2.5 V" in the Battery HA4-HC4.

In the same way, Figure 63 a) and b) show that the battery performs in a similar way but this time the voltage reaches 2.5 V as the method requires. Thus, the time employed on each cycle is longer since it takes more time to reach a higher voltage. Hence, the battery will keep charged at 1 mA while the voltage is less than 2.5V. Once reached this voltage, this value will remain constant until the current is equal to or less than 0.05 mA. Finally, it will be discharged at 1 mA until the voltage reaches 0.1 V. In this method, the first cycle takes 1 hour 19 minutes and the following ones only last for 11 minutes. Nevertheless, after the 14th cycle the battery takes around 20 minutes to complete one cycle.

Figure 63 c) shows that in the first cycle the battery reaches 0.25 mAh of capacity. In the following ones, the capacity is ranged from 0.03 mAh to 0.05 mAh. Consequently, it

can be stated that the capacity reached when the battery is charged until 2.5 V is higher than when it is charged until 2V.

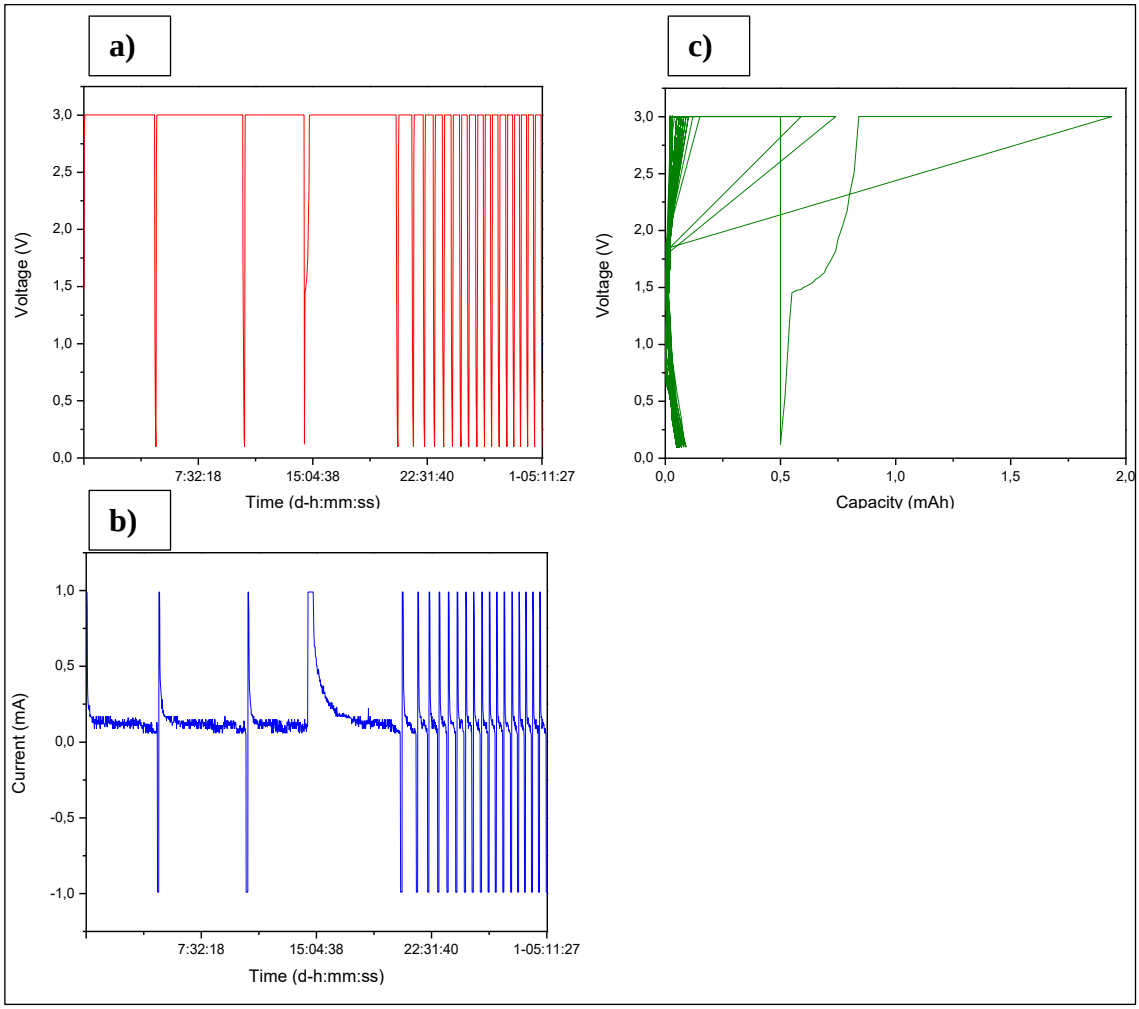

Figure 64. Plot Voltage vs. Time (a) and Current vs. Time (b) for the first 20 cycles; plot Voltage vs. Capacity for the 100 cycles (c) using the method "1mA- 3 V" in the Battery HA4-HC4.

From Figure 64, it can be observed that the battery performs in a different way when it is charged at a current voltage of 3V. Figure 64 a) and b) show that the first four cycles of the method take around 4 hours 40 minutes each one. After the 5^{th} cycle, the battery takes around 30 minutes to complete each charge-discharge cycle. Consequently, for the first 20 cycles the battery needs 1 day and 5 hours. As the charging voltage is higher, the battery requires more time to be charged and discharged.

Figure 64 c) shows that in this method the battery reaches a high capacity de 1.9 mAh in tone of the first four cycles. The rest of the four ones show 0.5 mAh of capacity and after this the capacity remains constant at around 0.05 mAh when the voltage reaches is

maximum (3V) and its minimum (0.1 V). Thus, the capacity achieved when charging the battery at a constant voltage of 3 V is very high.

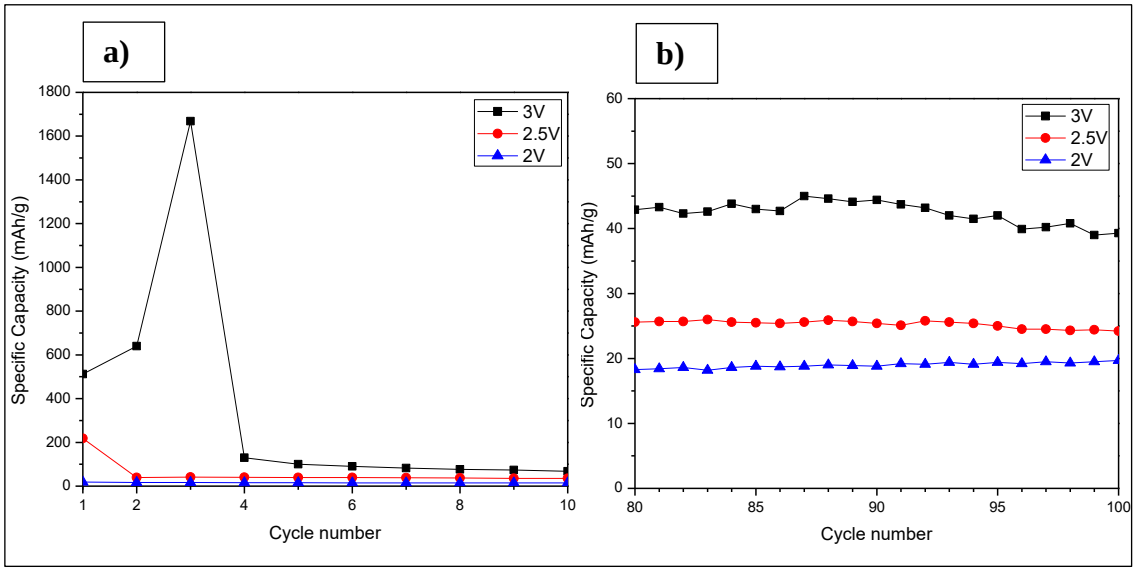

Figure 65. Plot Specific capacity vs. Cycle number for the first 10 cycles (a) and for the last 20 cycles (b) using the different methods showed in Table 11 in the Battery HA4-HC4.

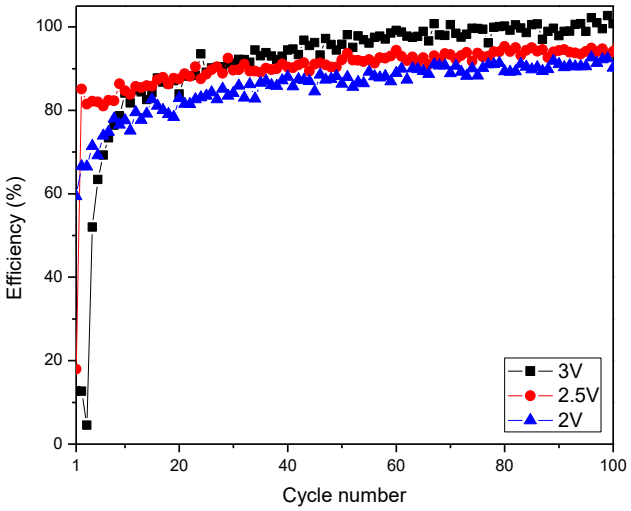

Figure 66. Plot Efficiency vs. Cycle number for the different methods showed in Table 11 in the Battery HA4-HC4.

In order to compare and to see how the charge voltage condition affects the battery, the specific capacity and the efficiency are plotted in Figure 65 and Figure 66, respectively.

On the one hand, Figure 65 a) shows that the specific capacity reached in the third cycle of the method "1mA- 3V" is very high. However, after the 4th cycle the specific

capacity remains practically constant until the last one for the three methods. In Figure 65 b) the specific capacity range has been extended for the last 20 cycles to better see the values reached. Thus, it can be seen that the method "1mA- 3V" reaches a specific capacity of around 43 mAh/g. For the method "1mA- 2.5V" the specific capacity is 26 mAh/g and for the "1mA- 2V" this is 19 mAh/g. Consequently, it can be stated that the specific capacity will be higher on the battery when the method to charge and discharge it requires a higher voltage.

On the other hand, Figure 66 shows that the efficiency of the battery is higher when the charge voltage condition is higher too. Thus, the efficiency for the battery testing the method "1mA- 3V" is around 100 % in the last cycles of the test. The one for the method "1mA- 2.5V" and "1mA- 2V" is around 95 %, being slightly higher the efficiency for the method with higher voltage.

4.4.1.4. Current condition influence

Finally, another group of methods was tested on Battery HA1-HC1, Battery HA3-HC3, Battery HA4-HC4 and Battery HA5-HC5 to see how changing the current condition to start discharging the battery can influence its performance. In Figure 67 the code written for this group of methods can be seen, highlighting with a yellow square the parameter that will change from method to method. This parameter is the value of the current in which once reached this value or a lower one, the battery will stop being charged at 2.5 V and it will be discharged at a constant current of 130 µA until the voltage is equal to or less than 0.1 V. All the methods will start charging the batteries with a constant current of 410 µA while the voltage is less than 2.5 V. Once the battery reaches the latter value, it will remain charged constantly at 2.5 V until the second condition becomes true. Table 12 shows the current value written on the second step's condition and the name given to each method.

Stp	Variables	Mode	End Cond1	(And) End Cond2	GOTO	Log Cond
1		Charge CC: 410 uA	Voltage >= 2.5 V		Next Step	01:00
2		Charge CV: 2.5 V	Current <= 100 uA		Next Step	01:00
3		Discharge CC: 130 uA	Voltage <= 0.1 V		Next Step	01:00
4		<IF>	Cycle <= 100 Times		1	
5		<IF>			End_OK	

Figure 67. Code for the methods implemented changing the current condition in step 2.

Name of method	Condition Step 2: Current <=
1mA- 2.5V- 0.1C- N	100 µA
1mA- 2.5V- 0.1C- N2	200 µA
1mA- 2.5V- 0.1C- N3	300 µA
1mA- 2.5V- 0.1C- N4	350 µA

Table 12. Methods tested to see how changing the current condition in step 2 to start discharging the battery affects the performance of the batteries.

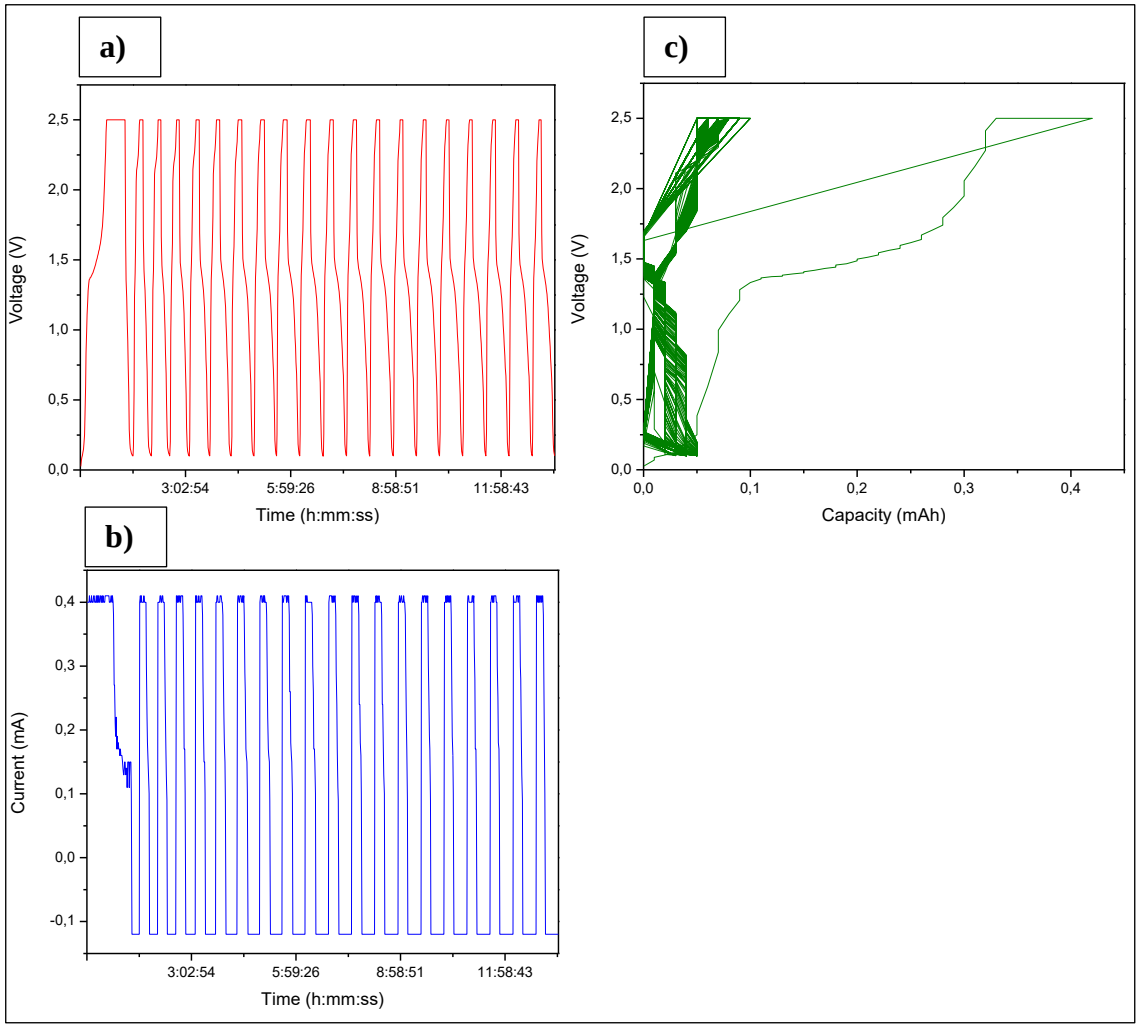

Figure 68. Plot Voltage vs. Time (a) and Current vs. Time (b) for the first 20 cycles; plot Voltage vs. Capacity for the 100 cycles (c) using the method "1mA- 2.5V- 0.1C- N" in the Battery HA4-HC4.

From Figure 68 a) and b), it can be seen how in the first cycle the battery takes some time to be charged at a constant voltage of 410 µA until it reaches 2.5 V. Then, the voltage remains constant while the current is higher than 100 µA. Once the current is below the

latter value, the battery is discharged with a constant current of 130 µA while the voltage is more than 0.1 V. This cycle is repeated for 100 times, and although the first cycle lasts around 1 hour 35 minutes, the other 99 ones only take approximately 40 minutes each one.

From Figure 68 c), it can be observed that the capacity of the battery reaches 0.42 mAh in the first cycle due to the chemical reaction that takes place between the electrolyte and the surface of the electrodes. However, for the following 99 cycles the capacity ranges from 0.01 to 0.05 mAh when the voltage decreases until 0.1 V but it varies from 0.05 to 0.09 mAh when the voltage rises until 2.5 V.

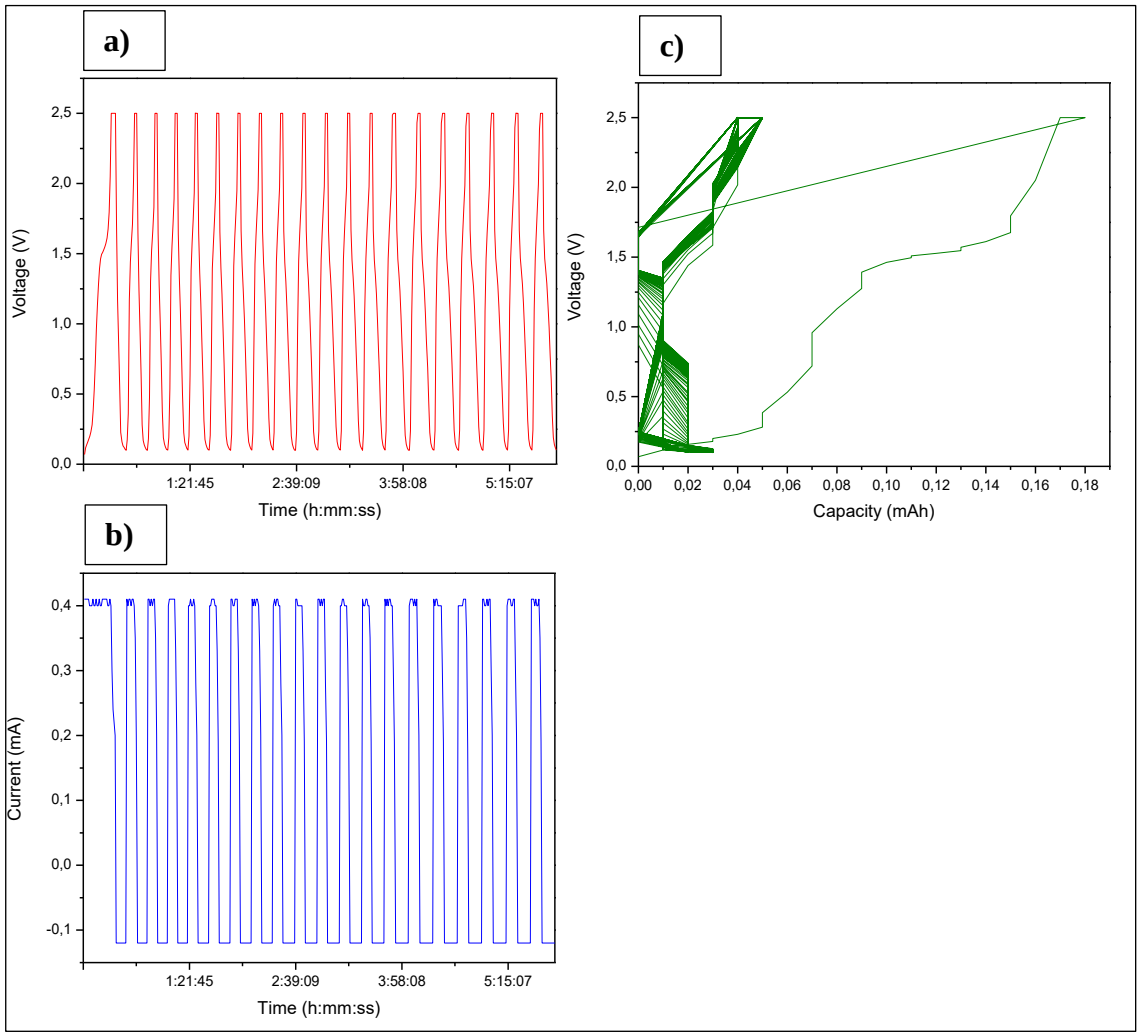

Figure 69. Plot Voltage vs. Time (a) and Current vs. Time (b) for the first 20 cycles; plot Voltage vs. Capacity for the 100 cycles (c) using the method "1mA- 2.5V- 0.1C- N2" in the Battery HA4-HC4.

Figure 69 a) and b) show that the battery performs just as the method requires. In this case, the time needed for each cycle is lower as the battery will pass to the discharging mode sooner since the current condition is higher. Thus, the first cycle takes 35 minutes and the rest ones take around 18 minutes each one. Nevertheless, the capacity reached vs. the voltage is lower for the method "1mA- 2.5V- 0.1C- N2" than for the method "1mA- 2.5V- 0.1C- N". Hence, Figure 69 c) shows that the capacity as it maximum is 0.18 mAh in the first cycle, thought for the rest of the cycles it varies from 0.01 to 0.03 mAh for the lowest voltages and from 0.04 to 0.05 mAh for the highest ones.

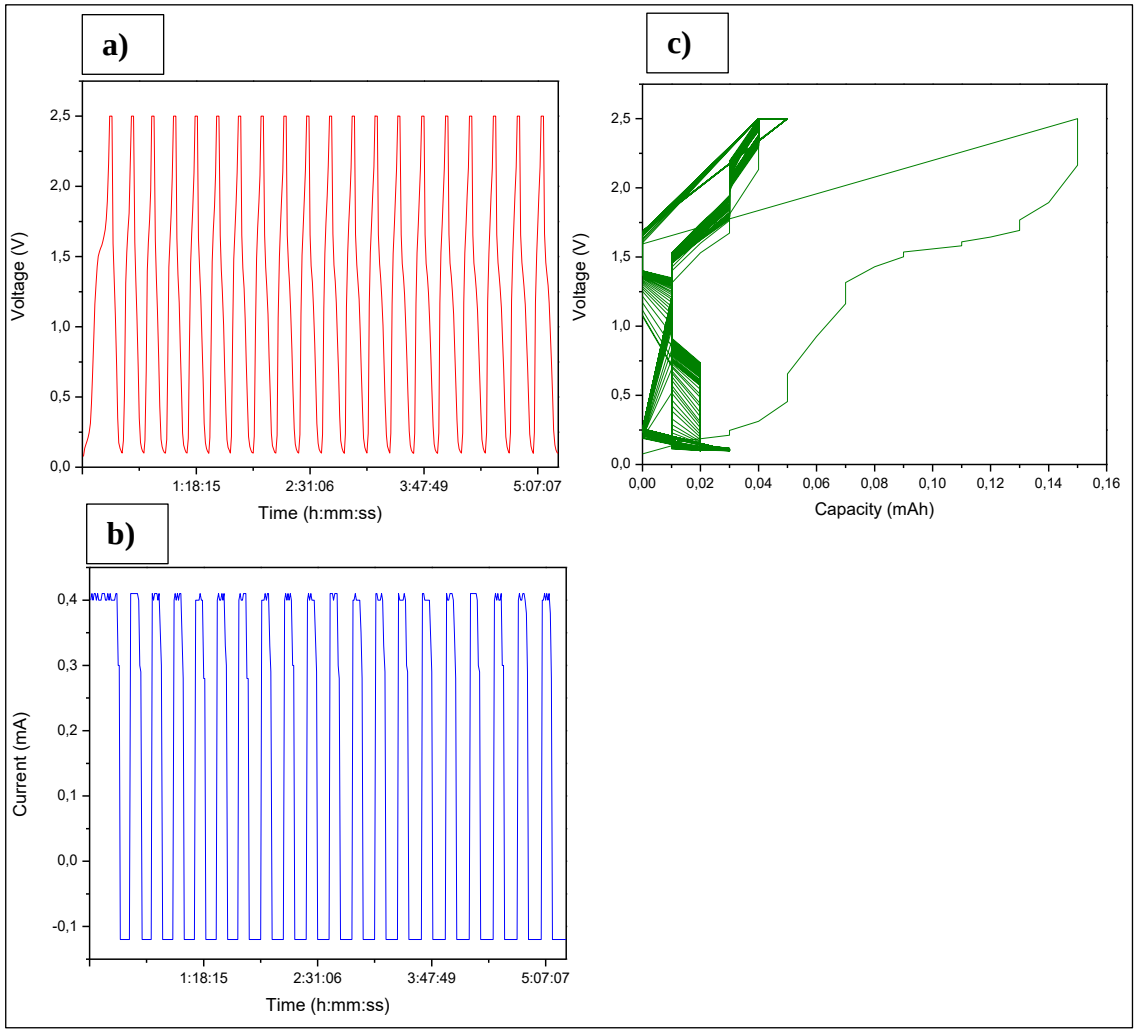

Figure 70. Plot Voltage vs. Time (a) and Current vs. Time (b) for the first 20 cycles; plot Voltage vs. Capacity for the 100 cycles (c) using the method "1mA- 2.5V- 0.1C- N3" in the Battery HA4-HC4.

When testing the method "1mA- 2.5V- 0.1C- N3" on the Battery HA4-HC4, the results plotted in Figure 70 a) and b) show that the first cycle lasts for around 31 minutes while the other ones take 17 minutes each one. The time where the battery remains

charged at a constant voltage of 2.5 V is low due to the high value of 300 µA implemented on this method that makes the software starts discharging the battery once the current is equal to or less than the latter value. Furthermore, with the method "1mA- 2.5V- 0.1C- N3" the battery reaches a lower capacity than on the methods tested before. Hence, from Figure 70 c), it can be seen that the capacity of the battery is 0.15 mAh in the first cycle and then it is 0.01 or 0.02 mAh when the voltage is 0.1 V and 0.03 or 0.04 mAh when the voltage is 2.5 V.

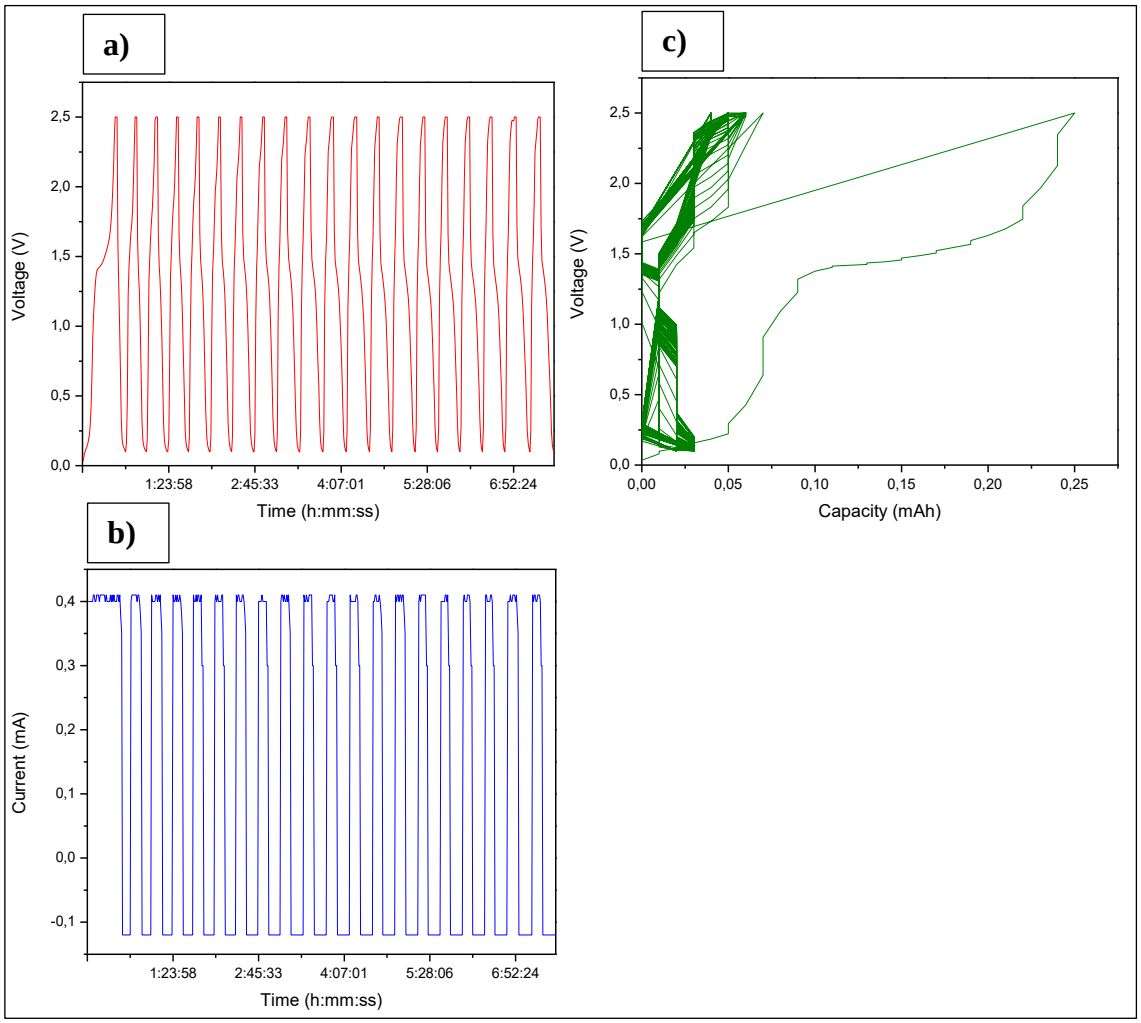

Figure 71. Plot Voltage vs. Time (a) and Current vs. Time (b) for the first 20 cycles; plot Voltage vs. Capacity for the 100 cycles (c) using the method "1mA- 2.5V- 0.1C- N4" in the Battery HA4-HC4.

Finally, in the last method tested called "1mA- 2.5V- 0.1C- N4" it can be observed from Figure 71 a) and b) that each cycle takes longer than in the last two methods tested. Thus, the first cycle lasts for 45 minutes and the other ones takes around 23 minutes. This could be because it takes more time when the battery is in the discharging mode than in

the charging mode, since in this method the discharging mode starts quite soon as the current value to cross is 350 µA and the battery is only charged at a constant value of 410 µA. However, as it takes longer to be charged and discharged, the accuracy is better, and the capacity achieved is higher than on the last two methods tested before. Hence, Figure 71 c) show that the maximum capacity reached in the first cycle is 0.25 mAh. For the following cycles the capacity ranges from 0.01 to 0.03 mAh when the voltage is 0.1V and from 0.03 to 0.06 mAh when the voltage is 2.5 V.

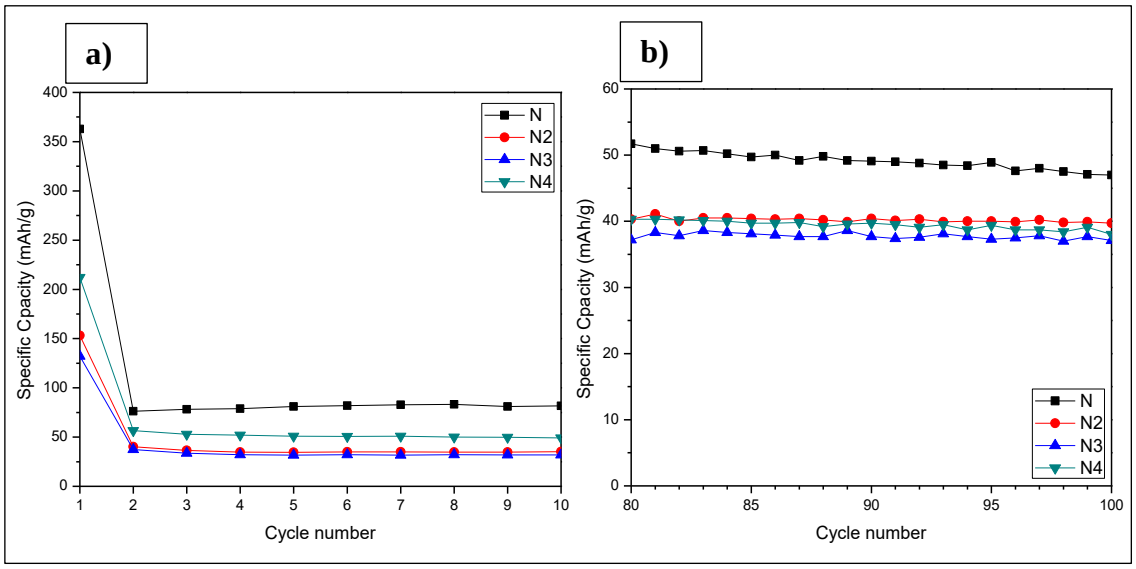

Figure 72. Plot Specific capacity vs. Cycle number for the first 10 cycles (a) and for the last 20 cycles (b) using the different methods showed in Table 12 in the Battery HA4-HC4.

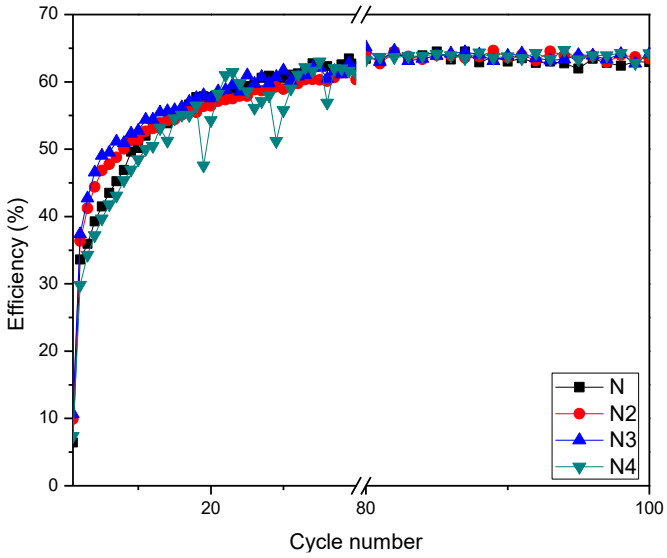

Figure 73. Plot Efficiency vs. Cycle number for the different methods showed in Table 12 in the Battery HA4-HC4.

Lastly, the specific capacity and the efficiency are plotted versus the cycle number (in Figure 72 and 73, respectively) for all the methods tested in this section in order to compare them.

Figure 72 shows that the specific capacity for the method "1mA- 2.5V- 0.1C- N" is relatively higher during all the cycles in comparison with the other ones. However, the specific capacity for the method "1mA- 2.5V- 0.1C- N4" starts being higher than for the method "1mA- 2.5V- 0.1C- N2" and "1mA- 2.5V- 0.1C- N3" but it starts decreasing and in the last cycles the specific capacity for the method "1mA- 2.5V- 0.1C- N2" is slightly higher than for the "1mA- 2.5V- 0.1C- N4" one. Moreover, at the last part of the tests the difference between the specific capacity for the method "1mA- 2.5V- 0.1C- N3" and for "1mA- 2.5V- 0.1C- N2" and "1mA- 2.5V- 0.1C- N4" is not that much, as the first one has a specific capacity of 38 mAh/g and the two latter ones have around 40 mAh/g. All these conclusions can be observed from Figure 72 a) and b).

Regarding the efficiency, Figure 73 shows that the efficiency for the different methods is practically the same after the cycle number 20. At this point, it is around 58 % for all the methods and increases along the cycles until reaching an efficiency of 65 % approximately. Taking Figure 73 a step further, it can be seen how the efficiency is a bit lower the first 10 cycles for the method "1mA- 2.5V- 0.1C- N" and "1mA- 2.5V- 0.1C- N4" than for the other two ones. Moreover, the method "1mA- 2.5V- 0.1C- N4" show some decreasing peaks in the efficiency for some cycles.

To sum up, it can be concluded that when charging-discharging the Battery HA4-HC4 with the method "1mA- 2.5V- 0.1C- N", the specific capacity is higher than for the other methods while the efficiency is the same for all of them. However, this test takes a lot of time to complete 100 cycles compared with the other three ones. Once again, as the battery is charged and discharged slowly, the specific capacity is higher due to the better accuracy.

4.4.1.5. Other results

Apart from Battery HA1-HC1, Battery HA3-HC3, Battery HA4-HC4 and Battery HA5-HC5 the rest of the batteries showed in Table 9 were not working in the Landt Battery Testing System. Even if the batteries were assembled following the same method and the electrolyte utilized was the same, the battery showed a wrong performance. For

instance, Battery HA2-HC2 had pure $BmimFeCl_4$ as electrolyte as the batteries previously mentioned. However, when testing "Method 1" some strange results appear.

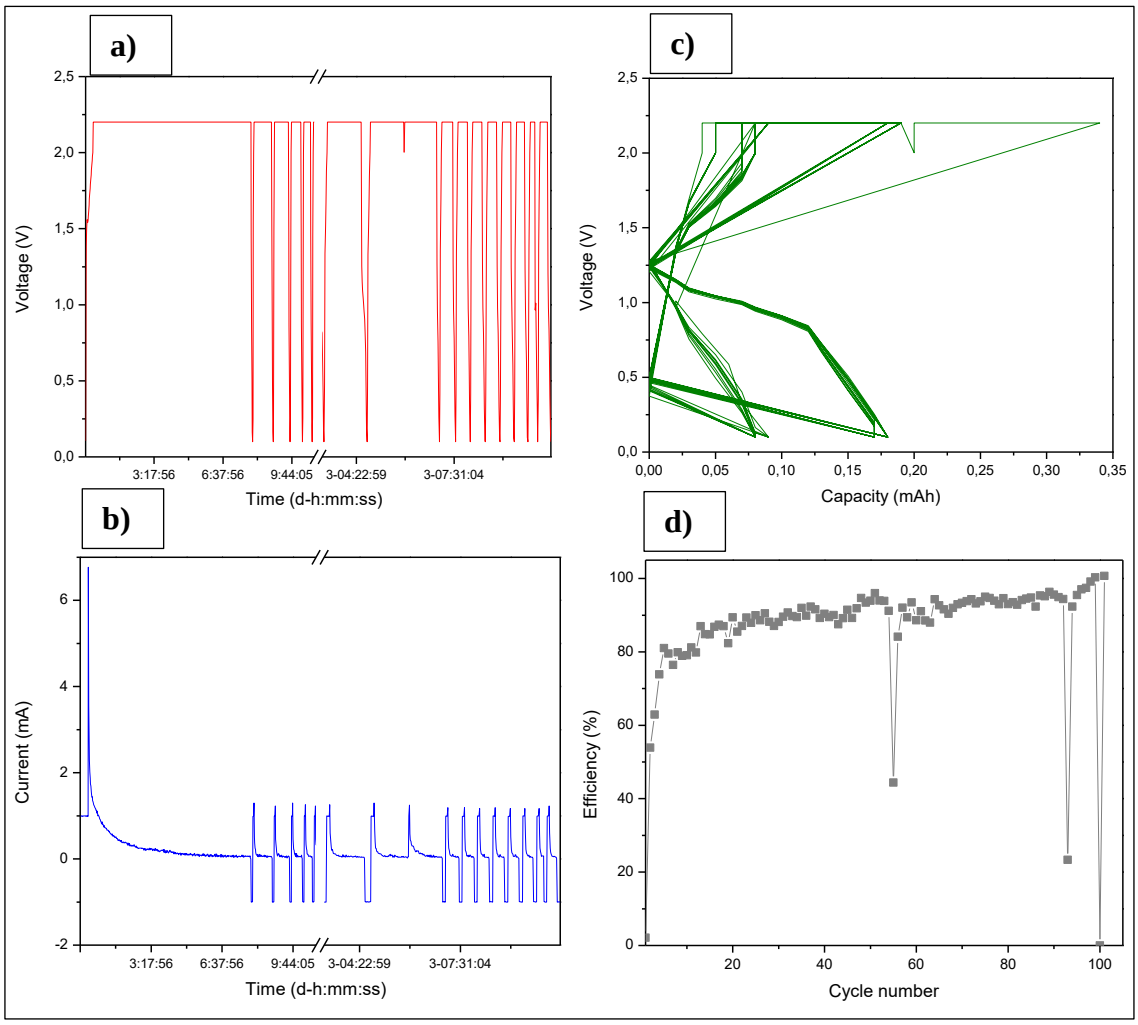

Figure 74. Plot Voltage vs. Time (a) and Current vs. Time (b) for the first 10 and the last 10 cyles; plot Voltage vs. Capacity for the 100 cycles (c); plot Efficiency vs. Cycle number (d) using "Method 1" in the Battery HA2-HC2.

From Figure 74 b), it can be seen that even if the method is coded to charge the battery until 1 mA, while testing Battery HA2-HC2 reaches almost 7 mA in the first cycle. Moreover, in the last 10 cycles, showed in Figure 74 a) and b), the time spent in each cycle is different and sometimes it does not follow the code in the method. Figure 74 c) shows that the battery has a high capacity during all the test. Figure 74 d) shows that the battery's efficiency is great but in some cycles the efficiency drops sharply.

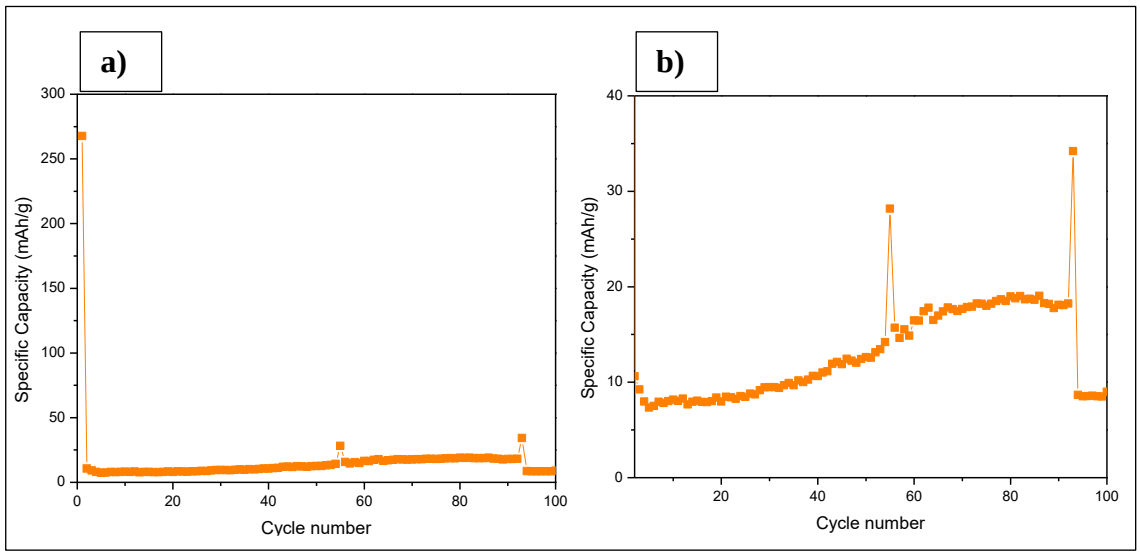

Figure 75. Plot Specific capacity vs. Cycle number for 100 cycles (a) and for the last 99 cycles (b) using "Method 1" in the Battery HA2-HC2.

Finally, from Figure 75 a) and b), it can be seen that the specific capacity is very high. In the first cycle Battery HA2-HC2 reaches almost 275 mAH/g and for the rest of the cycles it ranges from 10 to 20 mAh/g showing strange peaks in 2 cycles and decreasing in the last 5 cycles.

The high capacity together with the random peaks that the Battery HA2-HC2 means that it is not working correctly. To prove it, another method is implemented. This time, the method "1mA- 2.5V- 22.8C" is tested. However, the Battery HA2-HC2 does not work and it is not charged and discharged as the method requires. From Figure 76 the results obtained in the Landt Battery Tetsing System are shown.

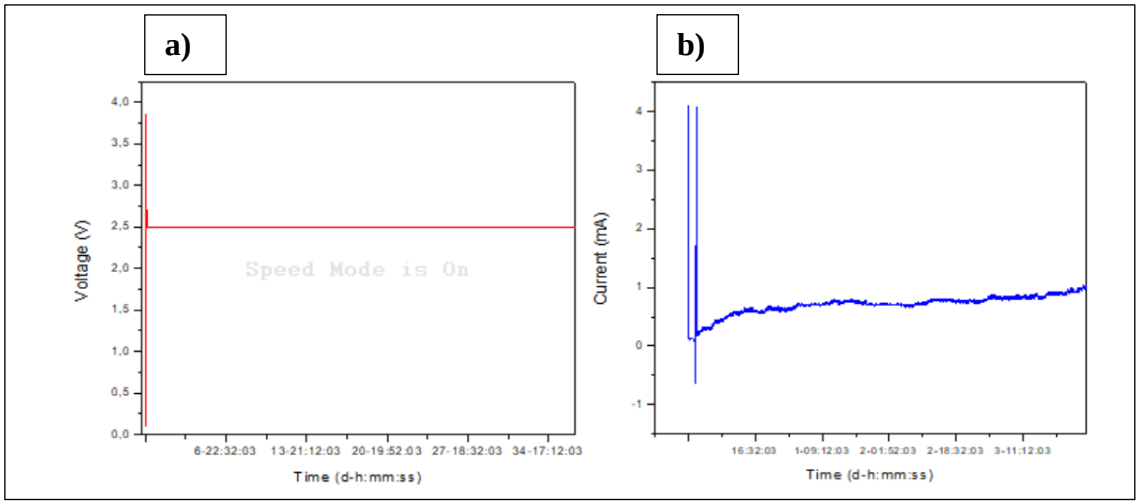

Figure 76. Plot Voltage vs. Time (a) and Current vs. Time (b) for the the method "1mA- 2.5V- 22.8C" tested on the Battery HA2-HC2.

Neither the voltage values nor the current ones match with the code implemented on the method used. Consequently, it can be concluded that the Battery HA2-HC2 does not work. Similarly, Battery HA6-HC6 which was also made with 100 % $BmimFeCl_4$ did not work and when "Method 1" was tested, the current and the voltage remained constant at 1 mA and 0.002 V, respectively.

Furthermore, the batteries made with 30 % $BmimFeCl_4$ in EC+DMC as electrolyte were also tested on the charge-discharge test showing a bad performance. None of these batteries work properly. From Figure 77, it can be seen how Battery HA9-HC9 performed when the method "1mA- 2.5V- 22.8C" was tested. The battery is not charged and discharged as the method requires. Thus, it can be concluded that this battery does not work. Similar results were obtained when testing on Battery HA10-HC10. Additionally, Battery HA7-HC7 and HA8-HC8 also based on 30 % $BmimFeCl_4$ in EC+DMC as electrolyte did not work and the current and voltage remained in a small constant value over the time. Consequently, it can be stated that the batteries using 30 % $BmimFeCl_4$ in EC+DMC did not work.

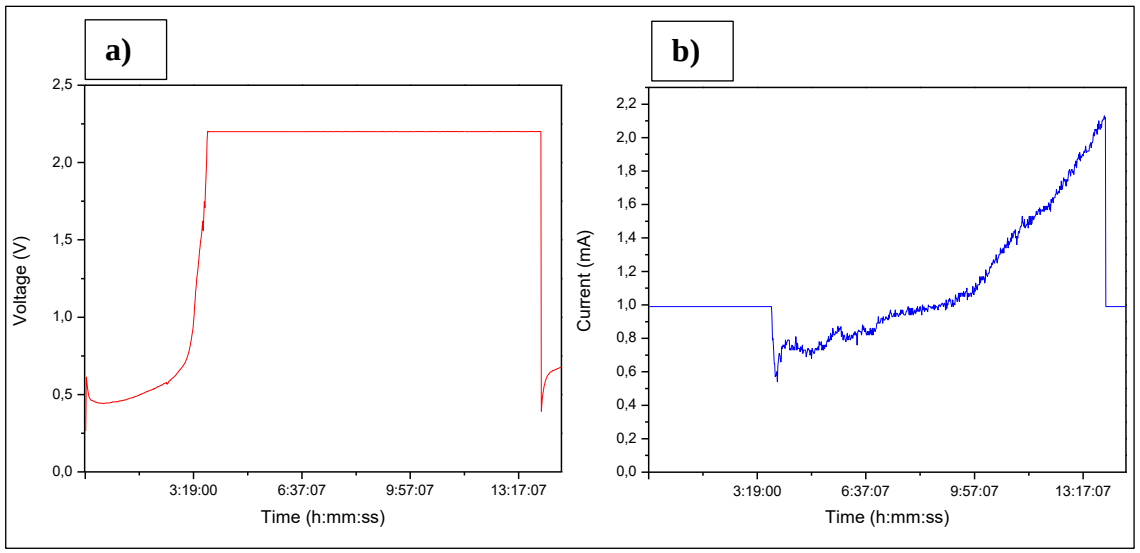

Figure 77. Plot Voltage vs. Time (a) and Current vs. Time (b) for the the method "1mA- 2.5V- 22.8C" tested on the Battery HA9-HC9 which has 30 % $BmimFeCl_4$ in EC+DMC as electrolyte.

In the same way, Battery HA11-HC11 based on 0.5 M $BmimFeCl_4$ in EC+DMC and Battery HA12-HC12 and Battery HA13-HC13 containing 5 % and 40 % $BmimFeCl_4$ in EC+DMC, respectively, did not work when tested on the Landt Battery Testing System. In conclusion, only the batteries with 100 % IL worked as expected.

Finally, two more batteries were assembled with another type of IL. Hence, Battery HA14-HC14 and Battery HA15-HC15 were made with 100 % $FeCl_3$. From Figure 78, the results obtained when testing Battery HA15-HC15 can be seen. The battery is supposed to be charged at a constant current of 1 mA while the voltage increases until 1.5V but this does not happen. This battery remains charging at 1 mA because the voltage is too low and does not reach 1.5 V. Thus, the batteries with 100 % $FeCl_3$ does not work either.

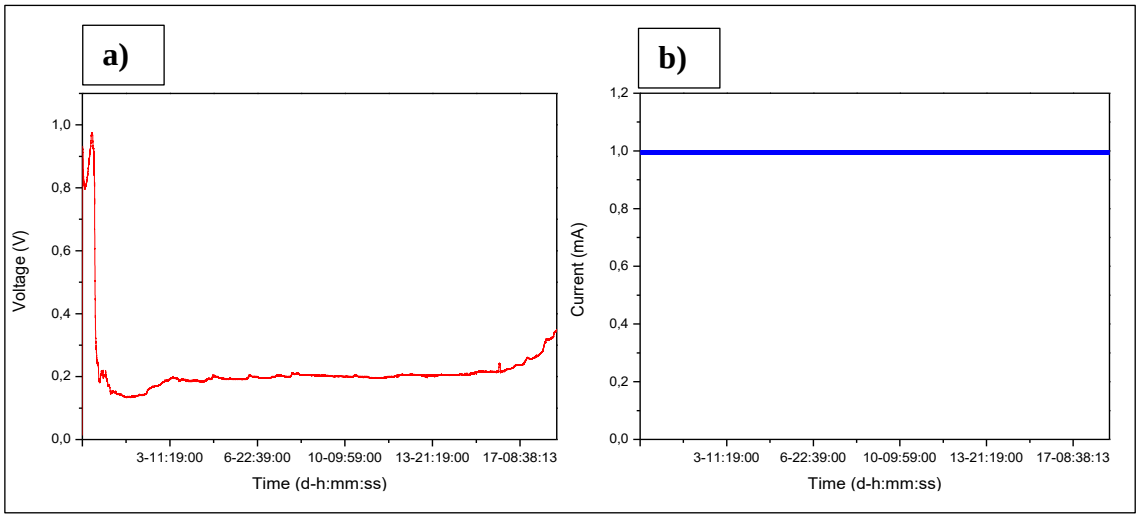

Figure 78. Plot Voltage vs. Time (a) and Current vs. Time (b) for the the method "1mA-1.5V" tested on the Battery HA15-HC15 which has 100% $FeCl_3$ as electrolyte.

4.4.2. Open Circuit Potential Test

Once the batteries were assembled and before connecting them to the Land Battery Testing System, an Open Circuit Potential Test was done. This is a passive experiment to measure the electrochemical stability of the battery. Thus, if the system is stable for a long period of time (minutes), then, it could also be stable enough for a perturbation-based experiment.

An Open Circuit Potential Test was done on all the batteries. Consequently, before connecting them to the Landt Battery Testing System it was already known if they were likely to work correctly or not. If the Open Circuit Potential Test showed a non-stable performance, the chance that the battery would work properly during the charge-discharge test was minimal.

Battery HA1-HC1, Battery HA3-HC3, Battery HA4-HC4 and Battery HA5-HC5 was tested with an Open Circuit Potential and all of them showed a stable performance. Figure

79 shows the plot obtained in the Open Circuit Potential tested on Battery HA4-HC4 as an example.

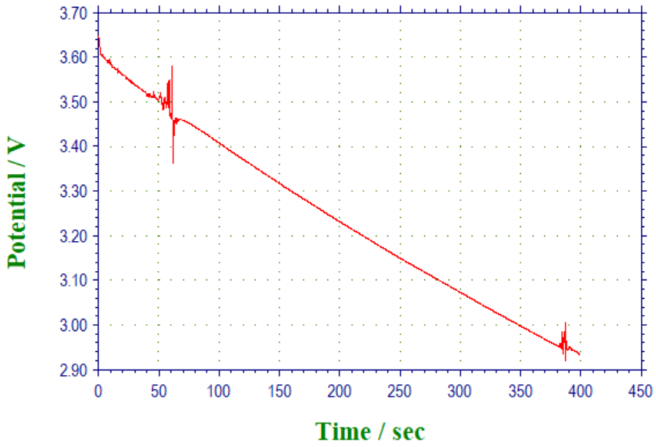

Figure 79. Plot potential vs. time obtained by the Open Circuit Potential tested on Battery HA4-HC4.

From Figure 79, it can be seen that the potential between anode and cathode for 400 seconds decreases with an almost constant slope of -0.0018 V/s. Although a system which only changes its voltage for ±5 mV over a long period of time is preferable, and therefore considered stable, when obtaining a well-defined line with a slight slope the system might be stable enough for a perturbation test. Thus, it was expected than Battery HA4-HC4 could work properly on the charge-discharge test.

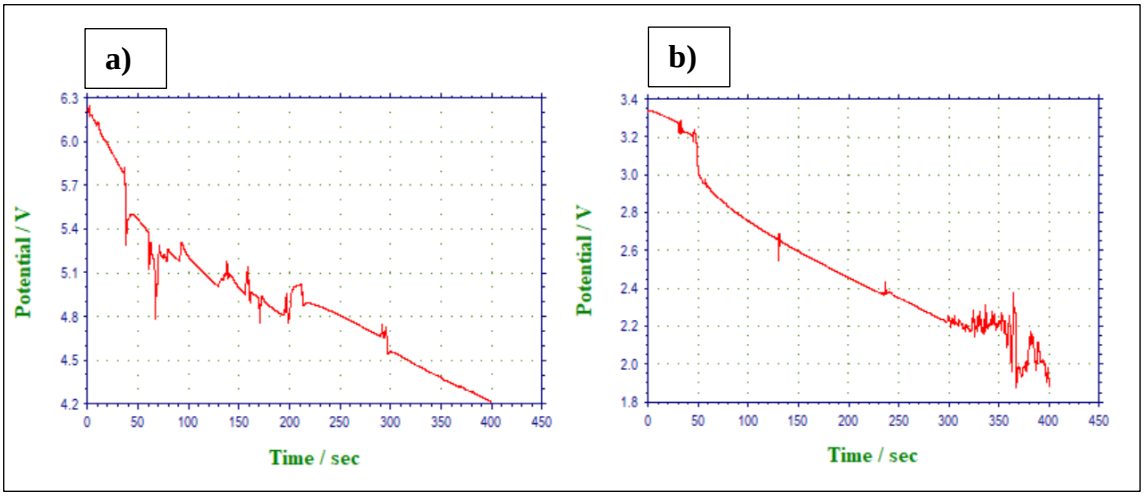

Figure 80. Plot potential vs. time obtained by the first round (a) and second round (b) of the Open Circuit Potential tested on Battery HA3-HC3.

Figure 80 shows the results obtained when testing an Open Circuit Potential on Battery HA3-HC3 for the first time (Figure 80 a) and for the second time (Figure 80 b).

When the first Open Circuit Potential is tested, the battery has a high potential of 6.25 V and it decreases around 2 V during the 400 seconds the test lasts showing a not well defined modelled. However, when the second round is tested, the battery starts with a potential of 3.35 V and it diminishes ca. 1.4 V with a more linear performance for most of the test. Hence, Battery HA3-HC3 was expected to work. The difference between Figure 80 a and b proves that each battery must be tested at least twice because the stability of the battery can change during the first period after having assembled it. This is due to the chemical reactions that take place when the electrolyte comes into contact with the electrodes.

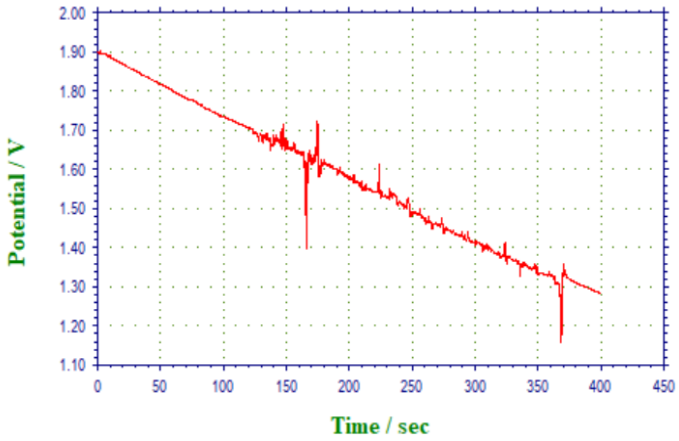

Figure 81. Plot potential vs. time obtained by the Open Circuit Potential tested on Battery HA2-HC2.

From Figure 81, it can be supposed that Battery HA2-HC2 may work correctly when testing on it in the Landt Battery Testing System. The potential only changes around 0.6 V for the 400 seconds tested and even if the plot shows some peaks the slope is quiet constant. However, when Battery HA2-HC2 is connected to the charge-discharge test it does not work as expected. Hence, when "Method 1" is tested the battery shows a very high capacity of around 0.17 mAh even which indicates that something is not working well. Later, when the method "1mA- 2.5V- 1C" is tested the battery is not charged and discharged as the method requires and it only shows two cycles with random voltage and current values.

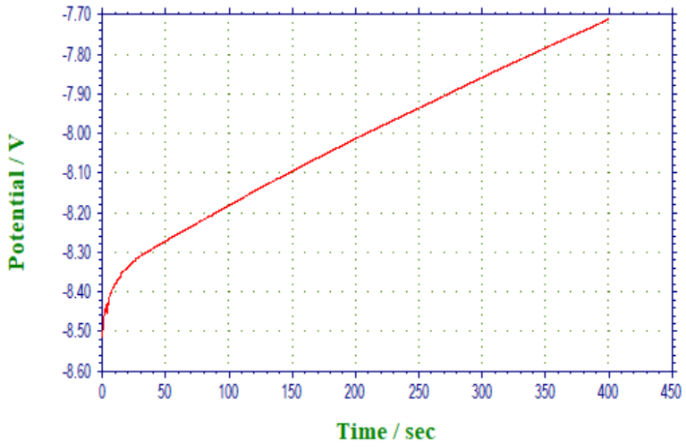

Figure 82. Plot potential vs. time obtained by the Open Circuit Potential tested on Battery HA9-HC9 which has 30 % $BmimFeCl_4$ in EC+DMC as electrolyte.

From the start, Battery HA9-HC9 was not expected to work as it can be deduced from Figure 82. The latter shows a very low potential with an increasing voltage over the time. Hence, it is known that this type of battery cannot have a potential of -8.5 V between anode and cathode. In addition, the potential is not constant during this time. As a consequence, the Battery HA9-HC9 containing 30 % $BmimFeCl_4$ in EC+DMC as electrolyte is not expected to work since it is not stable.

In conclusion, the Open Circuit Potential is a good measure to know if the battery is electrochemically stable. Consequently, by knowing if it is stable it can be predicted if the batteries will work correctly. However, this is just an estimation and the batteries sometimes will not perform as expected even if the results on the Open Circuit Potential show that they are quite stable.

4.5. Summary of discussion

The solutions based on various concentrations of $BmimFeCl_4$ in DMC and in EC+DMC have different values of conductivity, viscosity and density. The aim is to have an electrolyte which has high ionic conductivity, high density, and low viscosity. A high ionic conductivity implies more ions in movement between electrodes. A high density is wanted since the electrolyte will take less space in the same mass. Finally, a low viscosity means faster ion transportation in the electrolyte. However, there is a correlation between ionic conductivity and viscosity as increasing the amount of IL in the solvent means that the conductivity will be higher as there are more ions but the viscosity will be higher too because the pure IL $BmimFeCl_4$ has a high viscosity.

From the results shown it can be concluded that the solutions made with 30 % $BmimFeCl_4$ in DMC+EC or higher percentages than the latter have a good ionic conductivity. Nevertheless, the solutions made with DMC as a solvent have less conductivity when the percentages are less than 50 %. When the density is studied, it is stated that this parameter increases with the percentage of IL in solvent and with the loss of temperature. Furthermore, the density for the samples based on EC+DMC as solvent are higher than the ones made with DMC. The higher percentage of $BmimFeCl_4$ in the solution means that the density will be higher. Lastly, a low viscosity is achieved when the percentage of IL in solvent is little and the temperature of the sample is high. In this case, the solutions made with DMC have less viscosity than the ones made with EC+DMC. Therefore, a balance between conductivity, density and viscosity must be achieved in order to find the optimal electrolyte.

Besides studying the IL $BemimFeCl_4$, other ILs were prepared. Nevertheless, only the solution with 100 % $FeCl_3$ could be dissolved and used as electrolyte in the batteries. Thus, the solutions based on 1 M $Fe(CH_3COO)_3$ in EC+DMC and 1 M $FePO_4$ in EC+DMC were excluded to be used in the batteries because they could not be dissolved.

In addition, the corrosion test showed that the aluminium-foil is quickly corroded by all the solutions in DMC and in EC+DMC and therefore, it cannot be used as part of the electrodes. However, the nickel-foil and copper-foil were corrosion resistant for the samples based on 15 % and 20 % $BmimFeCl_4$ in DMC after 1 week. Furthermore, the latter foils were not either corroded after 72 hours when using the solutions made with EC+DMC. Although it can be said that the nickel-foil and copper-foil are good materials to use in the electrodes, the corrosion test should be studied for longer periods of time to prove that none sign of corrosion appears.

Finally, the battery tests show that only four batteries based on 100 % $BmimFeCl_4$ as electrolyte work correctly. Thus, a lot of methods are tested on these batteries to see how the current charging rate, the voltage charging rate and the current condition to start discharging the battery can influence the specific capacity and the efficiency of the battery. The results showed that a lower current charging rate implies higher specific capacity since the accuracy to charge and discharge the battery each cycle is better as it takes more time. However, the efficiency of the battery is better at high charging rates. On the other side, when the battery is charged at higher voltages each cycle takes longer

since the battery will be charging at a constant current until it reaches the desired value of voltage. Hence, the battery has higher specific capacity and higher efficiency when it is charged at higher voltages than when lower voltages are implemented. Lastly, the value for the current condition to start discharging the battery is studied. Higher values of current condition mean that the battery will start discharging before. In this case, the specific capacity is higher when the current condition is lower, but the efficiency does not change showing a low value around 65 % for the four methods tested.

Similarly, after studying all the tests done in all the batteries, it can be concluded that the ones made with 5 %, 30 % and 40 % $BmimFeCl_4$ in EC+DMC does not work. Moreover, the two batteries prepared with 100 % $FeCl_3$ does not perform in the Landt Battery Testing System as expected. Further batteries containing these electrolytes should be assembled in order to see if the problem is that the ionic conductivity is too low, or if it is an issue concerning short-circuits.

5. Conclusion

Using the IL $BmimFeCl_4$ as electrolyte shows a promising future for iron-ion batteries. This IL shows great results of specific capacity and efficiency when it is used as pure (100 % $BmimFeCl_4$) in the electrolyte. However, it would be better to use a solution of $BmimFeCl_4$ in DMC or in EC+DMC (in a ratio 1:1) as electrolyte since the solutions have higher ionic conductivity than if 100 % IL is used directly as electrolyte. Furthermore, a less percentage of IL implies less viscosity and faster ion transportation. Thus, further research must be done using the IL as an additive in iron-ion batteries to make them work properly and to gain a full understanding of their performance.

6. References

1. A. El Kharbachi, O. Zavorotynska, M. Latroche, F. Cuevas, V. Yartys and M. Fichtner, *Journal of Alloys and Compounds*, 2020, **817**.
2. Y. Zhao, Y. Zhen, T. B. Maristuen, S.P. Kuefergasse, D.B. Faulhaberstrasse, A. M. Heidenheimer Strasse, *Norwegian Industrial Property Office*, Patent No. 20180939, 2019.
3. Z. Yue, H. Dunya, X. Y. Mei, C. McGarry and B. K. Mandal, *Ionics*, 2019, **25**, 5979-5989.
4. B. J. Li, Y. J. Li, X. Y. Zhan, P. He and H. S. Zhou, *Green Energy & Environment*, 2019, **4**, 3-19.
5. Q. Yang, Z. Zhang, X.-G. Sun, Y.-S. Hu, H. Xing and S. Dai, *Chemical Society Reviews*, 2018, **47**, 2020-2064.
6. L. L. Fan, N. P. Deng, J. Yan, Z. H. Li, W. M. Kang and B. W. Cheng, *Chemical Engineering Journal*, 2019, **369**, 874-897.
7. S. K. Singh and A. W. Savoy, *Journal of Molecular Liquids*, 2020, **297**.
8. Z. Lei, B. Chen, Y. Koo, D. R. MacFarlane, *Chemical Reviews*, 2017.
9. G. G. Eshetu, M. Armand, B. Scrosati and S. Passerini, *Angewandte Chemie-International Edition*, 2014, **53**, 13342-13359.
10. Lowry, Brian J., *Access Science*, 2019. [Available from DOI: https://doi.org/10.1036/1097-8542.186000]
11. Johnson L. Importance of Density: Sciencing; 2018 [Available from: https://sciencing.com/importance-density-5484217.html.]
12. Antor Paar Products Catalogue. Densimeter: DMA 5000 M. [Available from: https://www.anton-paar.com/es-es/productos/detalles/densimetro-dmatm-5000-m/]
13. G. Elert, *The Physics Hypertextbook*, 1998-2020. [Available from: https://physics.info/viscosity/]
14. S. Dabir, K. Tushar, H.L. Dasika, V.K. Nidamarty and Y. Kalipatnapu, *Viscosity of Liquids: Theory, Estimation, Experiment, and Data*. Springer, 2007.
15. Antor Paar Products Catalogue. Viscometer: Rolling-ball viscometer Lovis 2000 M/ME. [Available from: https://www.anton-paar.com/uk-en/products/details/rolling-ball-viscometer-lovis-2000-mme/]
16. G. Allen and J.C. Bevington, *Comprehensive polymer Science and Supplements*, 1996.
17. Mettler Toledo Catalogue. Conductivity meter: Seven Compact S230, 2020. [Available from: https://www.mt.com/no/no/home/library/datasheets/lab-analytical-instruments/DS_S230.html]
18. X. Y. Cui, H. Y. Wu, T. J. Hu, J. K. Zhang, X. Zhong, X. X. Wu, J. S. Wang, X. F. Li, J. H. Yang and C. X. Gao, *Journal of Alloys and Compounds*, 2020, **823**.

19. M. Bates, *How does a battery work?*, *MIT School of Engineering*, 2012. [Available from: https://engineering.mit.edu/engage/ask-an-engineer/how-does-a-battery-work/]

20. C.D. Rahn and C. Wang, *Battery Systems Engineering*, *Wiley*, 2013.

21. T. Hordé, p. Achard and R. Metkemeijer, International Council for Aeronautial Sciences, 2012. [Available from: https://www.researchgate.net/figure/Schematic-of-the-working-principle-of-a-Li-ion-battery_fig1_281418222]

22. P. Dong, X. Zhang, Y. Cha, J.-I. Lee and M.-K. Song, *Nano Energy*, 2020, **69**, 104434.

23. X. W. Wang, Y. Q. Tan, G. H. Shen and S. G. Zhang, *Journal of Energy Chemistry*, 2020, **41**, 149-170.

24. S. Suriyakumar, M. Kathiresan and A. M. Stephan, *Acs Omega*, 2019, **4**, 3894-3903.

25. B. Sun, K. Liu, J. L. Lang, M. H. Fang, Y. Jin and H. Wu, *Electrochimica Acta*, 2018, **284**, 662-668.

26. A. Vizintin, R. Guterman, J. Schmidt, M. Antonietti and R. Dominko, *Chemistry of Materials*, 2018, **30**, 5444-5450.

27. X. M. Cai, B. W. Cui, B. Ye, W. Q. Wang, J. L. Ding and G. C. Wang, *Acs Applied Materials & Interfaces*, 2019, **11**, 38136-38146.

28. D. Fang, Y. Wang, C. Qian, X. Liu, X. Wang, S. Chen and S. Zhang, *Advanced Functional Materials*, 2019, **29**, 1900875.

29. H. Lu, Z. Chen, H. L. Du, K. Zhang, J. L. Wang, Z. Z. Hou and J. Fang, *Ionics*, 2019, **25**, 2685-2691.

30. H. Lu, Y. Zhu, B. Zheng, H. L. Du, X. Z. Zheng, C. C. Liu, Y. Yuan, J. Fang and K. Zhang, *New Journal of Chemistry*, 2020, **44**, 361-368.

31. B. J. Li, Y. J. Li, X. Y. Zhan, P. He and H. S. Zhou, *Green Energy & Environment*, 2019, **4**, 3-19.

32. S. Brutti, M. A. Navarra, G. Maresca, S. Panero, J. Manzi, E. Simonetti and G. B. Appetecchi, *Electrochimica Acta*, 2019, **306**, 317-326.

33. A. F. de Anastro, N. Lago, C. Berlanga, M. Galceran, M. Hilder, M. Forsyth and D. Mecerreyes, *Journal of Membrane Science*, 2019, **582**, 435-441.

34. M. Xie, S. J. Li, Y. X. Huang, Z. H. Wang, Y. Jiang, M. Wang, F. Wu and R. J. Chen, *Chemelectrochem*, 2019, **6**, 2423-2429.

35. K. H. Yang, Z. Liao, Z. X. Zhang, L. Yang and S. Hirano, *Materials Letters*, 2019, **236**, 554-557.

36. D. Y. Oh, Y. J. Nam, K. H. Park, S. H. Jung, K. T. Kim, A. R. Ha and Y. S. Jung, *Advanced Energy Materials*, 2019, **9**, 1802927.

37. Y. Yang, Q. Huang, L. Niu, D. Wang, C. Yan, Y. She and Z. Zheng, *Advanced Materials*, 2017, **29**, 1606679.

38. Y. Huang, H. Li, Z. Wang, M. Zhu, Z. Pei, Q. Xue, Y. Huang and C. Zhi, *Nano Energy*, 2016, **22**, 422-438.

39. N. Choudhary, C. Li, J. Moore, N. Nagaiah, L. Zhai, Y. Jung and J. Thomas, *Advanced Materials*, 2017, **29**, 1605336.

40. L. P. Yu and G. Z. Chen, *Frontiers in Chemistry*, 2019, **7**, 15.

41. Poonam, K. Sharma, A. Arora and S. K. Tripathi, *Journal of Energy Storage*, 2019, **21**, 801-825.

42. J. Tian, Z. Yang, Z. Yin, Z. Ye, J. Wang, C. Cui and W. Qian, *The Chemical Record*, 2019, **19**, 1256-1262.

43. A. Eftekhari, Y. Liu and P. Chen, *Journal of Power Sources*, 2016, **334**, 221-239.

44. G. Tian, in *Industrial Applications of Green Solvents, Vol Ii*, eds. Inamuddin, R. Mobin and A. M. Asiri, 2019, vol. 54, pp. 249-293.

45. E. Lindner, M. Guzinski, T. A. Khan and B. D. Pendley, *Acs Sensors*, 2019, **4**, 549-561.

46. Q. Yang, Z. Zhang, X.-G. Sun, Y.-S. Hu, H. Xing and S. Dai, *Chemical Society Reviews*, 2018, **47**, 2020-2064.

47. L. L. Fan, N. P. Deng, J. Yan, Z. H. Li, W. M. Kang and B. W. Cheng, *Chemical Engineering Journal*, 2019, **369**, 874-897.

48. Y. Cheng, Z. Chen, H. Wu, M. Zhu and Y. Lu, *Advanced Functional Materials*, 2016, **26**, 1338-1346.

49. J. Hao, Y. Yang, J. Zhao, X. Liu, F. Endres, C. Chi, B. Wang, X. Liu and Y. Li, *Nanoscale*, 2017, **9**, 8481-8488.

50. J. Hao, L. Pan, H. Zhang, C. Chi, Q. Guo, J. Zhao, Y. Yang, X. Liu, X. Ma and Y. Li, *Chemical Engineering Journal*, 2018, **346**, 427-437.

51. X. Liu, T. Ji, T. Nie, T. Wang, Z. Liu, S. Liu, J. Zhao and Y. Li, *Materials Letters*, 2020, **261**, 127157.

52. X.-G. Sun, C. Liao, N. Shao, J. R. Bell, B. Guo, H. Luo, D.-e. Jiang and S. Dai, *Journal of Power Sources*, 2013, **237**, 5-12.

53. X. Cao, X. He, J. Wang, H. Liu, S. Röser, B. R. Rad, M. Evertz, B. Streipert, J. Li, R. Wagner, M. Winter and I. Cekic-Laskovic, *ACS Applied Materials & Interfaces*, 2016, **8**, 25971-25978.

54. Q. Pang, X. Liang, C. Y. Kwok and L. F. Nazar, *Nature Energy*, 2016, **1**, 16132.

55. L. N. Wang, J. Y. Liu, S. Y. Yuan, Y. G. Wang and Y. Y. Xia, *Energy & Environmental Science*, 2016, **9**, 224-231.

56. L. M. Suo, Y. J. Zhu, F. D. Han, T. Gao, C. Luo, X. L. Fan, Y. S. Hu and C. S. Wang, *Nano Energy*, 2015, **13**, 467-473.

57. T. Stettner, F. C. Walter and A. Balducci, *Batteries & Supercaps*, 2019, **2**, 55-59.

58. Z. J. Liu, J. Huang, Y. T. Zhang, B. Tong, F. Guo, J. W. Wang, Y. Shi, R. Wen, Z. B. Zhou, L. M. Guo and Z. Q. Peng, *Advanced Energy Materials*, 2019, **9**.

59. U. Ulissi, G. A. Elia, S. Jeong, F. Mueller, J. Reiter, N. Tsiouvaras, Y. K. Sun, B. Scrosati, S. Passerini and J. Hassoun, *Chemsuschem*, 2018, **11**, 229-236.

60. H. Lee, D. J. Lee, M. Kim, H. Kim, Y. S. Cho, H. J. Kwon, H. C. Lee, C. R. Park and D. Im, *ACS applied materials & interfaces*, 2020, DOI: 10.1021/acsami.9b21962.

61. Z. Hou, C. Shu, P. Hei, T. Yang, R. Zheng, Z. Ran and J. Long, *Nanoscale*, 2020, **12**, 6785-6794.

62. H. Wang, H. Wang, J. Huang, X. Zhou, Q. Wu, Z. Luo and F. Wang, *Acs Applied Materials & Interfaces*, 2019, **11**, 44556-44565.

63. W.-J. Kwak, Rosy, D. Sharon, C. Xia, H. Kim, L. R. Johnson, P. G. Bruce, L. F. Nazar, Y.-K. Sun, A. A. Frimer, M. Noked, S. A. Freunberger and D. Aurbach, *Chemical Reviews*, 2020, DOI: 10.1021/acs.chemrev.9b00609.

64. H. Wang, H. Wang, J. Huang, X. Zhou, Q. Wu, Z. Luo and F. Wang, *ACS Applied Materials & Interfaces*, 2019, **11**, 44556-44565.

65. F. Mizuno, S. Nakanishi, A. Shirasawa, K. Takechi, T. Shiga, H. Nishikoori and H. Iba, *Electrochemistry*, 2011, **79**, 876-881.

66. M. Asadi, B. Sayahpour, P. Abbasi, A. T. Ngo, K. Karis, J. R. Jokisaari, C. Liu, B. Narayanan, M. Gerard, P. Yasaei, X. Hu, A. Mukherjee, K. C. Lau, R. S. Assary, F. Khalili-Araghi, R. F. Klie, L. A. Curtiss and A. Salehi-Khojin, *Nature*, 2018, **555**, 502-506.

67. J.-B. Park, S. H. Lee, H.-G. Jung, D. Aurbach and Y.-K. Sun, *Advanced Materials*, 2018, **30**, 1704162.

68. J. Zhang, B. Sun, Y. Zhao, A. Tkacheva, Z. Liu, K. Yan, X. Guo, A. M. McDonagh, D. Shanmukaraj, C. Wang, T. Rojo, M. Armand, Z. Peng and G. Wang, *Nature Communications*, 2019, **10**, 602.

69. A. Tkacheva, J. Zhang, B. Sun, D. Zhou, G. Wang and A. M. McDonagh, *The Journal of Physical Chemistry C*, 2020, **124**, 5087-5092.

70. Monti D, Jónsson E, Palacín R, Johansson P. *Journal of Power Sources*. 2014, **245**, 630-636.

71. Liu H, Yu H. *Journal of Materials Science & Technology*. 2019, **35**, 674-686.

72. J. G. Kim, B. Son, S. Mukherjee, N. Schuppert, A. Bates, O. Kwon, M. J. Choi, H. Y. Chung and S. Park, *Journal of Power Sources*, 2015, **282**, 299-322.

73. L. Fan, S. Y. Wei, S. Y. Li, Q. Li and Y. Y. Lu, *Advanced Energy Materials*, 2018, **8**.

74. J. H. Shin, W. A. Henderson, S. Scaccia, P. P. Prosini and S. Passerini, *Journal of Power Sources*, 2006, **156**, 560-566.

75. F. Gonzalez, P. Tiemblo, N. Garcia, O. Garcia-Calvo, E. Fedeli, A. Kvasha and I. Urdampilleta, *Membranes*, 2018, **8**.

76. G. P. Pandey, Y. Kumar and S. A. Hashmi, *Indian Journal of Chemistry Section a-Inorganic Bio-Inorganic Physical Theoretical & Analytical Chemistry*, 2010, **49**, 743-751.

77. J. H. Shin, W. A. Henderson and S. Passerini, *Electrochemistry Communications*, 2003, **5**, 1016-1020.

78. K. X. Lei, C. C. Wang, L. J. Liu, Y. W. Luo, C. N. Mu, F. J. Li and J. Chen, *Angewandte Chemie-International Edition*, 2018, **57**, 4687-4691.

79. Y. R. Wang, R. P. Chen, T. Chen, H. L. Lv, G. Y. Zhu, L. B. Ma, C. X. Wang, Z. Jin and J. Liu, *Energy Storage Materials*, 2016, **4**, 103-129.

80. R. Rajagopalan, Y. G. Tang, X. B. Ji, C. K. Jia and H. Y. Wang, *Advanced Functional Materials*, 2020, **30**.

81. S. L. Liu, J. F. Mao, Q. Zhang, Z. J. Wang, W. K. Pang, L. Zhang, A. J. Du, O. R. Sencadas, W. C. Zhang and Z. P. Guo, *Angewandte Chemie-International Edition*, 2020, **59**, 3638-3644.

82. K. Yoshii, T. Masese, M. Kato, K. Kubota, H. Senoh and M. Shikano, *Chemelectrochem*, 2019, **6**, 3901-3910.

83. J. Y. Hwang, S. T. Myung and Y. K. Sun, *Advanced Functional Materials*, 2018, **28**.

84. T. Yamamoto, K. Matsumoto, R. Hagiwara and T. Nohira, *The Journal of Physical Chemistry C*, 2017, **121**, 18450-18458.

85. K. Beltrop, S. Beuker, A. Heckmann, M. Winter and T. Placke, *Energy & Environmental Science*, 2017, **10**, 2090-2094.

86. J. Muldoon, C. B. Bucur, A. G. Oliver, T. Sugimoto, M. Matsui, H. S. Kim, G. D. Allred, J. Zajicek and Y. Kotani, *Energy & Environmental Science*, 2012, **5**, 5941-5950.

87. H. D. Yoo, I. Shterenberg, Y. Gofer, G. Gershinsky, N. Pour and D. Aurbach, *Energy & Environmental Science*, 2013, **6**, 2265-2279.

88. M. Matsui, *Journal of Power Sources*, 2011, **196**, 7048-7055.

89. G. Vardar, A. E. S. Sleightholme, J. Naruse, H. Hiramatsu, D. J. Siegel and C. W. Monroe, *Acs Applied Materials & Interfaces*, 2014, **6**, 18033-18039.

90. T. Sato, G. Masuda and K. Takagi, *Electrochimica Acta*, 2004, **49**, 3603-3611.

91. N. Yoshimoto, M. Matsumoto, M. Egashia and M. Morita, *Journal of Power Sources*, 2010, **195**, 2096-2098.

92. T. Kakibe, N. Yoshimoto, M. Egashira and M. Morita, *Electrochemistry Communications*, 2010, **12**, 1630-1633.

93. T. Kakibe, J. Y. Hishii, N. Yoshimoto, M. Egashira and M. Morita, *Journal of Power Sources*, 2012, **203**, 195-200.

94. P. Padigi, G. Goncher, D. Evans and R. Solanki, *Journal of Power Sources*, 2015, **273**, 460-464.

95. A. Ponrouch and M. R. Palacin, *Current Opinion in Electrochemistry*, 2018, **9**, 1-7.

96. S. Biria, S. Pathreeker, F. S. Genier, H. Li and I. D. Hosein, *ACS Applied Energy Materials*, 2020, **3**, 2310-2314.

97. C. J. Xu, B. H. Li, H. D. Du and F. Y. Kang, *Angewandte Chemie-International Edition*, 2012, **51**, 933-935.

98. Z. Liu, T. Cui, G. Pulletikurthi, A. Lahiri, T. Carstens, M. Olschewski and F. Endres, *Angewandte Chemie-International Edition*, 2016, **55**, 2889-2893.

99. Z. Liu, G. Pulletikurthi, A. Lahiri, T. Cui and F. Endres, *Dalton Transactions*, 2016, **45**, 8089-8098.

100. P. P. Wang, Z. Chen, H. Wang, Z. Y. Ji, Y. P. Feng, J. Q. Wang, J. Liu, M. M. Hu, J. B. Fei, W. Gan and Y. Huang, *Energy Storage Materials*, 2020, **25**, 426-435.

101. V. Verma, S. Kumar, W. Manalastas, R. Satish and M. Srinivasan, *Advanced Sustainable Systems*, 2019, **3**.

102. A. El Kharbachi, O. Zavorotynska, M. Latroche, F. Cuevas, V. Yartys and M. Fichtner, *Journal of Alloys and Compounds*, 2020, **817**.

103. N. Jayaprakash, S. K. Das and L. A. Archer, *Chemical Communications*, 2011, **47**, 12610-12612.

104. C. Wang, J. F. Li, H. D. Jiao, J. G. Tu and S. Q. Jiao, *Rsc Advances*, 2017, **7**, 32288-32293.

105. C.-Y. Chen, T. Tsuda, S. Kuwabata and C. L. Hussey, *Chemical Communications*, 2018, **54**, 4164-4167.

106. G. Z. Zhu, M. Angell, C. J. Pan, M. C. Lin, H. Chen, C. J. Huang, J. A. Lin, A. J. Achazi, P. Kaghazchi, B. J. Hwang and H. J. Dai, *Rsc Advances*, 2019, **9**, 11322-11330.

107. Landt Instruments 2012-2020. Battery Test Systems for Energy Materials Research. [Availabre from: https://landtinst.com/battery-test-systems-for-energy-materials-research/]

108. H. Saba, X. J. Zhu, Y. Chen and Y. M. Zhang, *Chinese Journal of Chemical Engineering*, 2015, **23**, 804-811.

109. X. Zhang, X. Fan, H. Niu and J. Wang, *Green Chemistry*, 2003, **5**, 267-269.

110. S. A. Sakal, Y. Z. Lu, X. C. Jiang, C. Shen and C. X. Li, *Journal of Chemical and Engineering Data*, 2014, **59**, 533-539.

111. S. K. Panja and S. Saha, *RSC Advances*, 2013, **3**, 14495-14500.

112. K. Buhl, C. Bond, D. Stone, National Pesticide Information Center, 2013. [Available from: http://npic.orst.edu/factsheets/ironphosphategen.html]

113. Royal Society if Chemistry 2020. [Available from: http://www.chemspider.com/Chemical-Structure.144555.html]

114. A. Laurikenas, J. Barkauskas, J. Reklaitis, G. Niaura, D. Baltrunas and A. Kareiva, *Lithuanian Journal of Physics*, 2016, **56**, 35-41.

115. S. H. Pyo, J. H. Park, T. S. Chang and R. Hatti-Kaul, *Current Opinion in Green and Sustainable Chemistry*, 2017, **5**, 61-66.

116. Y. Ein-Eli, *Electrochemistry Communications*, 2002, **4**, 644-648.

117. Mitsubishi Chemical Corporation. [Available from: https://www.m-chemical.co.jp/en/products/departments/mcc/c2/product/1200981_7910.html]

118. S. I. Tobishima, J. I. Yamaki and T. Okada, *Electrochimica Acta*, 1984, **29**, 1471-1476.

119. N. Ehteshami, L. Ibing, L. Stolz, M. Winter and E. Paillard, *Journal of Power Sources*, 2020, **451**.

7. Appendix

Appendix 1: Hazards identification for the chemicals used in the laboratory

In this section can be found the pictograms and the hazard and precautionary statements for the chemicals utilized in the laboratory. This data was obtained from the safety data sheet of each chemical which has been written following the standards of the Globally Harmonized System of Classification and Labelling of Chemicals by the company where the chemicals were bought.

- **Product name:** 1-Butyl-3-methylimidazolium chloride (BmimCl)

Pictogram: 

Signal word: Danger

Hazard statements:

H301 Toxic if swallowed.

H315 Causes skin irritation.

H319 Causes serious eye irritation.

H411 Toxic to aquatic life with long lasting effects.

Precautionary statements:

P273 Avoid release to the environment.

P301 + P310 + P330 IF SWALLOWED: Immediately call a POISON CENTER/doctor. Rinse mouth.

P302 + P352 IF ON SKIN: Wash with plenty of water.

P305 + P351 + P338 IF IN EYES: Rinse cautiously with water for several minutes.

Remove contact lenses, if present and easy to do. Continue rinsing.

- **Product name:** Iron (III) chloride hexahydrate ($FeCl_3 \cdot 6H_2O$)

Pictogram: 

Signal word: Danger

Hazard statements:

H290 May be corrosive to metals.

H302 Harmful if swallowed.

H315 Causes skin irritation.

H318 Causes serious eye damage.

Precautionary statements:

P280 Wear eye protection/ face protection.

P301 + P312 + P330 IF SWALLOWED: Call a POISON CENTER/doctor if you feel unwell. Rinse mouth.

P302 + P352 IF ON SKIN: Wash with plenty of water.

P305 + P351 + P338 + P310 IF IN EYES: Rinse cautiously with water for several minutes. Remove contact lenses, if present and easy to do. Continue rinsing. Immediately call a POISON CENTER/doctor.

- **Product name:** Iron phosphate ($FePO_4$)

Pictogram: 

Signal words: Warning

Hazard statements:

H315: Causes skin irritation.

H319: Causes serious eye irritation.

H335: May cause respiratory irritation.

Precautionary statements:

* P261: Avoid breathing dust/fume/gas/mist/vapours/spray.

P280: Wear protective gloves/protective clothing/eye protection/face protection.

P305+P351+P338: IF IN EYES: Rinse cautiously with water for several minutes. Remove contact lenses, if present and easy to do. Continue rinsing.

P304+P340: IF INHALED: Remove person to fresh air and keep comfortable for breathing.

P405: Store locked up.

P501: Dispose of contents/container to hazardous or special waste collection point, in accordance with local, regional, national and/or international regulation.

- **Product name:** Iron (III) acetate

Not a hazardous substance or mixture.

- **Product name:** Dimethyl carbonate (DMC)

Pictogram: 

Signal word: Danger

Hazard statements:

H225 Highly flammable liquid and vapour.

Precautionary statements:

P210 Keep away from heat, hot surfaces, sparks, open flames and other ignition sources. No smoking.

P403 + P235 Store in a well-ventilated place. Keep cool.

- **Product name:** Ethylene carbonate (EC)

Pictogram: 

Signal word: Warning

Hazard statements:

H302 Harmful if swallowed.

H319 Causes serious eye irritation.

H373 May cause damage to organs (Kidney) through prolonged or repeated exposure if swallowed.

Precautionary statements:

P301 + P312 + P330 IF SWALLOWED: Call a POISON CENTER/doctor if you feel unwell. Rinse mouth.

P305 + P351 + P338 IF IN EYES: Rinse cautiously with water for several minutes. Remove contact lenses, if present and easy to do. Continue rinsing.

P314 Get medical advice/ attention if you feel unwell.